NASA/TM–20230006634

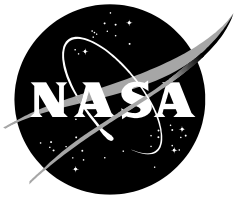

PMT F7
Silver Standard Material Properties Characterization

Jon R. Abramson
Convergent Manufacturing Technologies US
1101 N Northlake Way, Ste 200, Seattle WA 98103-8901

Juan M. Fernandez
NASA Langley Research Center, Hampton, Virginia

Joshua E. Salazar
NASA Langley Research Center, Hampton, Virginia

July 2023

NASA STI Program Report Series

Since its founding, NASA has been dedicated to the advancement of aeronautics and space science. The NASA scientific and technical information (STI) program plays a key part in helping NASA maintain this important role.

The NASA STI program operates under the auspices of the Agency Chief Information Officer. It collects, organizes, provides for archiving, and disseminates NASA's STI. The NASA STI program provides access to the NTRS Registered and its public interface, the NASA Technical Reports Server, thus providing one of the largest collections of aeronautical and space science STI in the world. Results are published in both non-NASA channels and by NASA in the NASA STI Report Series, which includes the following report types:

- TECHNICAL PUBLICATION. Reports of completed research or a major significant phase of research that present the results of NASA Programs and include extensive data or theoretical analysis. Includes compilations of significant scientific and technical data and information deemed to be of continuing reference value. NASA counterpart of peer-reviewed formal professional papers but has less stringent limitations on manuscript length and extent of graphic presentations.

- TECHNICAL MEMORANDUM. Scientific and technical findings that are preliminary or of specialized interest, e.g., quick release reports, working papers, and bibliographies that contain minimal annotation. Does not contain extensive analysis.

- CONTRACTOR REPORT. Scientific and technical findings by NASA-sponsored contractors and grantees.

- CONFERENCE PUBLICATION. Collected papers from scientific and technical conferences, symposia, seminars, or other meetings sponsored or co-sponsored by NASA.

- SPECIAL PUBLICATION. Scientific, technical, or historical information from NASA programs, projects, and missions, often concerned with subjects having substantial public interest.

- TECHNICAL TRANSLATION. English-language translations of foreign scientific and technical material pertinent to NASA's mission.

Specialized services also include organizing and publishing research results, distributing specialized research announcements and feeds, providing information desk and personal search support, and enabling data exchange services.

For more information about the NASA STI program, see the following:

- Access the NASA STI program home page at http://www.sti.nasa.gov

- Help desk contact information:

https://www.sti.nasa.gov/sti-contact-form/
and select the "General" help request type.

NASA/TM–20230006634

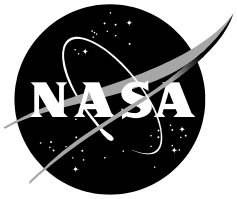

PMT F7
Silver Standard Material Properties Characterization

Jon R. Abramson
Convergent Manufacturing Technologies US
1101 N Northlake Way, Ste 200, Seattle WA 98103-8901

Juan M. Fernandez
NASA Langley Research Center, Hampton, Virginia

Joshua E. Salazar
NASA Langley Research Center, Hampton, Virginia

National Aeronautics and
Space Administration

Langley Research Center
Hampton, Virginia 23681-2199

July 2023

Available from:

NASA STI Program / Mail Stop 148
NASA Langley Research Center
Hampton, VA 23681-2199
Fax: 757-864-6500

Table of Contents

1. Report Version Log

Table 1.1: Report Version Log.

Version #	Date	Description	Material Files	Approval
1	10/28/2021	Final Report Revision 2	MATRIX-PMT-F7-v1 COMPOSITE-PMT-F7-M30S-PW-Fabric-v1 COMPOSITE-PMT-F7-MR60H-UD-Tape-v1 FIBRE-TORAY-M30S-v2 FIBRE-MITSUBISHI-MR60H-v2	Alastair McKee

2. Material File Permissions

Convergent material files have different security/permission levels of release depending on the source of the data, client or other restrictions. These permission have both a Convergent ‘internal’ permission level and an external client ‘release’ permission level. The details of the permission level are captured in the material file and enforced through encryption or other security measures within CCA. Details of the permission levels for both release (external) and internal categories are listed below.

Release

- Open: Available to everyone, no restrictions
- Proprietary: Available only to the customer
- Secret: Available only to the customer and encrypted

Internal

- Open: Available company wide
- Project/Group Name: Available only to people working on the named project or internal group
- Employee: Restricted to only the named employee and the file is encrypted

In addition to the permission level, each material file has an owner of record who is considered the ‘customer’. This is typically the individual within a company that was the primary technical contact for project or the source of the data. This information is captured within the material file. In the case of proprietary or secret permissions, Convergent requires permission from the material file owner to release the file to any other person or entity.

The following material file permissions and contact information are used for the materials characterized in this report:

Release: Open

Internal: Material Data Group

Customer: NASA

Juan M. Fernandez (juan.m.fernandez@nasa.gov)

3. Overview

3.1. Terminology

BMB: Bi-Material Beam

CCA: Convergent Common Component Architecture, the library used in composites processing analysis codes such as COMPRO and RAVEN

CMM: Coordinate Measuring Machine

Cp: Specific Heat Capacity

CHILE: Cure Hardening Instantaneously Linear Elastic

CTE: Coefficient of Thermal Expansion

DMA: Dynamic Mechanical Analyzer

DoC or *x*: Degree of Cure

DoM: Date of Manufacturing

DSC: Differential Scanning Calorimetry

Dyn or Dynamic: DSC tests where the specimen temperature is increased at a constant rate until the reaction completes

EI: Beam Stiffness

Iso or Isothermal: Tests where the specimen is held at a constant temperature long enough so that the reaction slows down significantly due to diffusion

IntIso or Interrupted Isothermal: Isothermal tests where the hold segment terminates before the reaction stops due to diffusion

MDSC: Temperature-Modulated DSC

MRCC: Manufacturer's Recommended Cure Cycle

Res or Residual: Dynamic DSC tests performed after the hold segment of Iso and Int tests to complete the remainder of the chemical reaction

TGA: Thermo-Gravimetric Analyzer

TMA: Thermo-Mechanical Analyzer

3.2. Abstract

Patz F7 epoxy resin was characterized to capture the thermo-chemical and thermo-mechanical properties of the material. Differential scanning calorimeter (DSC) testing was performed and the data was used to develop a cure kinetics model which predicts the cure response and specific heat capacity of the material. Thermo-mechanical analyzer (TMA) and dynamic mechanical analyzer (DMA) testing were performed and the data was used to develop thermo-mechanical models which predict the material coefficient of thermal expansion (CTE), cure shrinkage, and modulus evolution with cure. Convergent Manufacturing Technologies US determined test parameters, analyzed data, and performed model fitting. NASA completed tests and provided data to Convergent Manufacturing Technologies US.

3.3. Scope of Characterization

In this report, the results of material characterization testing and model fitting performed for Patz Materials and Technologies (PMT) F7 epoxy resin will be presented. The material database was specifically developed for use with the Convergent Common Component Architecture (CCA) material library. This library is used in composites processing analysis codes such as COMPRO and RAVEN.

The models are based on a set of experiments which represent the typical manufacturing conditions recommended for the material. The model has been validated against these experiments. Use of the model for process simulations which include conditions outside those that are presented in this report should be avoided.

3.4. Composites Processing Analysis

Composites processing analysis is supported by thermo-chemical, flow-compaction, and thermo-mechanical characterizations. Material models developed from these characterizations are used in thermo-chemical, flow-compaction, and stress-deformation analyses, respectively. The materials database (CCA) is used for all analyses. Brief descriptions of these types of analyses are as follows:

- Thermo-chemical analyses calculate the internal temperature in the part and tooling, as well as the degree of cure, in composites structural components.
- Flow-compaction analyses calculate the resin flow and fiber bed compaction in composite materials.
- Stress-deformation analyses calculate the development of residual strains and deformation in the structure and tooling.

The composites process models require a substantial amount of input data to describe the time and temperature dependent evolution of material properties. The quality of this material property data is of paramount importance for producing accurate model results.

The range of property data necessary for different analysis types, and the properties characterized within the scope of this project and report, are shown in Table 3.1. Property data not needed for certain analysis types are marked as N/A.

Table 3.1: The Spectrum of Material Property Data Characterized for Composites Processing Analysis.

Analysis type	Material properties required for the simulation	Characterized material properties for this report		
		Fibre	Resin	Fiber Bed
Thermo-Chemical Analysis	Degree of Cure	N/A	Characterized By Convergent/NASA	N/A
	Heat of Reaction	N/A	Characterized By Convergent/NASA	N/A
	Glass Transition	N/A	Characterized By Convergent/NASA	N/A
	Density	Data sheet or Open literature	Data sheet or Open literature	N/A
	Specific Heat Capacity	Data sheet or Open literature	Characterized By Convergent/NASA	N/A
	Thermal Conductivity	Data sheet or Open literature	Data sheet or Open literature	N/A
Flow-Compaction Analysis	Initial Fibre Volume Fraction	Data sheet or Open literature	N/A	N/A
	Resin Viscosity	N/A	Not Characterized	N/A
	Fibre Bed Compaction	N/A	N/A	Not Characterized
	Fibre Bed Permeability	N/A	N/A	Not Characterized
Stress-Deformation Analysis	Elastic / Viscoelastic Constants	Data sheet or Open literature	Characterized By Convergent/NASA	N/A
	Coefficient of Thermal Expansion	Data sheet or Open literature	Characterized By Convergent/NASA	N/A
	Cure Shrinkage	N/A	Characterized By Convergent/NASA	N/A

All characterization tests with the exception of bi-material beam (BMB) dynamic mechanical analyzer (DMA) tests and a limited set of differential scanning calorimeter (DSC) tests were performed by NASA and test data was supplied to Convergent US. The remaining testing and all model fitting was performed by Convergent US.

This report presents results of the following characterization procedures performed to the Silver Standard:

Thermo-Chemical

- Cure Kinetics (Degree of Cure, Heat of Reaction and Glass Transition)
- Specific Heat Capacity

Thermo-Mechanical

- Resin Modulus
- Coefficient of Thermal Expansion (CTE)
- Cure Shrinkage

3.5. Material Forms Available

NASA tested samples of the material manufactured by PMT. One batch of each of the following material forms were tested:

Neat Resin

- CMTUS Form Designation: **NR B1**
- Manufacturer's Designation: PMT F7
- CMTUS Form Designation: NR
- CMTUS Batch Designation: B1
- Date of Manufacture: 2020-01-06

Prepregs

- CMTUS Form Designation: **UD B1**
- Manufacturer's Designation: PMT F7/MR60H UD Tape
- CMTUS Form Designation: UD (Unidirectional)
- CMTUS Batch Designation: B1
- Fiber Type: Mitsubishi Pyrofil MR60H 24K
- Fabric Architecture: UD

- CMTUS Form Designation: **PW B1**
- Manufacturer's Designation: PMT F7/M30S PW Fabric
- CMTUS Form Designation: PW (Plain Weave)
- CMTUS Batch Designation: B1
- Fiber Type: Torayca M30S
- Fabric Architecture: PW

Convergent Manufacturing Technologies US received a sample of material from NASA on 03/10/2021. One batch of the aforementioned UD B1 material was received and labeled separately as UD B2 and UD B3 to account for cure advancement during material transit:

Prepregs

- CMTUS Form Designation: **UD B2**
- Manufacturer's Designation: PMT F7/MR60H UD Tape
- CMTUS Form Designation: UD
- CMTUS Batch Designation: B2
- Fiber Type: Mitsubishi Pyrofil MR60H 24K
- Fabric Architecture: Unidirectional

- CMTUS Form Designation: **UD B3**
- Manufacturer's Designation: PMT F7/MR60H UD Tape
- CMTUS Form Designation: UD
- CMTUS Batch Designation: B3
- Fiber Type: Mitsubishi Pyrofil MR60H 24K
- Fabric Architecture: Unidirectional

3.6. Manufacturer's Recommended Cure Cycle

The manufacturer's recommended cure cycle (MRCC) based on the F7 material datasheet is shown in Figure 3.1 and defined as follows:

Manufacturer's Recommended Cure Cycle

- Ramp 1.1ºC/min to 120ºC
- Hold for 80 min
- Ramp 1.1ºC/min to 180ºC
- Hold for 125 min
- Ramp 1.1ºC/min to 20ºC

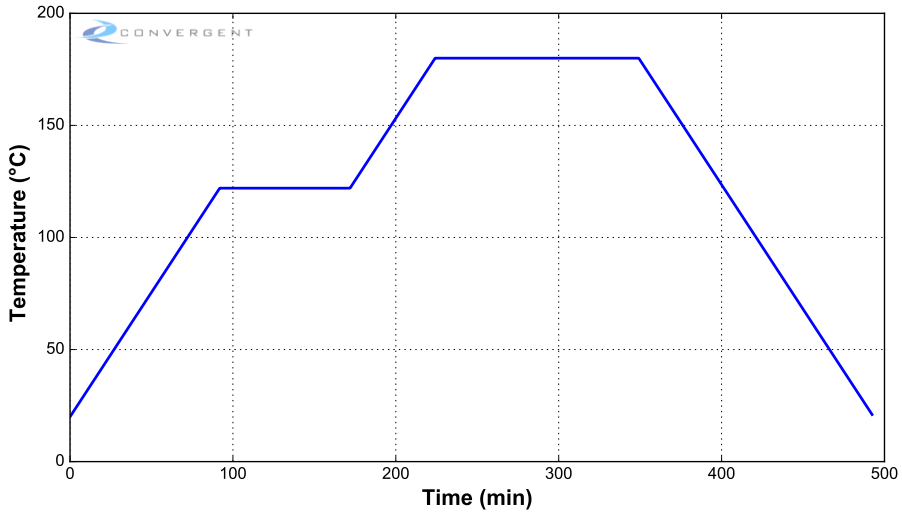

Figure 3.1: Manufacturer's Recommended Cure Cycle.

4. Density and Fiber Volume Fraction

The density and mass fractions of the constituents were obtained from the material datasheet and confirmed through correspondence with NASA. These values were used to support the analysis in this report. Based on the resin mass fraction, the resin density and the fiber density, the fiber volume fraction and density of the prepreg form(s) was calculated using:

$$V_f = \frac{\rho_r(1 - m_r)}{\rho_r(1 - m_r) + \rho_f m_r}$$

$$\rho = \rho_f V_f + \rho_r(1 - V_f)$$

Unidirectional Tape

- Resin Type: F7
- Resin Density: 1.24 g/cm^3
- Resin Mass Fraction: 0.314

- Fiber Type: Mitsubishi Pyrofil MR60H-24k
- Fiber Density: 1.81 g/cm^3
- Fiber Mass Fraction: 0.686
- Fiber Areal Weight: 40 g/m^2

This yielded the Fiber Volume Fraction: 0.599

Fabric

- Resin Type: F7
- Resin Density: 1.24 g/cm^3
- Resin Mass Fraction: 0.338

- Fiber Type: Torayca M30S-18k
- Fiber Density: 1.73 g/cm^3
- Fiber Mass Fraction: 0.662
- Fiber Areal Weight: 60 g/m^2

This yielded the Fiber Volume Fraction: 0.584

5. Material Degradation Temperature

Thermogravimetric Analysis (TGA) tests were performed to determine the degradation temperature of the material prior to Differential Scanning Calorimetry (DSC) testing. Testing was performed on a TA Instruments Discovery Thermogravimetric Analyzer. During the tests, the material was heated at a rate of 3ºC/min while continuously measuring the mass of the sample. The raw data is shown in the Fig. 5.1. Reported sample masses in excess of 100% are attributed to uncertainty in instrument measurement and recorded initial sample mass.

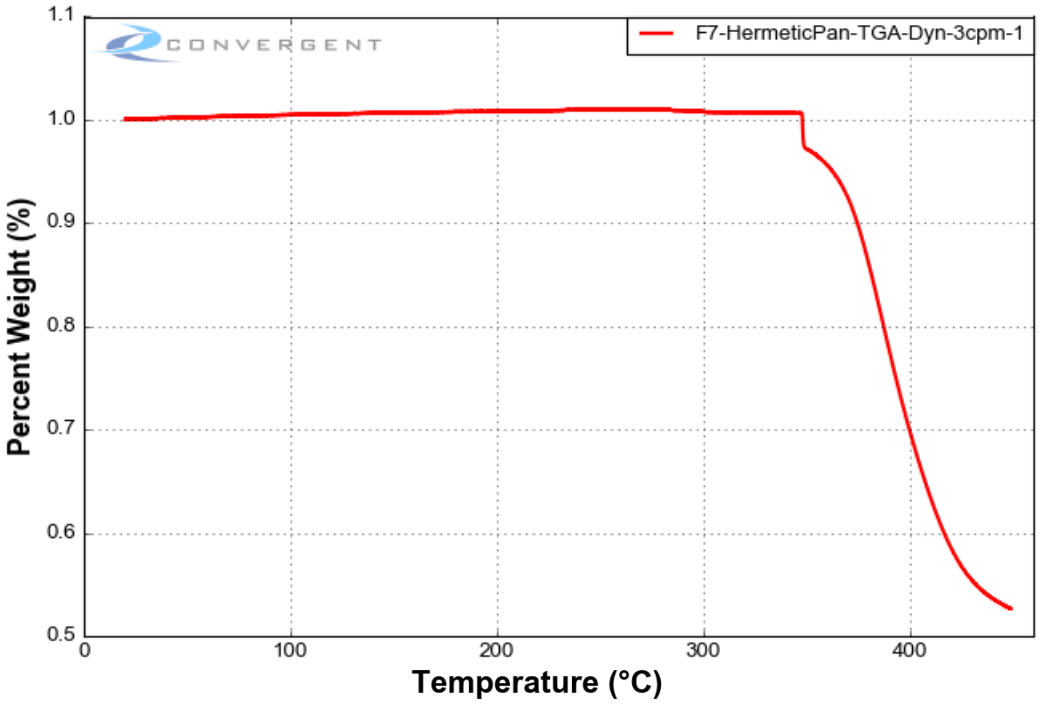

Figure 5.1: TGA Dynamic Ramp Raw Data Overlay.

As shown in Fig. 5.2, seal failure of the Tzero Aluminum Hermetic pan due to material offgassing occurs at 347°C in the 3°C/min sample. The upper temperature limit of 320°C was chosen for DSC testing.

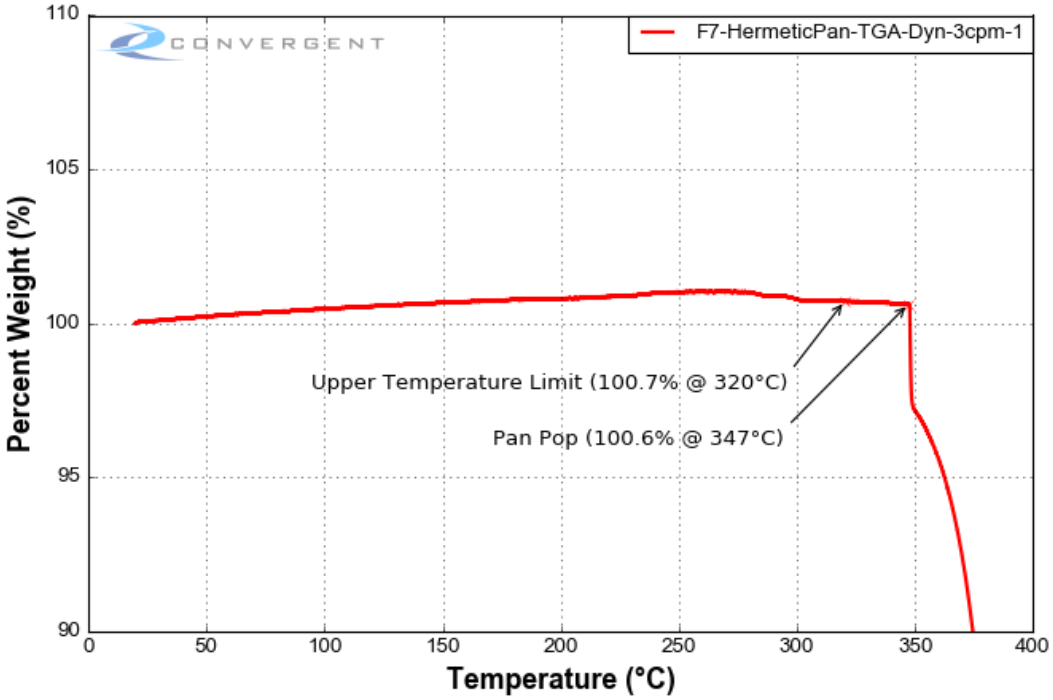

Figure 5.2: Material Degradation Temperature.

6. Thermo-Chemical Characterization: Cure Kinetics

6.1. Nomenclature

x: Degree of Cure

$\dot{x}$: Cure Rate: $\frac{dx}{dt}$

T_g: Glass Transition Temperature (°C or K)

HF: Heat Flow, measured in the DSC experiments (W)

HR: Heat of Reaction (J/kg)

HR_{Ramp}: HR released during the ramp segment of the DSC tests

HR_{Hold}: HR released during the hold segment of the DSC tests

$HR_{preTest}$: HR released due to the cure advancement in material before the start of the test (material handling, mixing, storing, etc.)

HR_{Test}: The total HR measured through various stages of the DSC test $(HR_{Ramp} + HR_{Hold})$

HR_{Total}: The total HR of the material $(HR_{preTest} + HR_{Test})$

HR_{Iso}^{avg}: The average of the total HR measured through various stages of the isothermal DSC tests

HR_{Dyn}^{avg}: The average of the total HR measured through various stages of the dynamic DSC tests

HR_{Model}: Model HR; the nominal total HR value used in the model.

6.2. Introduction

DSC tests were performed to characterize the cure kinetics of F7. A model for cure rate ($\dot{x}$) as a function of temperature and degree of cure was developed.

A TA Instruments Q25 DSC instrument was used for the characterization. Samples of 5 mg to 20 mg were encapsulated in T-Zero Aluminum Hermetic pans and the thermal analysis was run using a nitrogen purge of 50 ml/min.

6.3. DSC Test Procedures

Dynamic Ramp Tests

In a dynamic test, the sample is equilibrated at a temperature at least 50ºC below the initial T_g of the material and then heated at a predetermined ramp rate, as shown in Fig. 6.1. This provides the initial T_g of the material and the total heat of reaction to fully cure the sample.

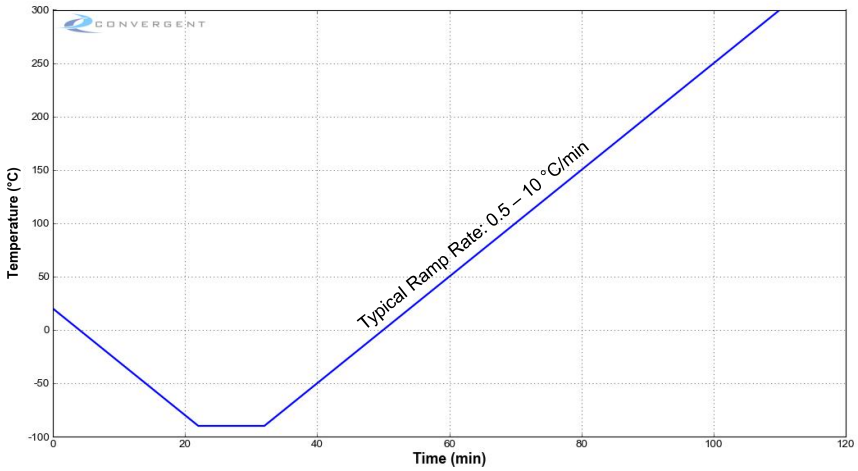

Figure 6.1: DSC Dynamic Test Definition.

The temperature range is selected such that the sample cures to completion on the ramp without degrading the material. The ramp rates are selected to include and bracket any ramp rates that are expected to be used in the manufacturing cure cycle(s), as shown in Fig. 6.2.

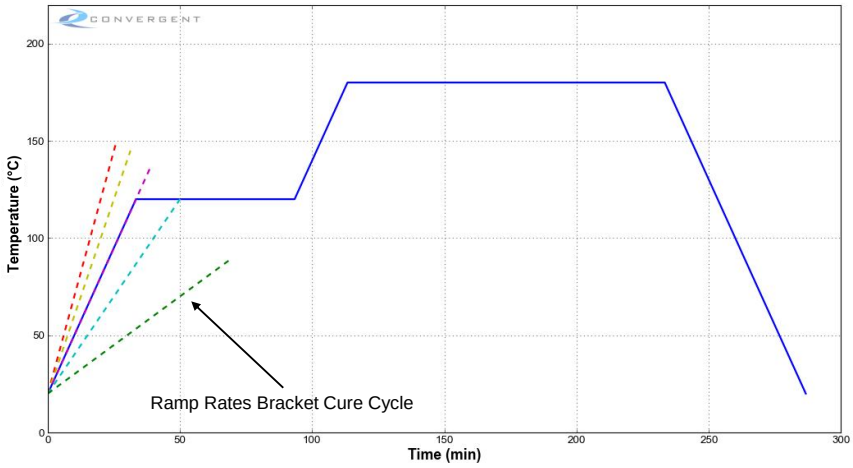

Figure 6.2: DSC Dynamic Test Selection of Ramp Rates.

Isothermal Tests

In an isothermal test, the sample is equilibrated at a temperature at least 50ºC below the initial T_g of the material and then heated to a predefined hold temperature at a very high ramp rate (50ºC/min). The sample is held at this temperature for a predetermined duration until the reaction slows down significantly due to diffusion or full cure of the sample. The sample is then cooled down again, followed by a residual ramp. The residual ramp provides the T_g after the hold and the residual heat of reaction to fully cure the sample. An example of this test type is shown in Fig. 6.3.

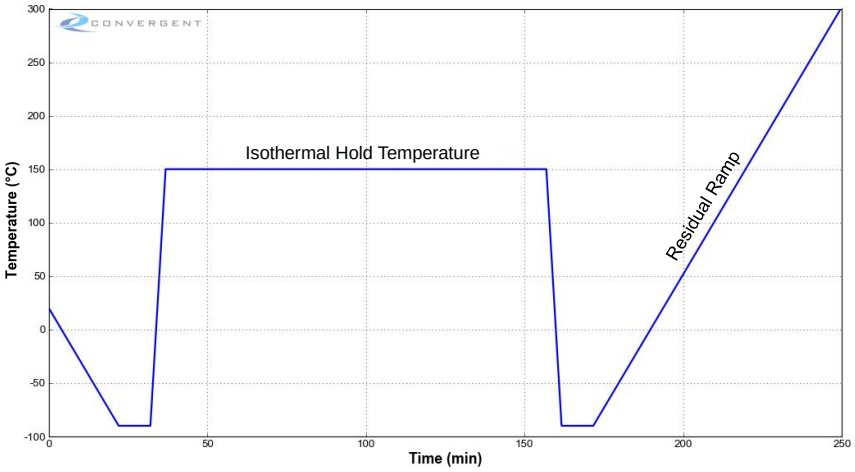

Figure 6.3: DSC Isothermal Test Definition.

The hold temperatures are selected to include and bracket any hold temperature(s) that are expected to be used in manufacturing cure cycle(s), as shown in Fig. 6.4.

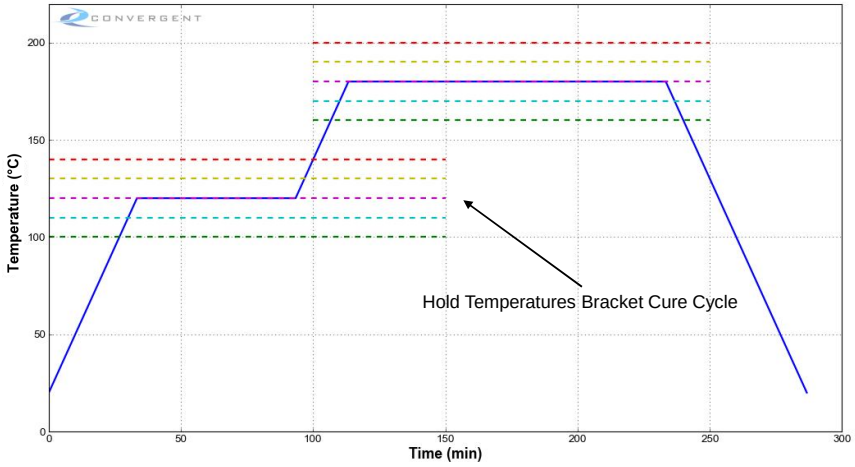

Figure 6.4: DSC Isothermal Test Selection of Hold Temperatures.

Interrupted Isothermal Tests

In an interrupted isothermal test, the hold segment of an isothermal test is terminated before the reaction slows down significantly. The sample is then cooled down again, followed by a residual ramp. Interrupted isothermal tests are performed to generate additional information on the degree of cure versus glass transition temperature relationship by only partially curing the sample in the hold. An example of this test type is shown in Fig. 6.5.

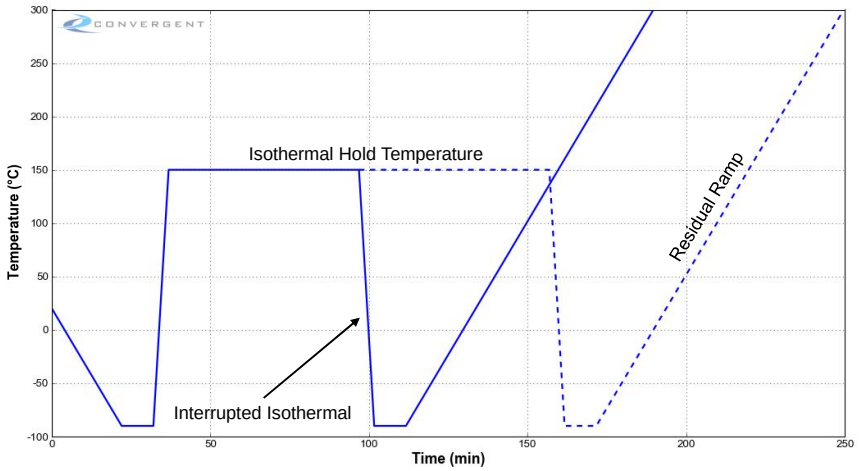

Figure 6.5: DSC Interrupted Isothermal Test Definition.

Aging Tests

In an aging test, the sample is held at a relatively low temperature for an extended period of time before testing in the DSC. The hold temperature is selected such that the reaction progresses slowly and various hold times are selected such that the final degree of cure is low. A residual ramp is performed in the DSC where the post aging T_g and residual heat of reaction are measured.

Cure Cycle Tests

The ramp rates and hold temperatures used in the dynamic and isothermal tests are selected to include any rates and hold temperatures used in the MRCC as well as any other typical or expected manufacturing cure cycle(s). However, the ultimate test of the success of a cure kinetics model is in predicting the cure behaviors of a practical cure cycle. Cure cycle tests are comprised of a series of tests where a typical thermal cure cycle (e.g. manufacturer's recommended cure cycle) is interrupted at various stages, where T_g and degree of cure are measured. The calculated T_g and degree of cure were then compared against the measured value to gauge the accuracy of the model. An example of this test type is shown in Fig. 6.6.

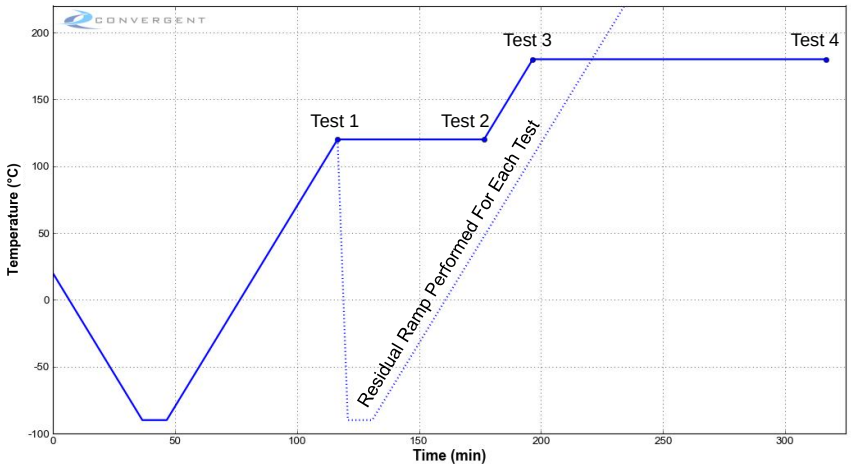

Figure 6.6: DSC Cure Cycle Test Definition.

Reheat Tests

Reheat tests are simply an additional residual ramp at the end of any given test described above. These residual ramps can be appended to any DSC tests and are conducted without removing the sample from the DSC. A reheat test can be used to confirm that a given sample has been fully cured or to gain additional information regarding data deconvolution (e.g. baseline shapes).

6.4. Material Form and Batch Comparison

Three forms of F7 were provided by Patz and tested by NASA. A section of batch UD B1 was sent to CMTUS for testing, referred to as UD B2. The specific details of these forms and designations assigned by CMTUS are listed in Section 3.5. Limited screening tests were performed on NR B1, UD B1 and UD B2 to investigate batch dependent behavior within the forms provided. A UD B3 batch was separated to account for nominal cure advancement in bi-material beam samples during sample preparation. UD B2 and UD B3 were ultimately deemed equivalent in cure state. All remaining thermo-chemical characterization tests were performed on PW B1 based on material availability.

Dynamic modulated differential scanning calorimeter (MDSC) tests were performed for all screened forms at ramp rates of 0.5ºC/min, 1.5ºC/min, and 3ºC/min with additional dynamic MDSC tests performed for NR B1 at 1ºC/min and 2ºC/min. The non-reversing heat flow signals were baselined to determine the total heat of reaction (HR_{Total}) and cure rate profile for each form. In addition, the reversing Cp signals were used to determine the initial Tg for each form.

Total Heat of Reaction Screening Results

The total heat of reaction (HR) for each screening test is shown in Fig. 6.7.

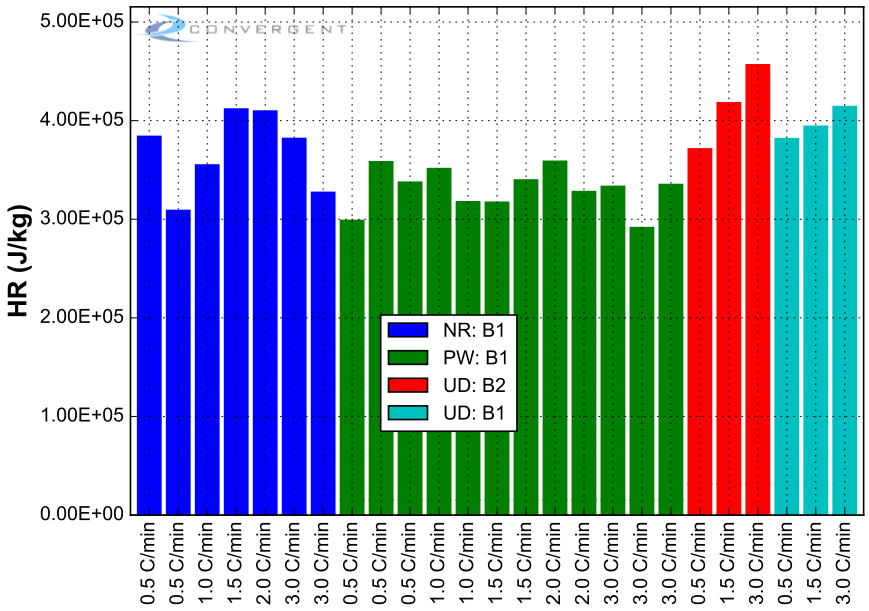

Figure 6.7: HR (Dynamic Form Comparison).

It has been observed that PW B1 possesses a lower average HR than NR B1, followed by UD B2 and UD B1.

Initial Tg Screening Results

The initial Tg result for each screening test is shown in Fig. 6.8.

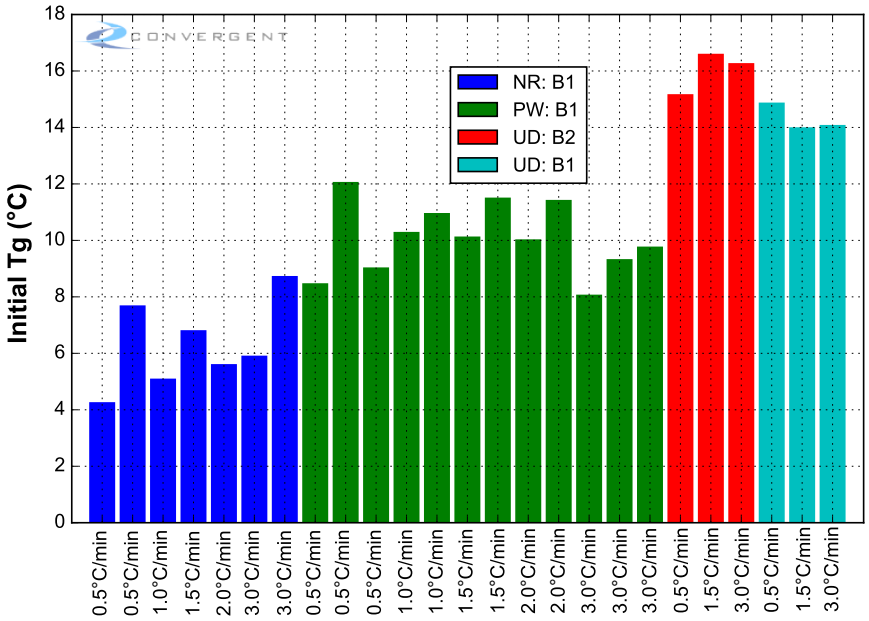

Figure 6.8: Initial Tg (Dynamic Form Comparison).

NR B1 possesses the lowest average initial Tg of all tested forms, followed by PW B1, UD B1, and UD B2.

Based on consistent differences in average HR and initial glass transition temperature between all tested forms, some level of initial cure advancement is assumed in most forms. NR B1, possessing a higher average HR and the lowest initial Tg of all tested forms, is assumed to be in a fully uncured state and is used as the comparative standard for all other forms. PW B1 is assumed to be 4.2% cured prior to testing and both UD B1 and UD B2 are assumed to be 8.5% cured prior to testing. Using these initial cure states creates agreement in cure behavior and allows for cure kinetics model applicability between all forms.

6.5. DSC Tests Performed

The DSC tests performed are summarized below:

- Dynamic tests: 25 tests at 0.5ºC/min to 3ºC/min
- Isothermal tests: 16 tests at 125ºC to 190ºC
- Interrupted Isothermal tests: 20 tests at 125ºC to 180ºC
- Cure Cycle tests: 10 tests of the MRCC cycle

A summary of the DSC tests performed are shown in Tables 6.1, 6.2, 6.3, and 6.4.

Table 6.1: DSC Dynamic Test Summary.

Test name	Mass (mg)	Ramp rate (°C/min)
F7-NR-B1-DSC-Dyn-0.5cpm-1	5.04	0.5
F7-NR-B1-DSC-Dyn-0.5cpm-2	5.06	0.5
F7-NR-B1-DSC-Dyn-1cpm-1	4.9	1
F7-NR-B1-DSC-Dyn-1.5cpm-1	4.8	1.5
F7-NR-B1-DSC-Dyn-2cpm-1	4.9	2
F7-NR-B1-DSC-Dyn-3cpm-1	5.0	3
F7-NR-B1-DSC-Dyn-3cpm-2	5.1	3
M30S F7-PW-B1-DSC-Dyn-0.5cpm-1	9.97	0.5
M30S F7-PW-B1-DSC-Dyn-0.5cpm-2	10.5	0.5
M30S F7-PW-B1-DSC-Dyn-0.5cpm-3	10.03	0.5
M30S F7-PW-B1-DSC-Dyn-1cpm-1	10.1	1
M30S F7-PW-B1-DSC-Dyn-1cpm-2	9.99	1
M30S F7-PW-B1-DSC-Dyn-1.5cpm-1	10.25	1.5
M30S F7-PW-B1-DSC-Dyn-1.5cpm-2	10.7	1.5
M30S F7-PW-B1-DSC-Dyn-2cpm-1	10.86	2
M30S F7-PW-B1-DSC-Dyn-2cpm-2	10.1	2
M30S F7-PW-B1-DSC-Dyn-3cpm-1	9.9	3
M30S F7-PW-B1-DSC-Dyn-3cpm-2	10.0	3
M30S F7-PW-B1-DSC-Dyn-3cpm-3	10.01	3
MR60H F7-UD-B1-DSC-Dyn-0.5cpm-1	10	0.5
MR60H F7-UD-B1-DSC-Dyn-1.5cpm-1	10.09	1.5
MR60H F7-UD-B1-DSC-Dyn-3cpm-1	9.9	3
MR60H F7-UD-B2-DSC-Dyn-0.5cpm-1	10.7	0.5
MR60H F7-UD-B2-DSC-Dyn-1.5cpm-1	14.7	1.5
MR60H F7-UD-B2-DSC-Dyn-3cpm-1	13.3	3

Table 6.2: DSC Isothermal Test Summary.

Test name	Mass (mg)	Hold temp (°C)	Hold time (min)
M30S F7-PW-B1-DSC-Iso-125C-1600min-1	10.9	125	1600
M30S F7-PW-B1-DSC-Iso-125C-1600min-2	9.98	125	1600
M30S F7-PW-B1-DSC-Iso-125C-1600min-3	10.03	125	1600
M30S F7-PW-B1-DSC-Iso-140C-900min-1	10.11	140	900
M30S F7-PW-B1-DSC-Iso-140C-900min-2	10.1	140	900
M30S F7-PW-B1-DSC-Iso-155C-600min-1	10	155	600
M30S F7-PW-B1-DSC-Iso-155C-600min-2	9.99	155	600
M30S F7-PW-B1-DSC-Iso-170C-400min-1	10.58	170	400
M30S F7-PW-B1-DSC-Iso-170C-400min-2	9.9	170	400
M30S F7-PW-B1-DSC-Iso-180C-300min-1	10.13	180	300
M30S F7-PW-B1-DSC-Iso-180C-300min-2	10.01	180	300
M30S F7-PW-B1-DSC-Iso-190C-200min-1	10.16	190	200
M30S F7-PW-B1-DSC-Iso-190C-225min-2	10.1	190	225
M30S F7-PW-B1-DSC-Iso-190C-225min-3	10	190	225
MR60H F7-UD-B2-DSC-Iso-120C-1600min-1	9.8	120	1600
MR60H F7-UD-B2-DSC-Iso-190C-225min-1	10.1	190	225

Table 6.3: DSC Interrupted Isothermal Test Summary.

Test name	Mass (mg)	Hold temp (°C)	Hold time (min)
F7-PW-B1-DSC-InterIso-125C-75min-1	10.02	125	75
F7-PW-B1-DSC-InterIso-125C-160min-1	10.04	125	160
F7-PW-B1-DSC-InterIso-125C-300min-1	10	125	300
F7-PW-B1-DSC-InterIso-125C-475min-1	10.07	125	475
F7-PW-B1-DSC-InterIso-125C-700min-1	9.98	125	700
F7-PW-B1-DSC-InterIso-140C-30min-1	10.04	140	30
F7-PW-B1-DSC-InterIso-140C-80min-1	10.2	140	80
F7-PW-B1-DSC-InterIso-140C-150min-1	10.21	140	150
F7-PW-B1-DSC-InterIso-140C-300min-1	10.1	140	300
F7-PW-B1-DSC-InterIso-140C-475min-1	10	140	475
F7-PW-B1-DSC-InterIso-155C-15min-1	9.9	155	15
F7-PW-B1-DSC-InterIso-155C-50min-1	10.09	155	50
F7-PW-B1-DSC-InterIso-155C-100min-1	10.13	155	100
F7-PW-B1-DSC-InterIso-155C-165min-1	10.1	155	165
F7-PW-B1-DSC-InterIso-155C-250min-1	9.9	155	250
F7-PW-B1-DSC-InterIso-180C-10min-1	9.9	180	10
F7-PW-B1-DSC-InterIso-180C-20min-1	10.4	180	20
F7-PW-B1-DSC-InterIso-180C-35min-1	10.2	180	35
F7-PW-B1-DSC-InterIso-180C-55min-1	9.9	180	55
F7-PW-B1-DSC-InterIso-180C-90min-1	9.99	180	90

Table 6.4: DSC Cure Cycle Test Summary.

Test name	Mass (mg)	Segment ID	Cycle ID
M30S F7-PW-B1-DSC-MRCC1-A-1	9.96	A	1
M30S F7-PW-B1-DSC-MRCC1-A-2	10.1	A	1
M30S F7-PW-B1-DSC-MRCC1-B-1	10.12	B	1
M30S F7-PW-B1-DSC-MRCC1-B-2	10.05	B	1
M30S F7-PW-B1-DSC-MRCC1-C-1	10.15	C	1
M30S F7-PW-B1-DSC-MRCC1-C-2	10.1	C	1
M30S F7-PW-B1-DSC-MRCC1-D-1	9.97	D	1
M30S F7-PW-B1-DSC-MRCC1-D-2	10	D	1
M30S F7-PW-B1-DSC-MRCC1-E-1	10.03	E	1
M30S F7-PW-B1-DSC-MRCC1-E-2	10	E	1

6.6. DSC Raw Data and Data Analysis

The first step in the analysis is to calculate the baseline. In general, the baseline represents the part of the measured heat flow that is unrelated to the curing of the specimen such as heat lost to the surroundings or heat that contributes to increasing the specimen temperature. In the case of temperature-modulated DSC tests (MDSC), the deconvolution of the data not only provides the information traditionally obtainable from conventional DSCs, it also captures the response of the material to the temperature modulation. The total heat flow data (equivalent to the one measured in a non-modulated test) is obtained by averaging the modulated heat flow. The modulation component of the heat flow is used to determine the reversing component of the heat flow which is a measure of instantaneous heat capacity. In this study, the non-reversing heat flow component was used to analyze the curing process of the material when the underlying temperature rate was non-zero. In the zones where temperature was constant (e.g. during hold temperature in isothermal tests), the total heat flow was used in the analysis.

Baseline Calculations for Dynamic Tests

The baseline for the dynamic runs and the residual scans of the interrupted isothermal tests are calculated using the non-reversing component of the specific heat flow. All dynamic scans exhibit a characteristic local minimum in the specific heat flow and this point is taken as the start of the reaction. Typically, a linear baseline is extended from this point to the end of the reaction, where the heat flow measured reduces back to its initial level. In certain cases, alternate baseline approaches can be taken.

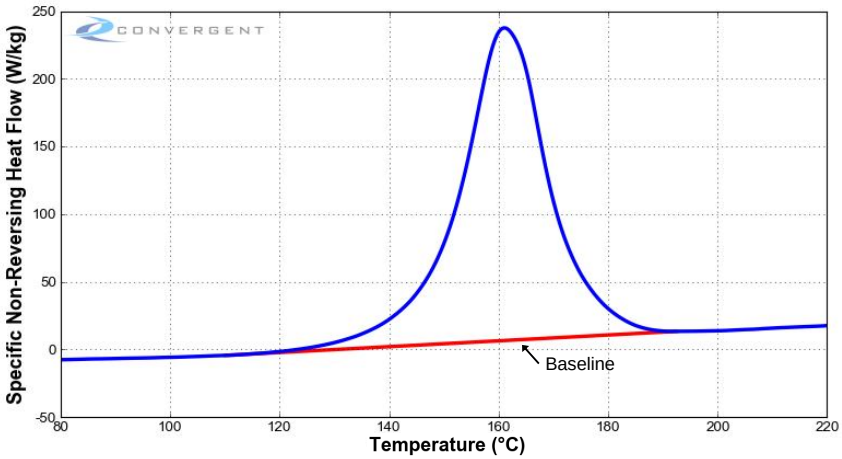

Figure 6.9: Baseline for Dynamic Tests.

Baseline Calculations for Isothermal Tests

The heat flow measured by the DSC after the reaction slows down significantly is a measure of the "baseline" in isothermal tests. The reaction slows due to diffusion at the end of the hold segment. The baseline was found by extending the heat flow at the end of the hold segment back to the start of the scan.

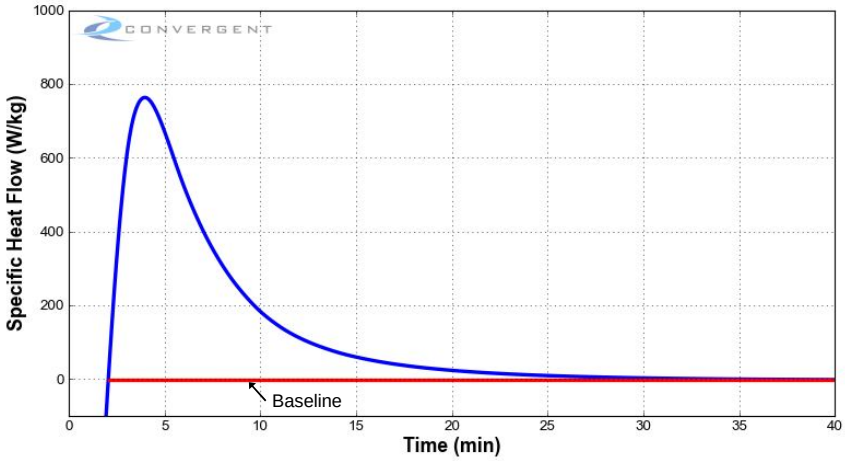

Figure 6.10: Baseline for Isothermal Tests.

The baseline definition discussed above assumes that no reaction occurs prior to the time that corresponds to the beginning of the baseline. This can introduce some uncertainty into the analysis, specifically in the case of high temperature isothermals where a certain amount of curing occurs on the ramp to the hold temperature. This effect was taken into account by using the model developed from dynamic tests to estimate the cure on the ramp and re-analyzing the isothermal tests with an updated initial degree of cure.

Heat of Reaction

Once the baselines were established, the HR generated in each of the tests was determined. The HR was found by integrating the difference between the specific heat flow ($\dot{q}$) and the baseline ($\dot{q}_{baseline}$) over the time the reaction occurs:

$$HR_{Total} = \int (\dot{q} - \dot{q}_{baseline})dt$$

The total HR calculation for dynamic and isothermal tests are shown in Figures 6.11 and 6.12.

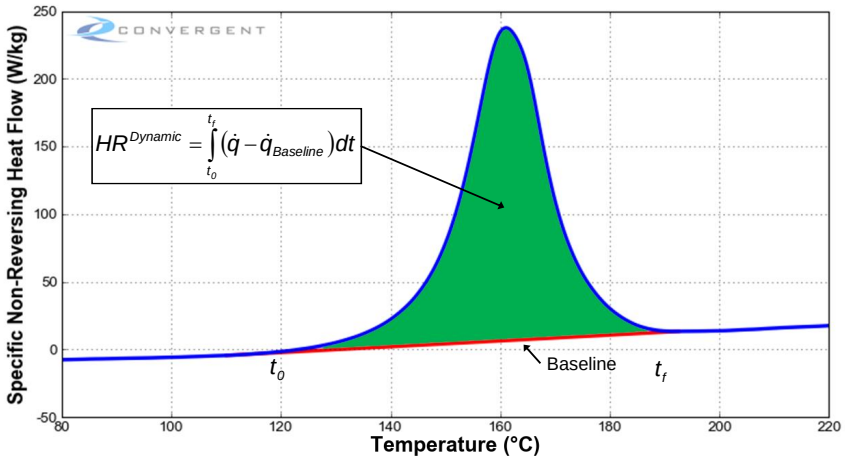

Figure 6.11: HR Calculation for Dynamic Tests.

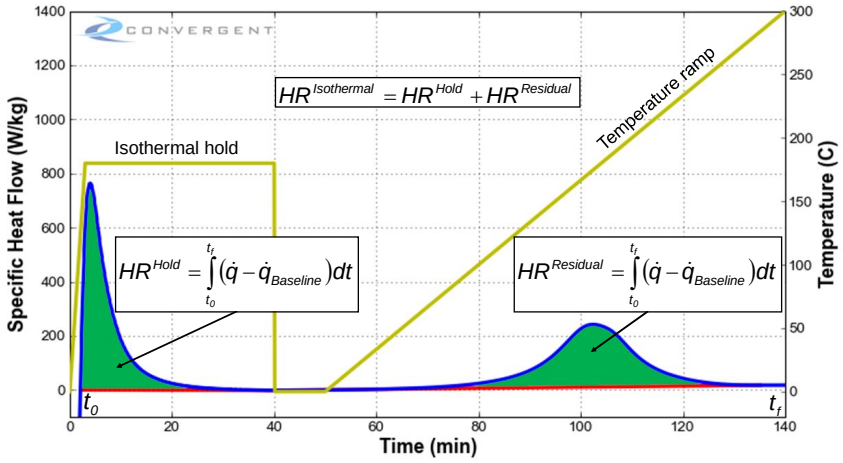

Figure 6.12: HR Calculation for Isothermal Tests.

The non-zero components of the total HRs for all of the dynamic and isothermal tests are shown in Table 6.5 and Fig. 6.13. The cooldown HR value accounts for the 4.2% cure advancement observed in batch PW B1 in Section 6.4.

Total HR - Dynamic Tests

Table 6.5: HR (Dynamic).

Test name	Cooldown (J/kg)	Ramp (J/kg)	Total (J/kg)
0.5°C/min	15540	283236	298776
0.5°C/min	15540	342668	358208
0.5°C/min	15540	322003	337543
1.0°C/min	15540	335806	351346
1.0°C/min	15540	302136	317676
1.5°C/min	15540	301649	317189
1.5°C/min	15540	324226	339766
2.0°C/min	15540	343185	358725
2.0°C/min	15540	312478	328018
3.0°C/min	15540	317751	333291
3.0°C/min	15540	275943	291483
3.0°C/min	15540	319669	335209

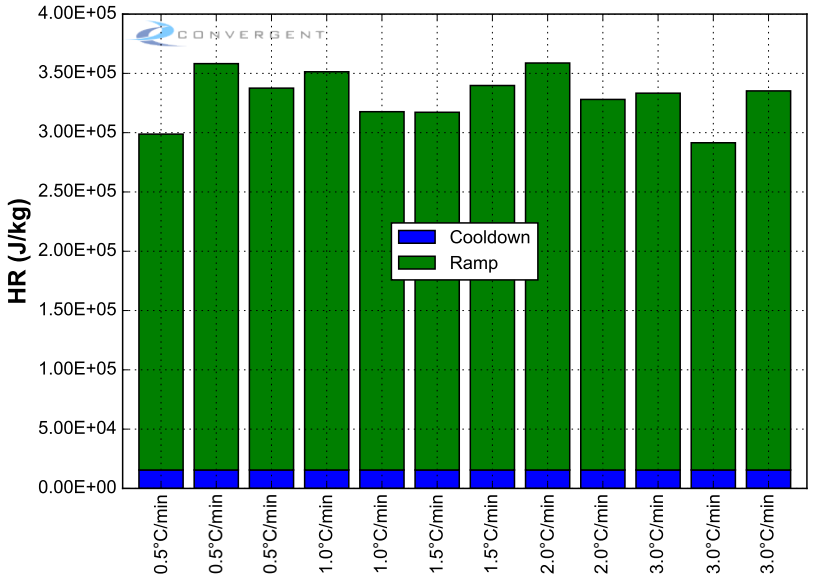

Figure 6.13: HR (Dynamic).

Total HR - Isothermal Tests

Note: the "Cooldown" column refers to the temperature ramp segment before the temperature hold. The HR here was calculated based on the dynamic tests to account for any heat lost in the initial ramp to the hold temperature.

Table 6.6: HR (Isothermal).

Test name	Cooldown (J/kg)	Hold (J/kg)	Ramp (J/kg)	Total (J/kg)
125°C	15540	235650	58854	310044
125°C	15540	223600	62711.8	301852
125°C	15540	261128	65722	342390
140°C	16000	298984	22281.3	337265
140°C	16000	296419	28984.5	341403
155°C	16600	328500	22285.4	367386
155°C	16600	320467	14659.3	351727
170°C	18200	344320	11265.5	373786
170°C	18200	328050	7218.39	353468
180°C	20500	340553	5727.83	366781
180°C	20500	308382	4783.4	333665
190°C	24500	312229	3155.23	339884
190°C	24500	322765	3096.21	350362
190°C	24500	326574	26589.5	377663

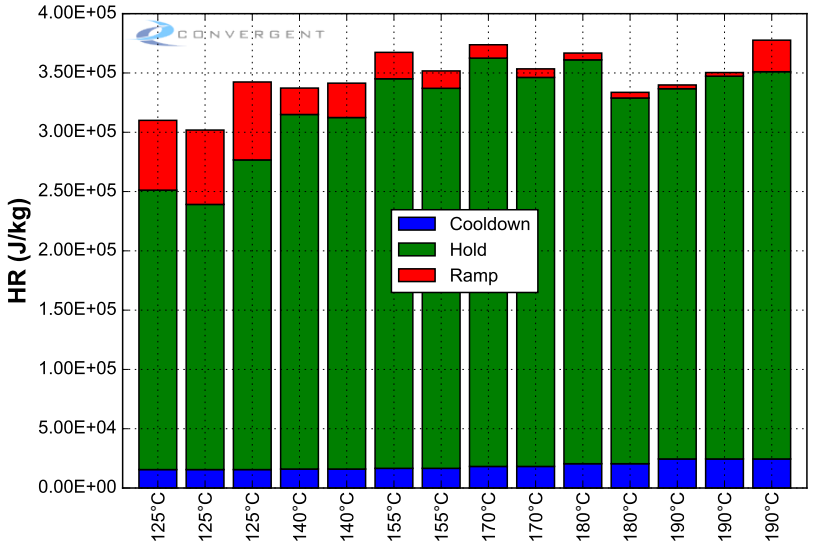

Figure 6.14: HR (Isothermal).

Based on the HR values measured in the dynamic and isothermal tests, the following values were calculated:

$$HR_{Iso}^{avg} = 346262.54 J/kg$$

$$HR_{Dyn}^{avg} = 330602.38 J/kg$$

The difference between the isothermal and dynamic HR values can be associated to the error embedded in the HR measurement on the hold and ramp segments of the DSC tests, respectively, by using the total and reversing heat flow signals. The measured average HR is 339,000 J/kg. The HR of the model was set to 370,000 J/kg based on measured HR from the NR B1 form only.

Calculation of Degree of Cure and Resin Cure Rate

With the baseline heat flow and the total heat of reaction known, the degree of cure was determined by a second analysis of the specific heat flow data. The degree of cure was found by dividing the heat evolved from the start of the reaction at time t_0 to the current time t by the total heat of reaction.

$$x(t) = \frac{1}{HR_{Total}} \int_{t_0}^{t} (\dot{q} - \dot{q}_{baseline}) dt$$

The degree of cure calculation at a given time for dynamic and isothermal tests are shown in Figures 6.15 and 6.16.

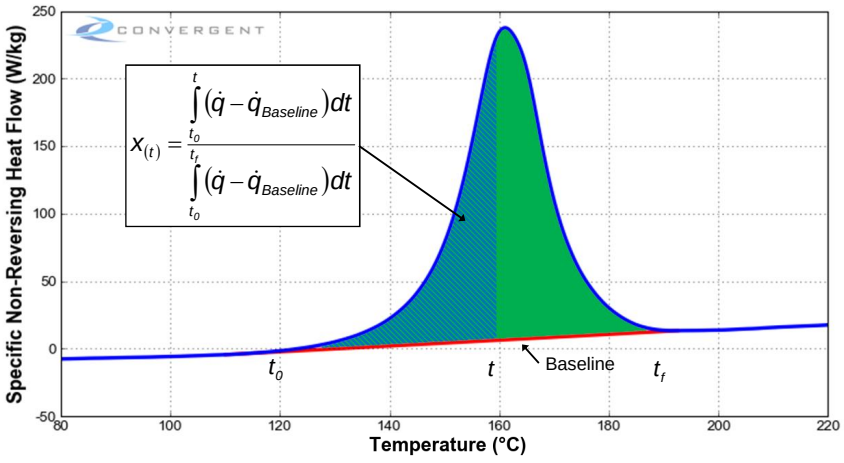

Figure 6.15: Degree of Cure Calculation for Dynamic Test.

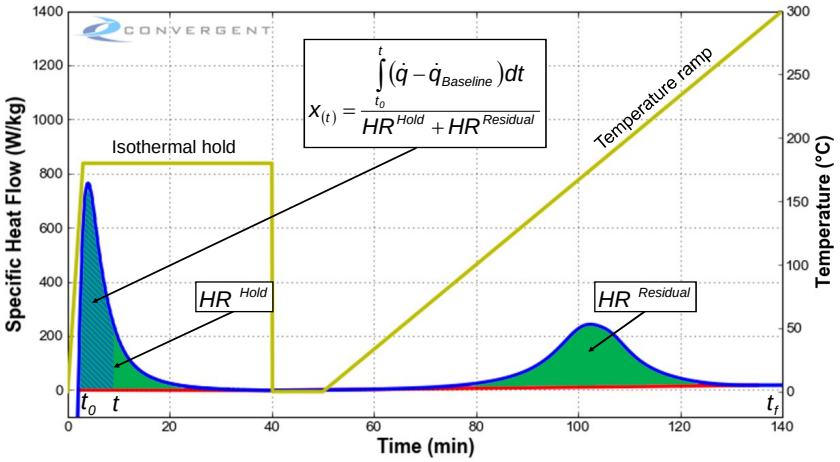

Figure 6.16: Degree of Cure Calculation for Isothermal Test.

The resin cure rate was then determined by considering the degree of cure as a function of time:

$$\dot{x} = \frac{dx}{dt} = \frac{x_t - x_{t-\Delta t}}{\Delta t}$$

DSC Raw Data

The raw heat flow and baselines for the dynamic tests are shown in Figures 6.17, 6.18, 6.19, 6.20, and 6.21.

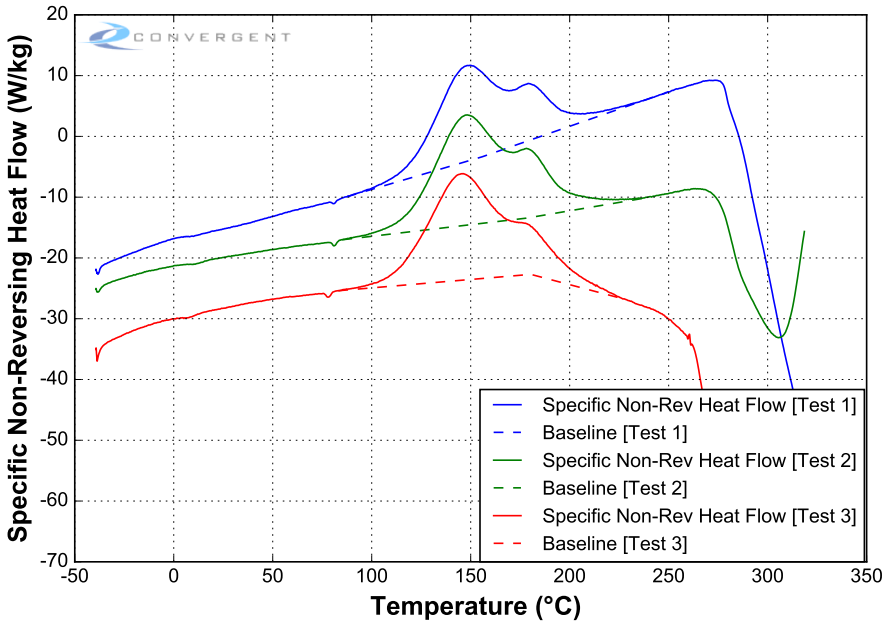

Figure 6.17: Raw Data: Dynamics 0.5°C/min.

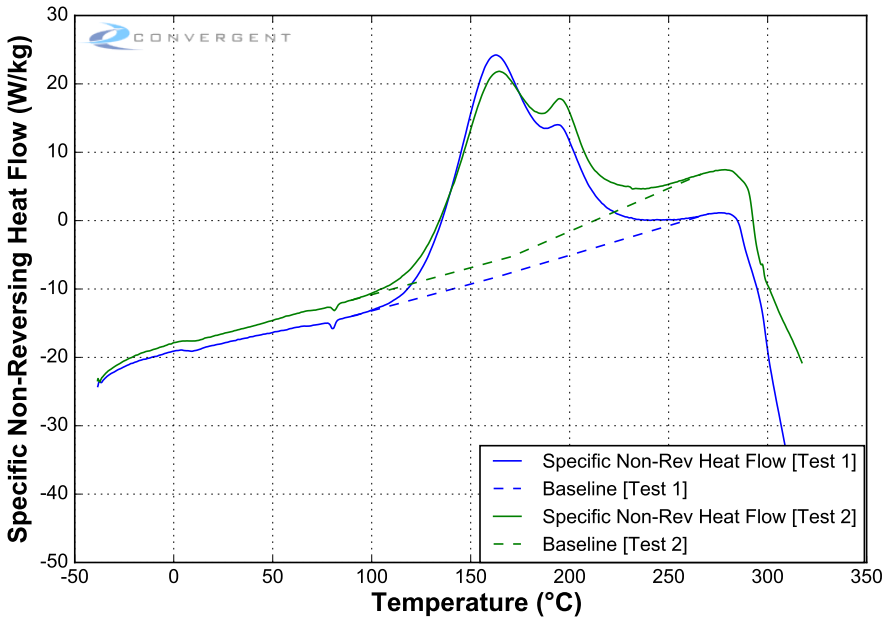

Figure 6.18: Raw Data: Dynamics 1°C/min.

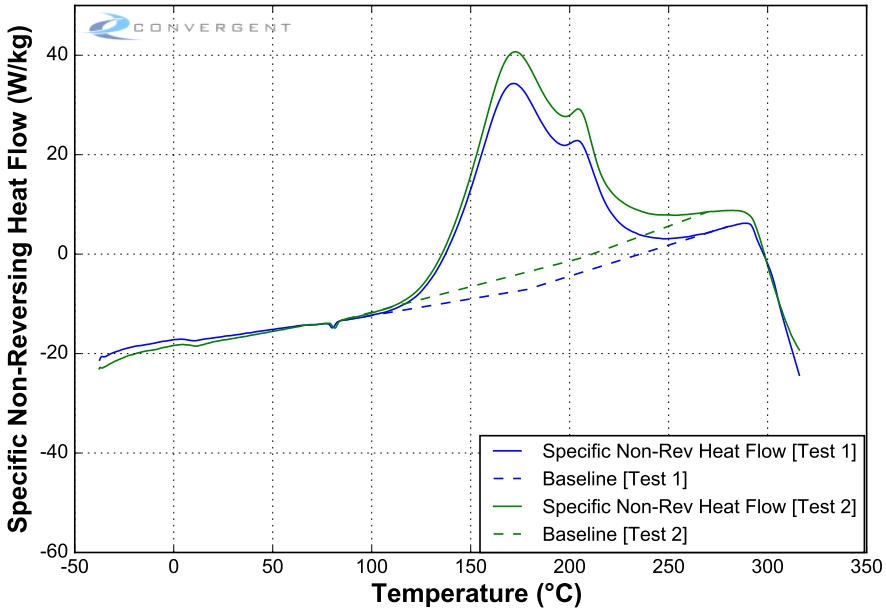

Figure 6.19: Raw Data: Dynamics 1.5°C/min.

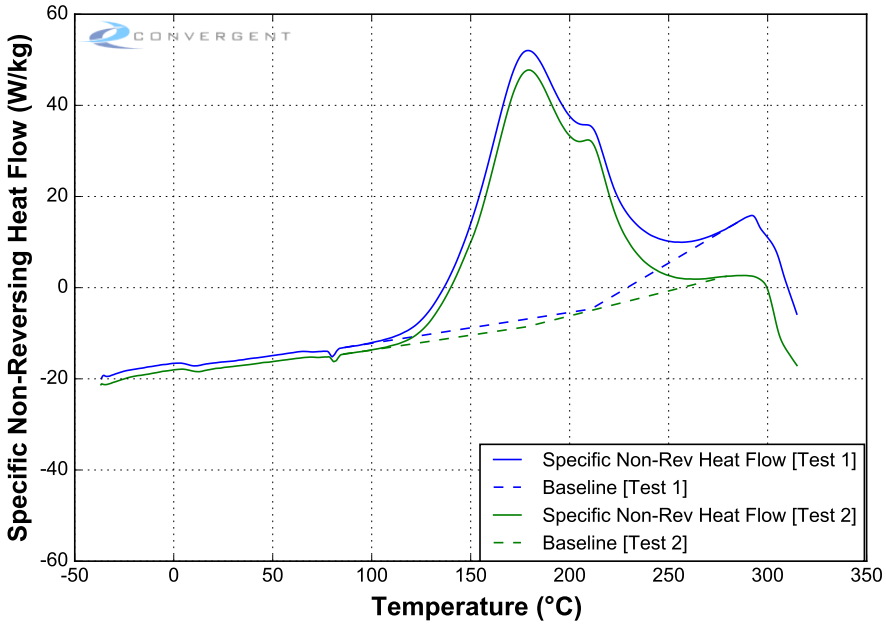

Figure 6.20: Raw Data: Dynamics 2°C/min.

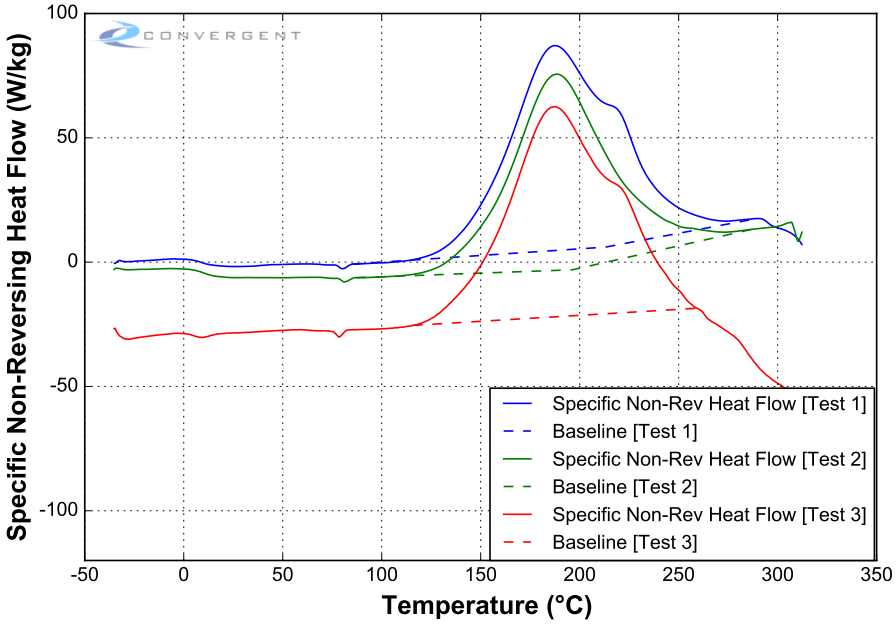

Figure 6.21: Raw Data: Dynamics 3°C/min.

Isothermal Hold Data Comment

Isothermal hold tests display abnormal behavior in reported total heat flow signals. Total heat flow is typically baselined in hold segments but data received from NASA contained significant signal modulation in these regions, preventing effective baselining. The reported non-reversing heat flow, typically a flat line, displayed the characteristic behavior of a total heat flow signal. A software error is suspected which causes mislabeling and subsequent storage of test signals in data files. At the time of reporting, a resolution had not been reached between NASA who provided the test data and the DSC equipment manufacturer. As a result, the reported non-reversing heat flow signals in isothermal hold segments are assumed to be the total heat flow signals.

The raw heat flow and baselines for the isothermal tests are shown in Figures 6.22, 6.23, 6.24, 6.25, 6.26, and 6.27.

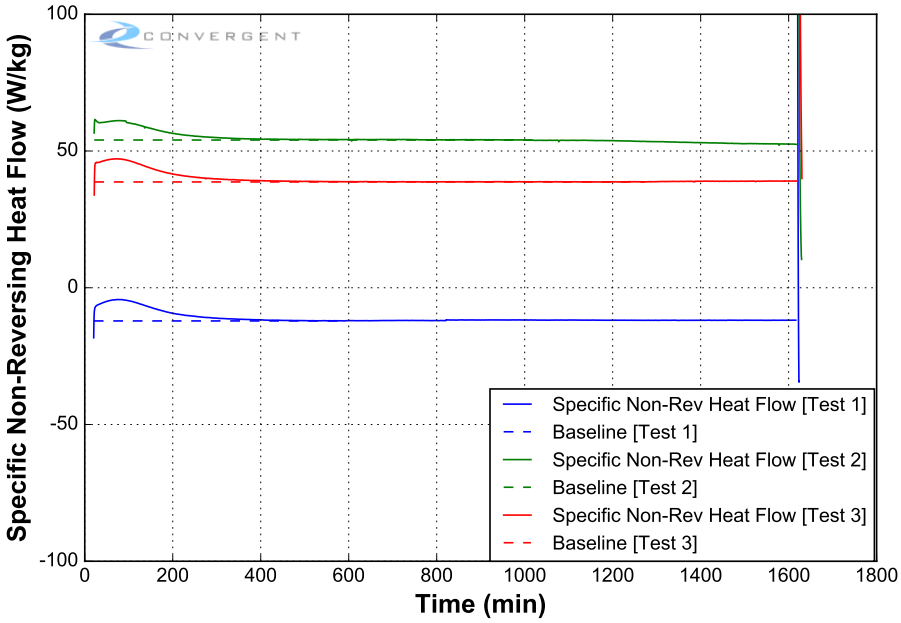

Figure 6.22: Raw Data: Isothermals 125°C [Hold].

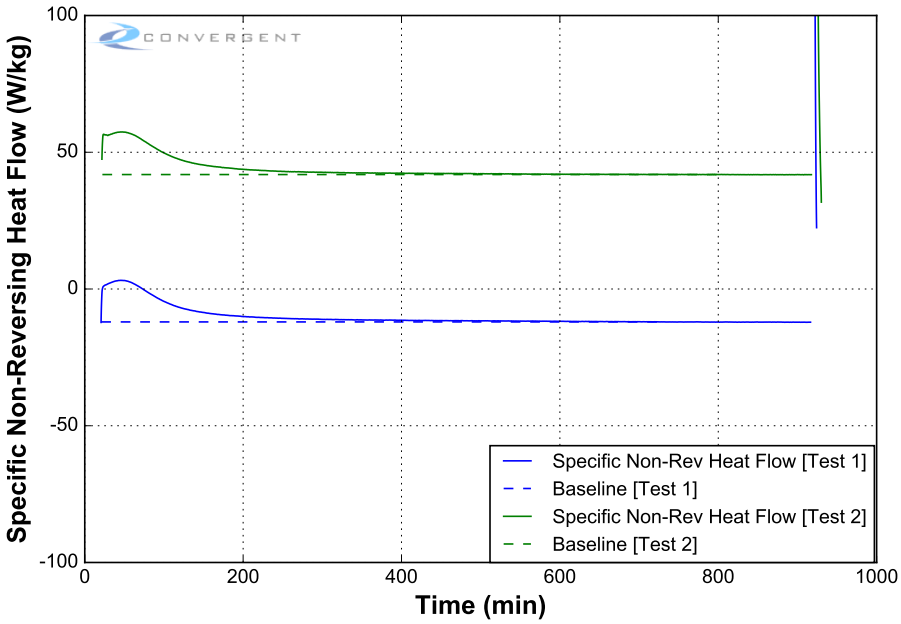

Figure 6.23: Raw Data: Isothermals 140°C [Hold].

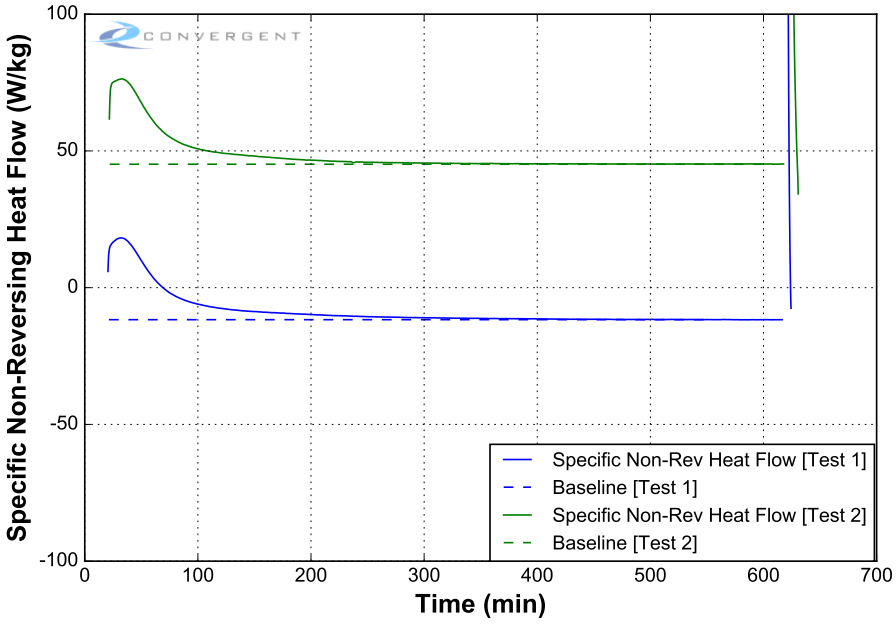

Figure 6.24: Raw Data: Isothermals 155°C [Hold].

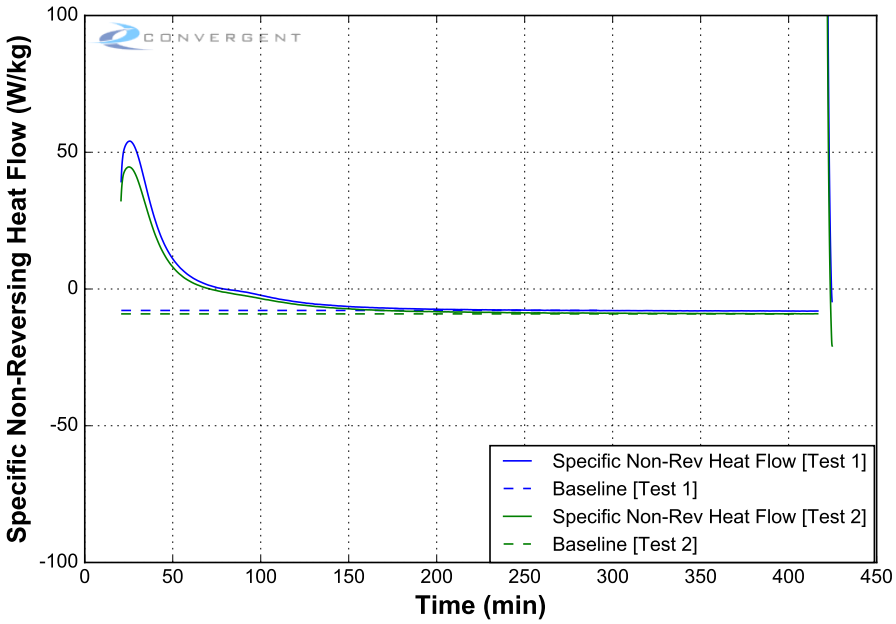

Figure 6.25: Raw Data: Isothermals 170°C [Hold].

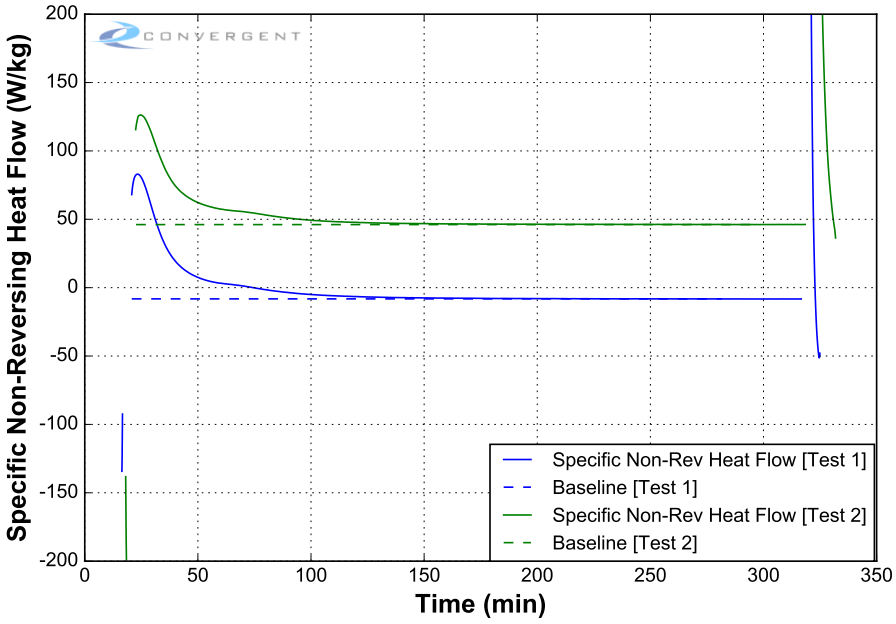

Figure 6.26: Raw Data: Isothermals 180°C [Hold].

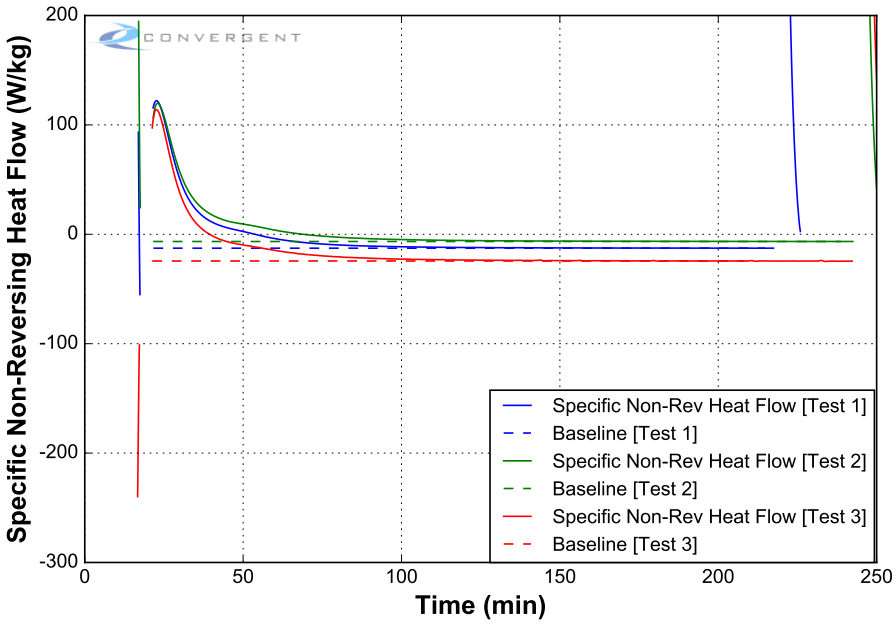

Figure 6.27: Raw Data: Isothermals 190°C [Hold].

Glass Transition Temperature

The step change in the heat capacity response is understood to be the temperature at which the material transitions from glassy to rubbery during heat-up or rubbery to glassy during the cool-down segments of the DSC tests. The midpoint of this transition is defined as the T_g. Several methods to define this point can be used. This analysis used the half height method to define the T_g.

The half height method extends a straight line along the rubbery and glassy heat capacity signals and calculates the vertical midpoint between these. The point where this vertical midpoint intersects the heat capacity signal during the transition is taken as the T_g.

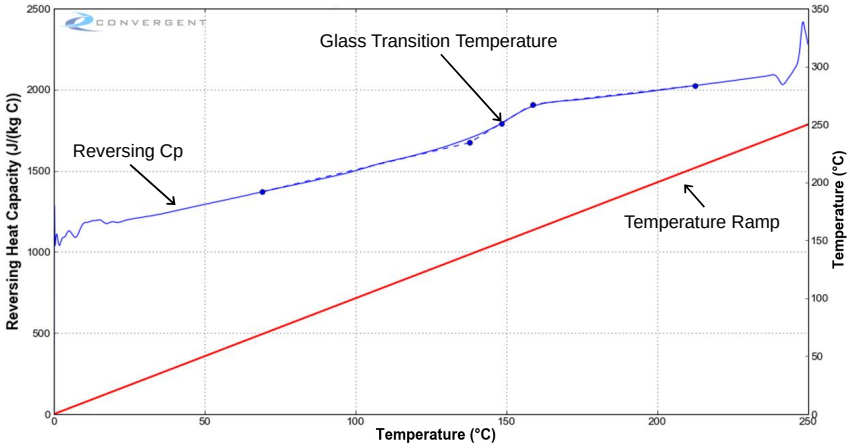

Figure 6.28: Tg Calculation.

The initial T_g of the material was determined using the temperature ramp of dynamic tests. Measuring the final T_g at the end of dynamic tests was not possible since the material degrades due to the high temperature it was exposed to during the test.

The T_g at the end of isothermal hold of an isothermal test was determined using the residual ramp of the test.

The measured T_g and corresponding degree of cure for each test are found in Tables 6.7, 6.8, 6.9, and 6.10 grouped by test type.

Table 6.7: Tg Summary (Dynamic).

Test name	Initial DoC	Initial Tg (°C)
0.5°C/min	0.0520122	8.45321
0.5°C/min	0.0433827	12.0415
0.5°C/min	0.0460386	9.01426
1.0°C/min	0.0442299	10.2719
1.0°C/min	0.0489178	10.9412
1.5°C/min	0.0489929	10.1084
1.5°C/min	0.0457374	11.4869
2.0°C/min	0.0433201	10.0083
2.0°C/min	0.0473754	11.4052
3.0°C/min	0.0466259	8.04954
3.0°C/min	0.0533136	9.30743
3.0°C/min	0.0463592	9.75187

Table 6.8: Tg Summary (Isothermal).

Test name	Post-Hold DoC	Post-Hold Tg (°C)
125°C	0.810175	156.931
125°C	0.792243	158.268
125°C	0.808049	158.237
140°C	0.933935	169.908
140°C	0.915102	171.455
155°C	0.939341	187.307
155°C	0.958322	184.482
170°C	0.969861	197.417
170°C	0.979578	195.762
180°C	0.984384	204.044
180°C	0.985664	207.004
190°C	0.990717	203.664
190°C	0.991163	212.245
190°C	0.929595	205.276

Table 6.9: Tg Summary (Interrupted Isothermal).

Test name	Post-Hold DoC	Post-Hold Tg (°C)
125°C - 75.0 min	0.348093	45.7461
125°C - 160.0 min	0.567586	84.639
125°C - 300.0 min	0.731913	123.374
125°C - 475.0 min	0.778793	142.771
125°C - 700.0 min	0.811177	150.655
140°C - 30.0 min	0.307812	38.5061
140°C - 80.0 min	0.527245	84.9086
140°C - 150.0 min	0.671543	120.634
140°C - 300.0 min	0.800551	158.579
140°C - 475.0 min	0.873	164.408
155°C - 15.0 min	0.28775	39.979
155°C - 50.0 min	0.548362	101.447
155°C - 100.0 min	0.730099	143.493
155°C - 165.0 min	0.816281	169.903
155°C - 250.0 min	0.858522	180.486
180°C - 10.0 min	0.398801	64.723
180°C - 20.0 min	0.594977	96.299
180°C - 35.0 min	0.746187	137.44
180°C - 55.0 min	0.87662	156.49
180°C - 90.0 min	0.913617	182.783

Table 6.10: Tg Summary (Cure Cycle).

Test name	Post-Hold DoC	Post-Hold Tg (°C)
M30S F7-PW-B1-DSC-MRCC1-A-1	0.137863	16.0339
M30S F7-PW-B1-DSC-MRCC1-A-2	0.0999183	16.0961
M30S F7-PW-B1-DSC-MRCC1-B-1	0.304063	45.4623
M30S F7-PW-B1-DSC-MRCC1-B-2	0.316647	47.5405
M30S F7-PW-B1-DSC-MRCC1-C-1	0.472139	61.5734
M30S F7-PW-B1-DSC-MRCC1-C-2	0.43832	64.9411
M30S F7-PW-B1-DSC-MRCC1-D-1	0.605726	117.68
M30S F7-PW-B1-DSC-MRCC1-D-2	0.684186	121.007
M30S F7-PW-B1-DSC-MRCC1-E-1	0.906742	200.713
M30S F7-PW-B1-DSC-MRCC1-E-2	0.915539	196.698

6.7. Cure Kinetics Model Fit

Glass Transition Temperature

The DiBenedetto equation was used to select parameter values to fit the T_g and DoC data. The DiBenedetto equation is shown below.

$$T_g = T_g^0 + \frac{\lambda x}{1-(1-\lambda)x}\left(T_g^\infty - T_g^0\right)$$

The DiBenedetto fit is shown in Fig. 6.29. The model constants are given in the subsequent table.

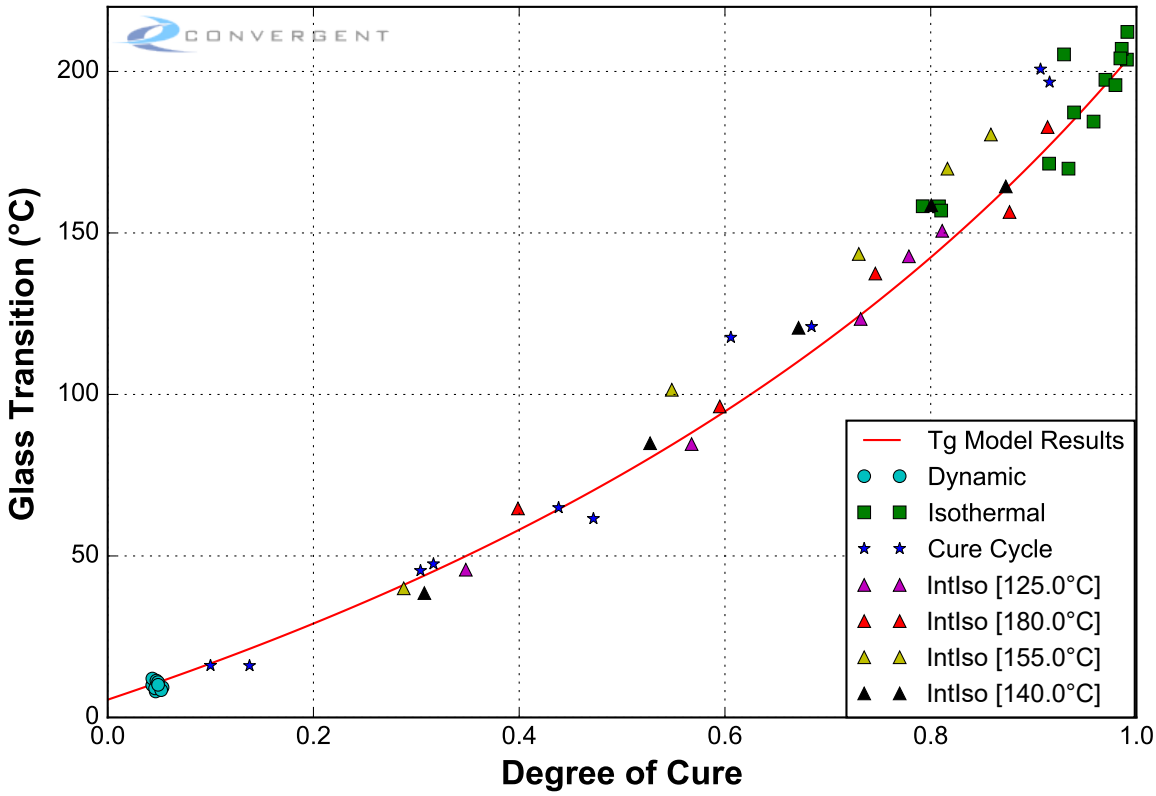

Figure 6.29: Tg vs DoC.

Cure Kinetics

The experimental data was fit using Cure Kinetics Model 24. Two reaction terms were used. The first reaction term represents the chemical cross-linking reaction. The second reaction term represents behavior after vitrification, where the cure rate is limited due to diffusion.

Cure kinetics model 24 is defined by:

$$\dot{x} = \left(\sum_{i=1}^{n} \frac{1}{\dot{x}_i} \right)^{-1}$$

$$\dot{x}_i = A_i e^{-\frac{B_i}{C_i T - D_i T_g + e_i}}$$

$$T_g = T_g^0 + \frac{\lambda x}{1 - (1 - \lambda)x} \left(T_g^\infty - T_g^0 \right) + CtoK$$

Note: CtoK is a conversion factor from degrees Celsius to kelvin.

Where the fit parameters are defined in Table 6.11.

Table 6.11: Cure Kinetics Model Parameters.

Constant	Value	Units
HR	370000	J/kg
T_g^0	5.5	$°C$
T_g^∞	207.0	$°C$
λ	0.53	–
$Initial\ DoC$	0.001	–

Reaction	A	B	C	D	E
1	-	-	1	0	0
2	1000	1500	1	1	-

The following reaction terms are defined as a function of degree of cure in Figures 6.30 and 6.31.

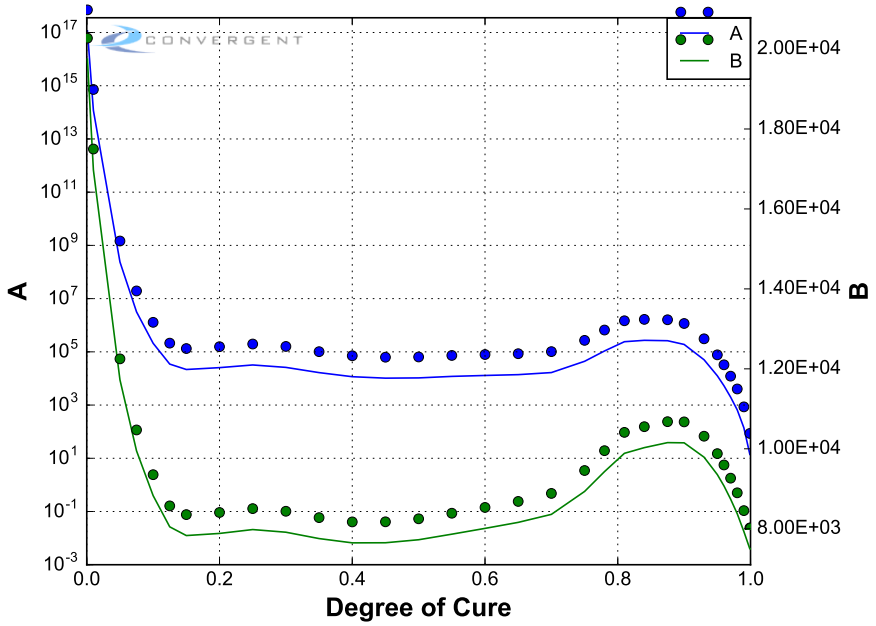

Figure 6.30: CK Model Reaction 1.

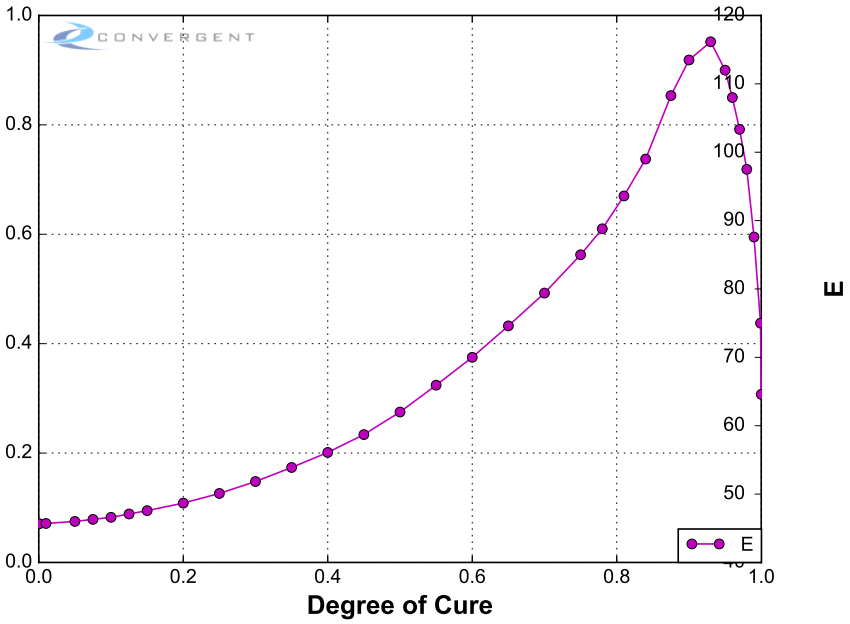

Figure 6.31: CK Model Reaction 2.

The model was fit in the space of the natural logarithm of the cure rate versus inverse absolute temperature for a given degree of cure. Overlays of the model and test data are shown in Figures 6.32 to 6.40.

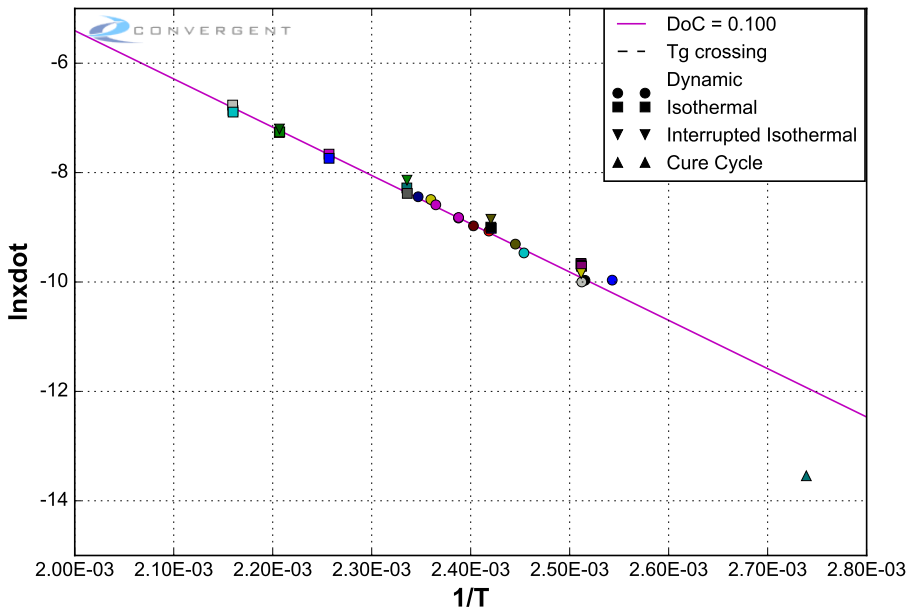

Figure 6.32: DoC=0.100.

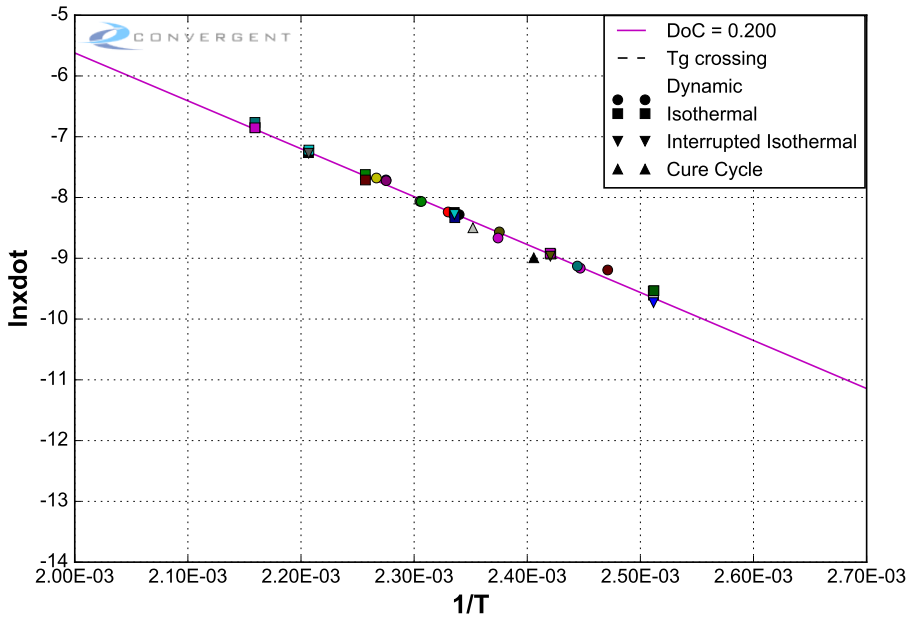

Figure 6.33: DoC=0.200.

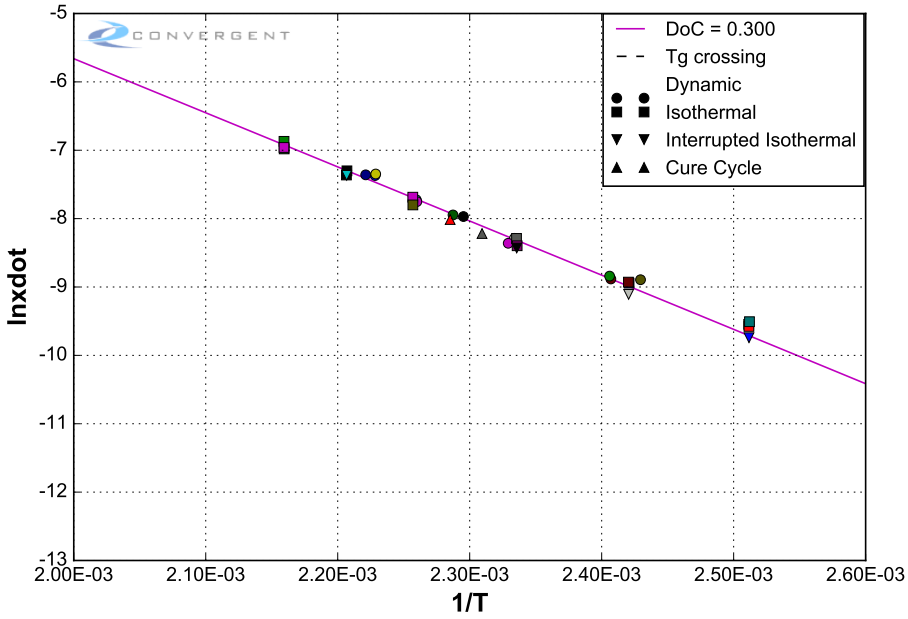

Figure 6.34: DoC=0.300.

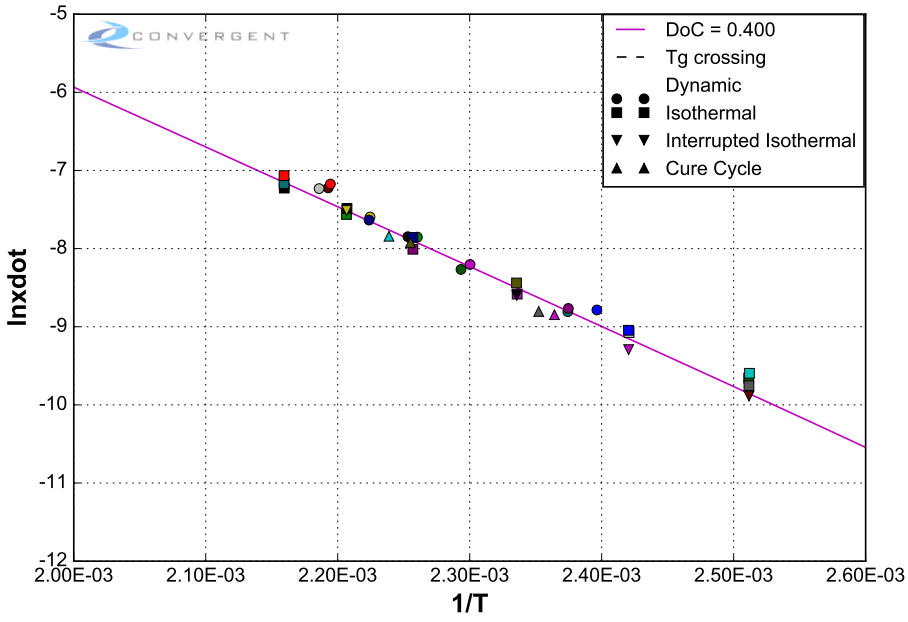

Figure 6.35: DoC=0.400.

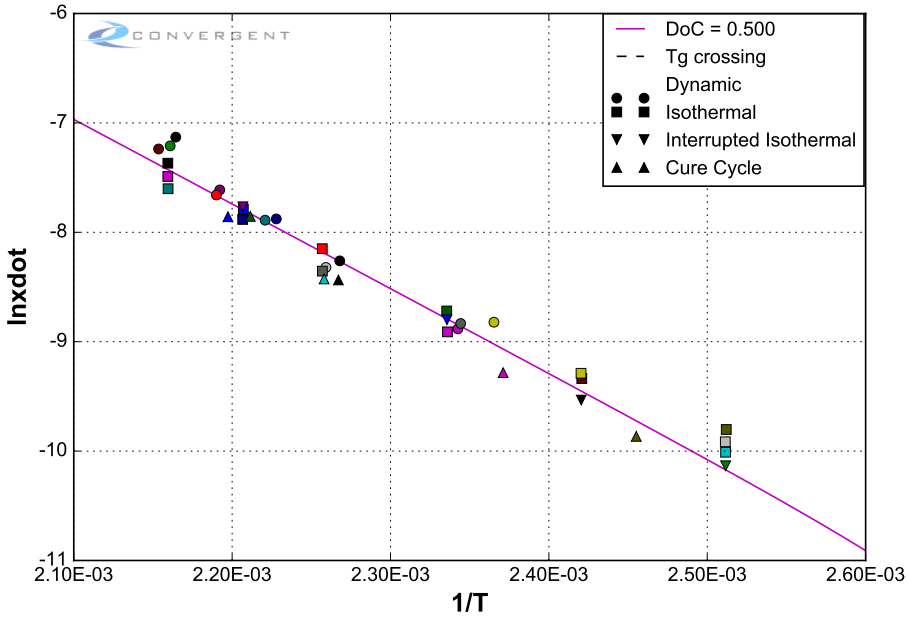

Figure 6.36: DoC=0.500.

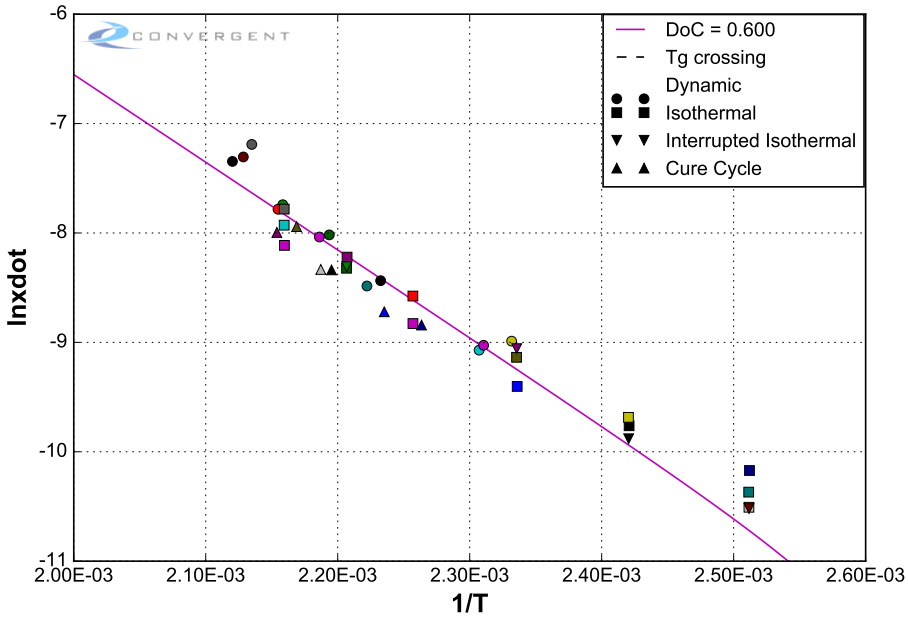

Figure 6.37: DoC=0.600.

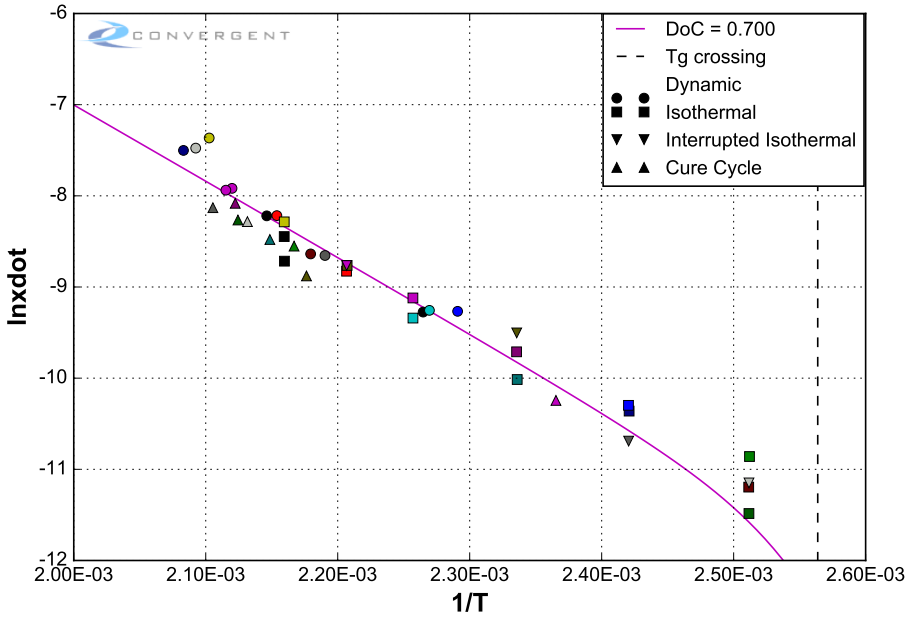

Figure 6.38: DoC=0.700.

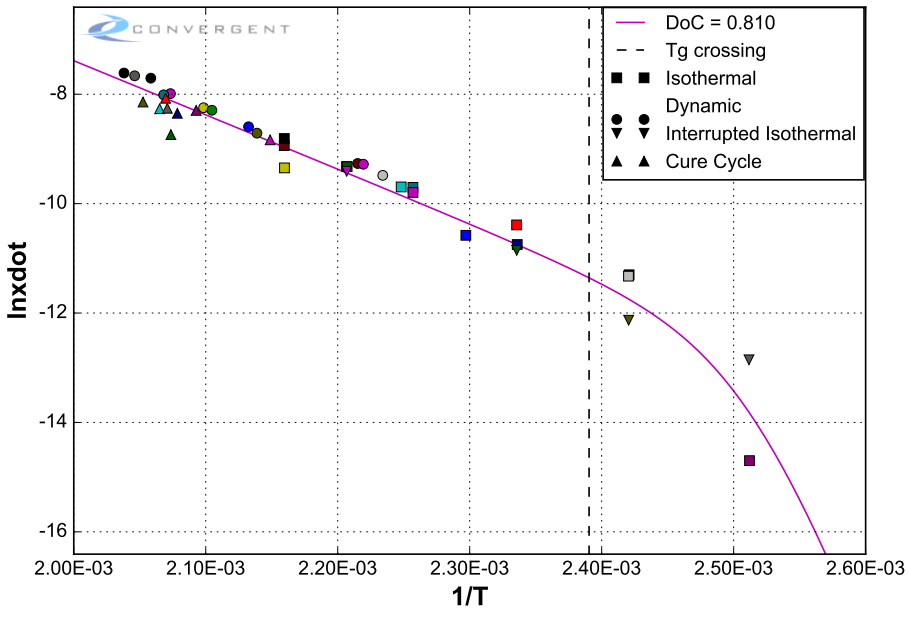

Figure 6.39: DoC=0.810.

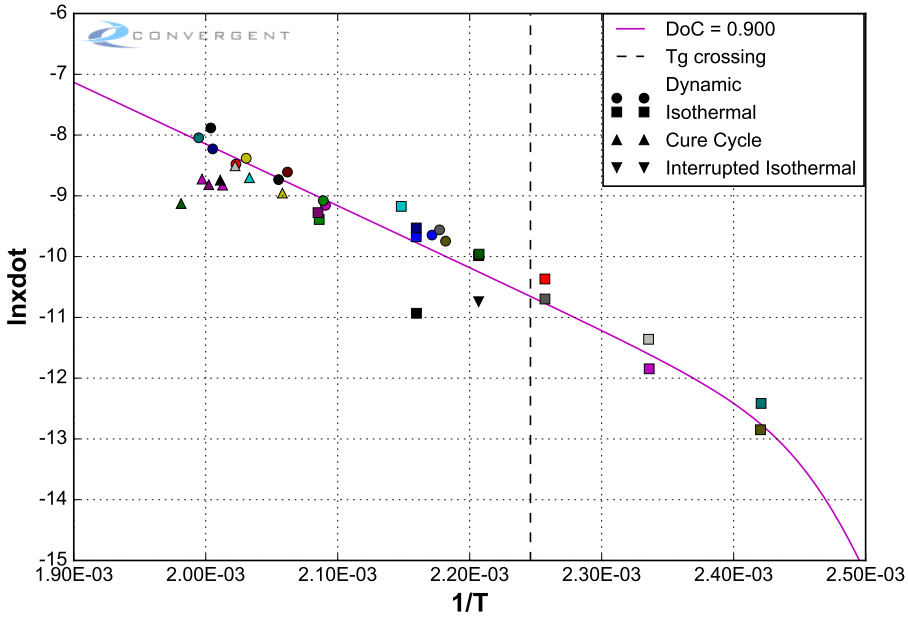

Figure 6.40: DoC=0.900.

6.8. Cure Kinetics Quality of Fit

A comparison of the degree of cure and cure rate from experimental data and as calculated by the model are shown in Figures 6.41 to 6.57.

Dynamic Tests

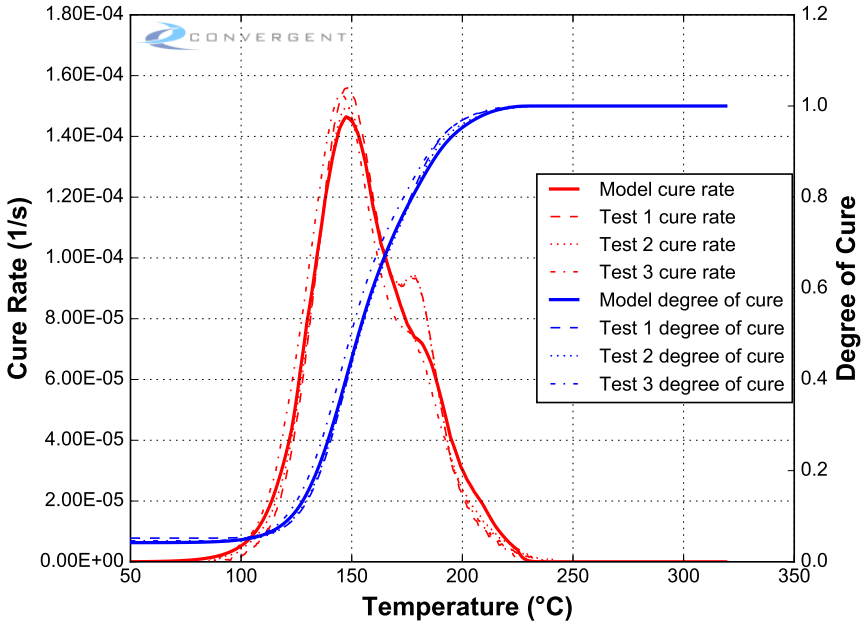

Figure 6.41: Model Prediction: Dynamics 0.5°C/min.

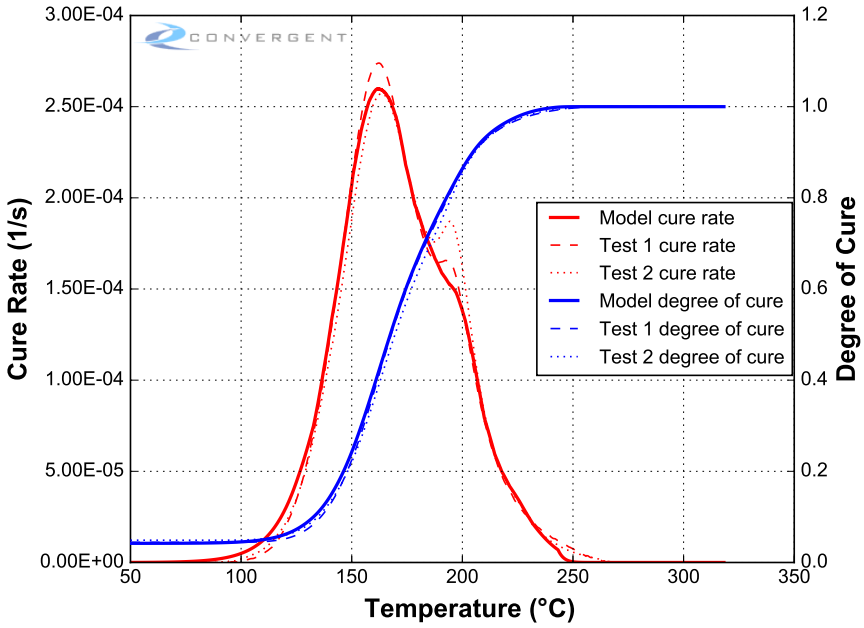

Figure 6.42: Model Prediction: Dynamics 1°C/min.

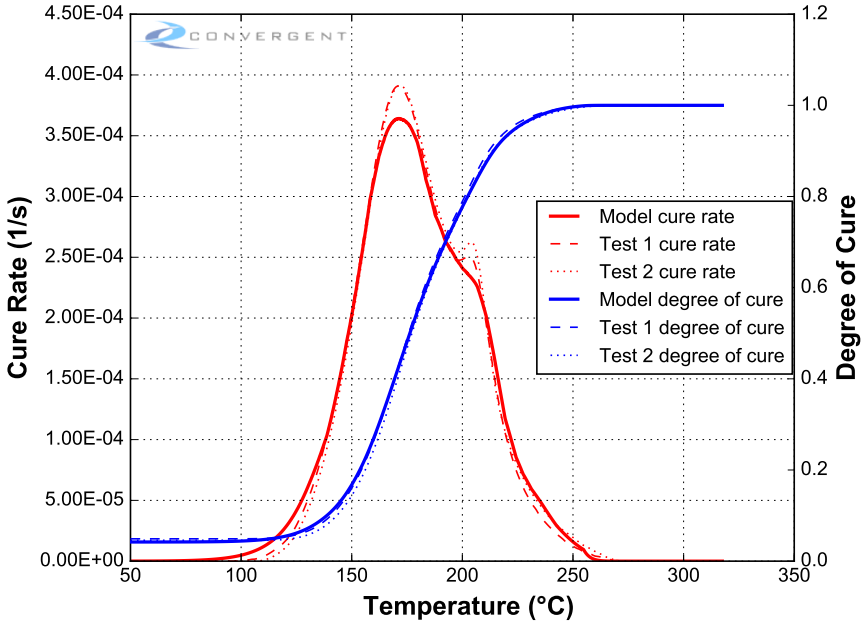

Figure 6.43: Model Prediction: Dynamics°1.5 C/min.

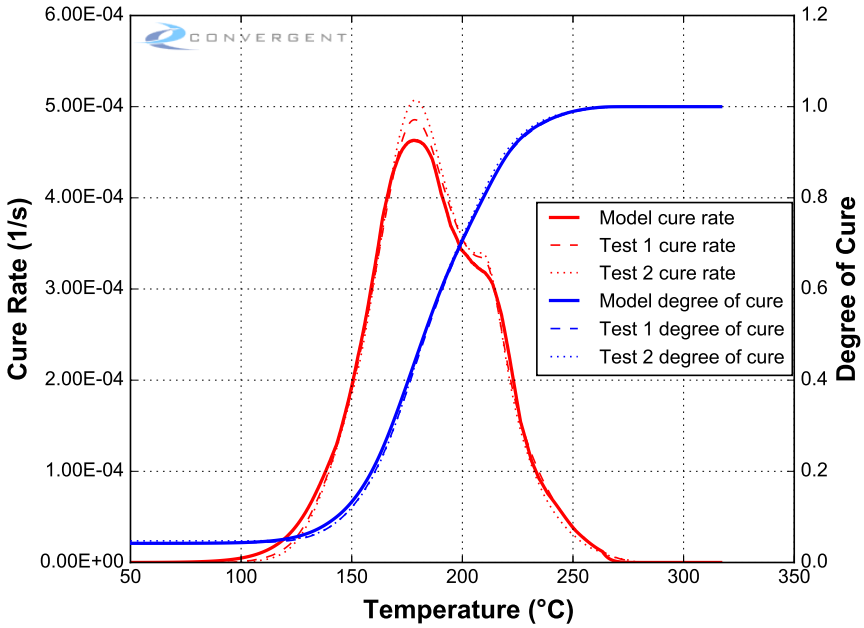

Figure 6.44: Model Prediction: Dynamics 2°C/min.

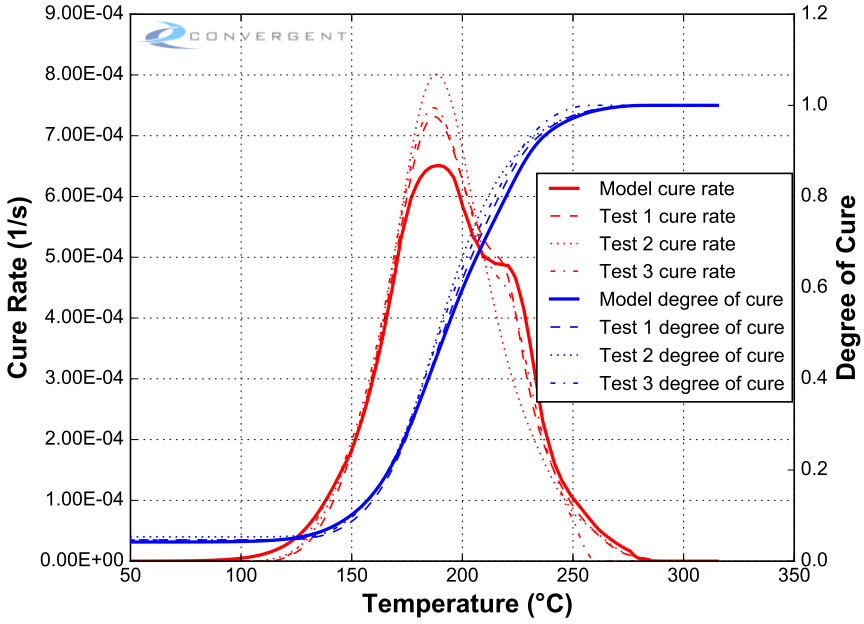

Figure 6.45: Model Prediction: Dynamics 3°C/min.

Isothermal Tests: Hold Segment

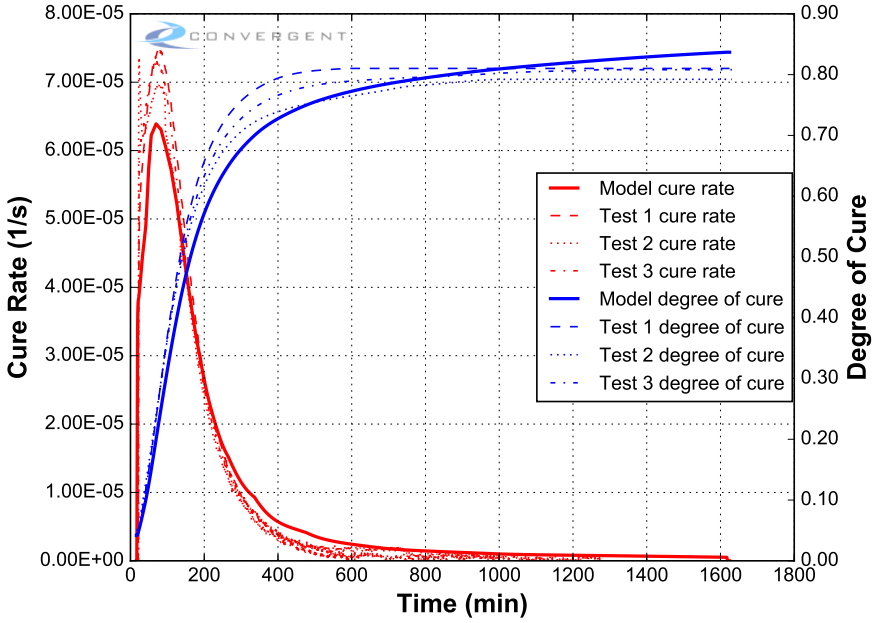

Figure 6.46: Model Prediction: Isothermals 125°C [Hold].

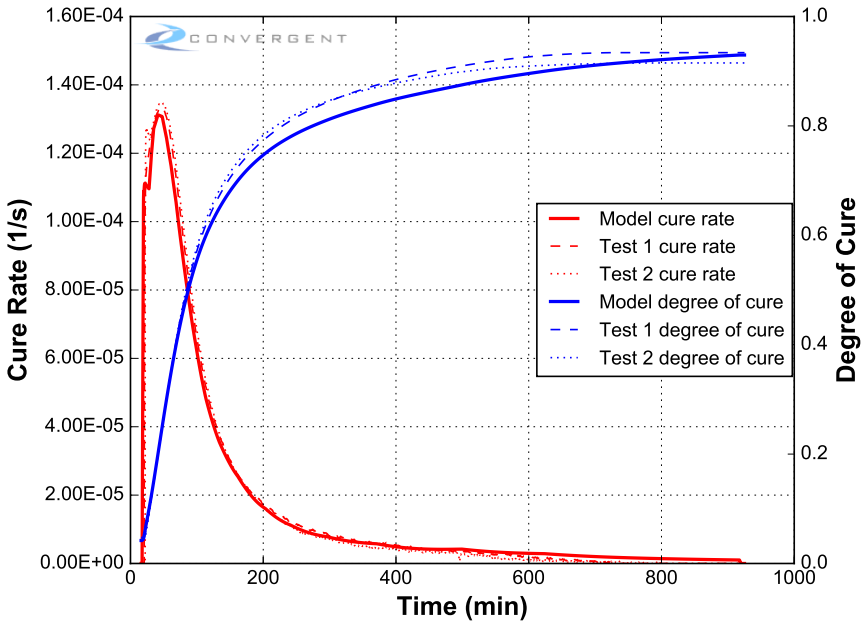

Figure 6.47: Model Prediction: Isothermals 140°C [Hold].

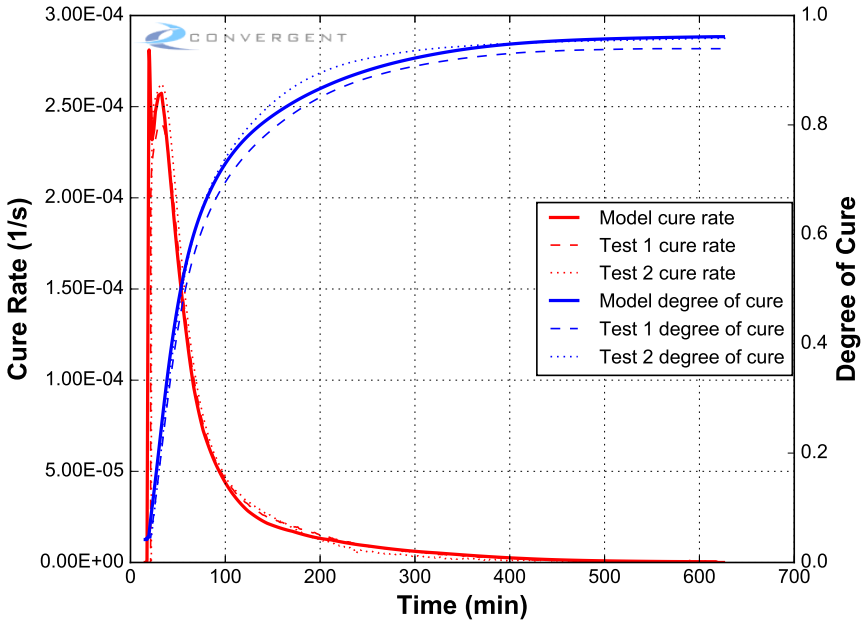

Figure 6.48: Model Prediction: Isothermals 155°C [Hold].

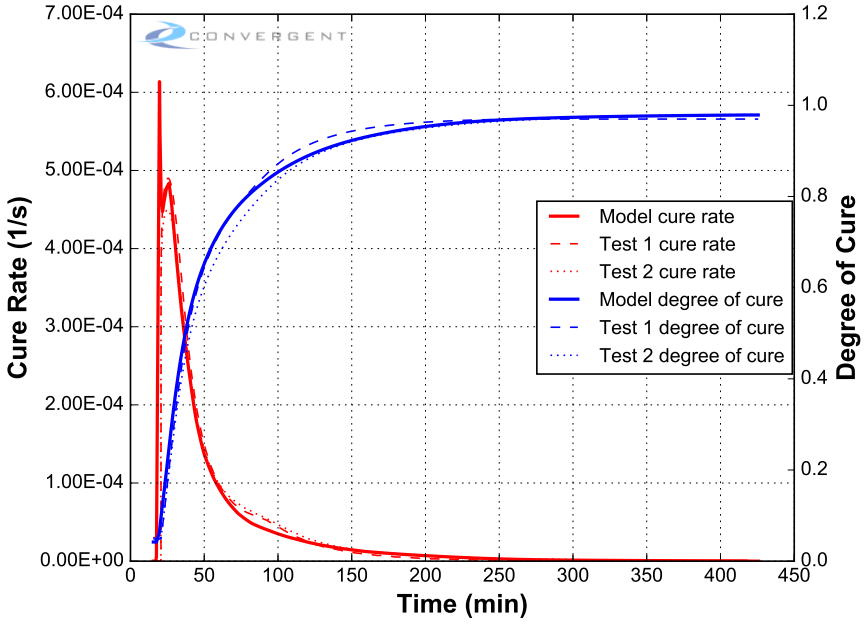

Figure 6.49: Model Prediction: Isothermals 170°C [Hold].

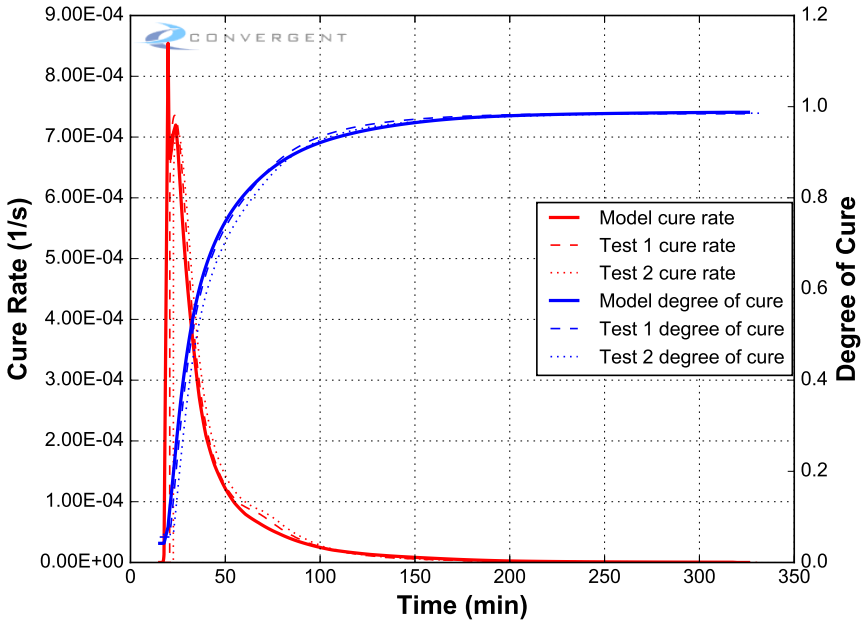

Figure 6.50: Model Prediction: Isothermals 180°C [Hold].

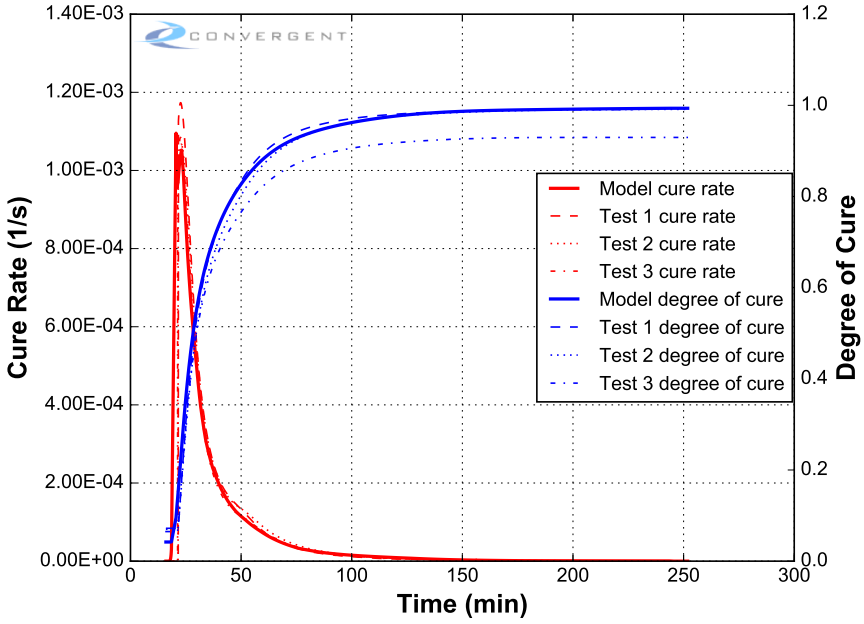

Figure 6.51: Model Prediction: Isothermals 190°C [Hold].

Isothermal Hold Model Comment

Isothermal hold model predictions contain an abnormal spike in the cure rate profiles located in the rapid ramp up to the peak test cure rate at the beginning of each test. Some isothermal tests feature a similar spike in cure rate at this point, although at a lesser magnitude than the model prediction. This spike is a result of bifurcation in instantaneous cure rate measurements at very early degrees of cure between dynamic and isothermal tests of the three tested material forms. To capture the curing behavior of the neat resin and prepreg forms, the average response at the early stages of cure was fit. This results in the cure rate spike when predicting the PW B1 form shown. Note that the effect on degree of cure predictions is negligible.

Isothermal Tests: Ramp Segment

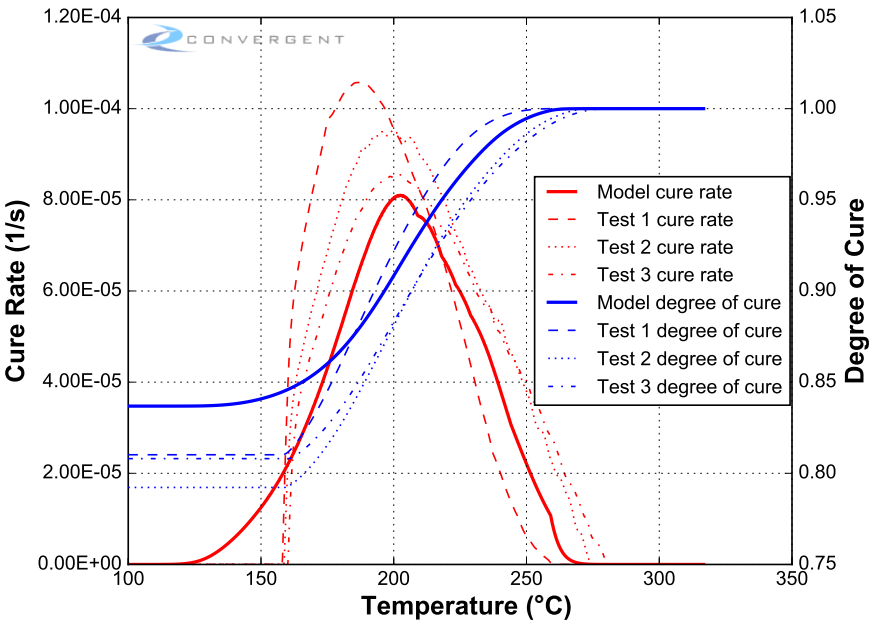

Figure 6.52: Model Prediction: Isothermals 125°C [Ramp].

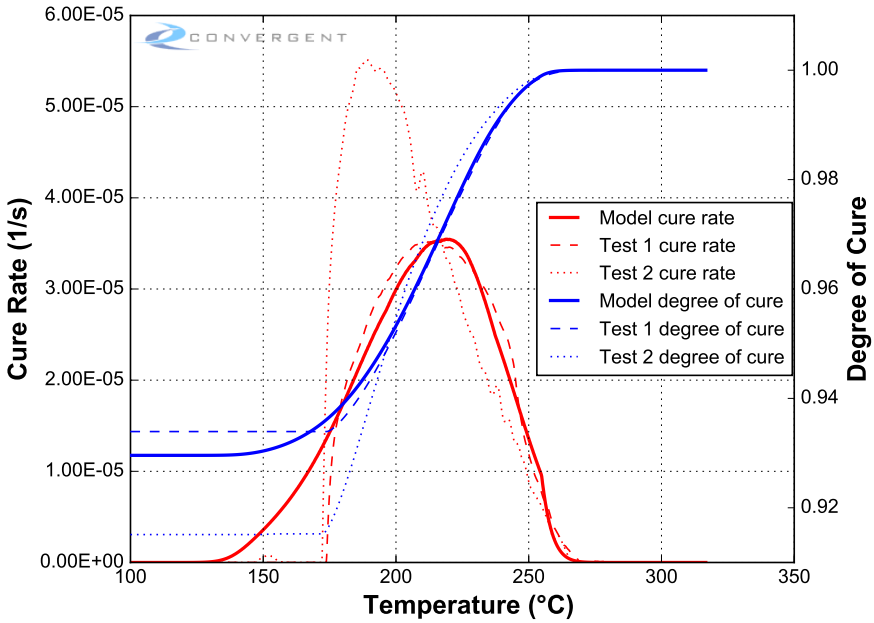

Figure 6.53: Model Prediction: Isothermals 140°C [Ramp].

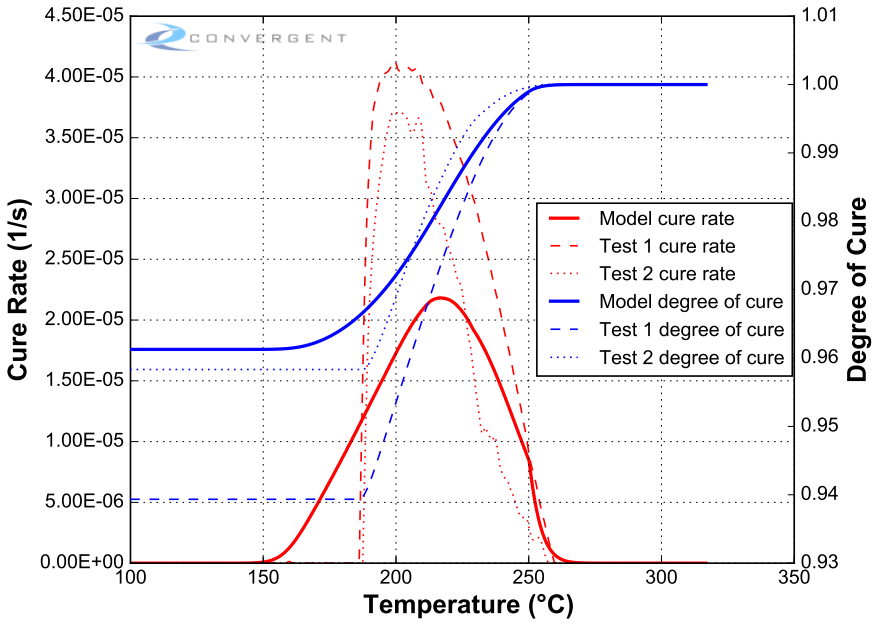

Figure 6.54: Model Prediction: Isothermals 155°C [Ramp].

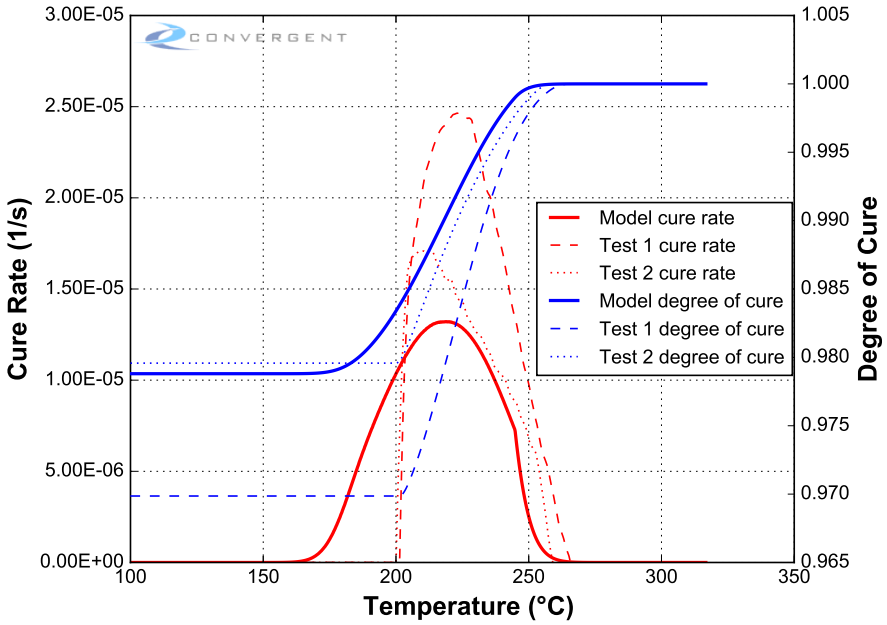

Figure 6.55: Model Prediction: Isothermals 170°C [Ramp].

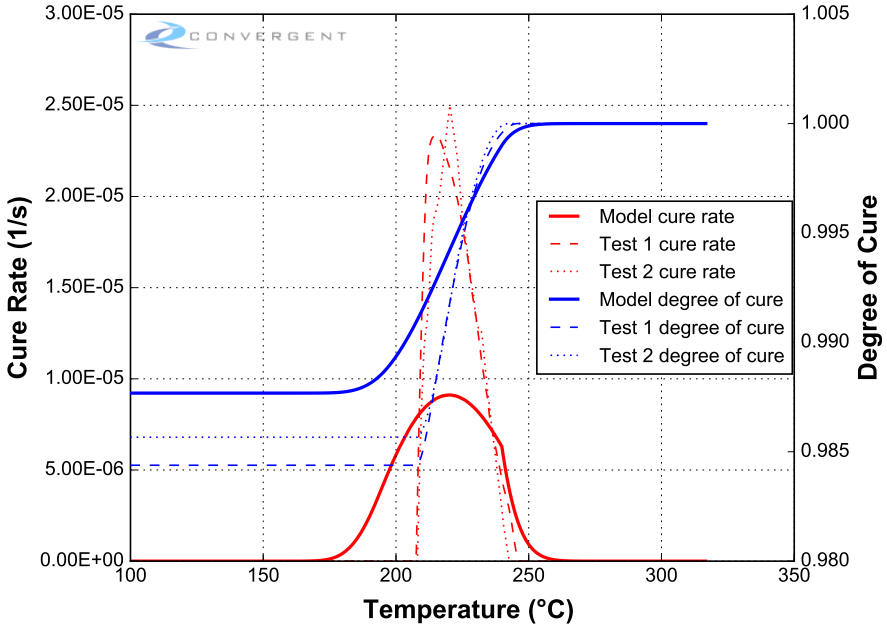

Figure 6.56: Model Prediction: Isothermals 180°C [Ramp].

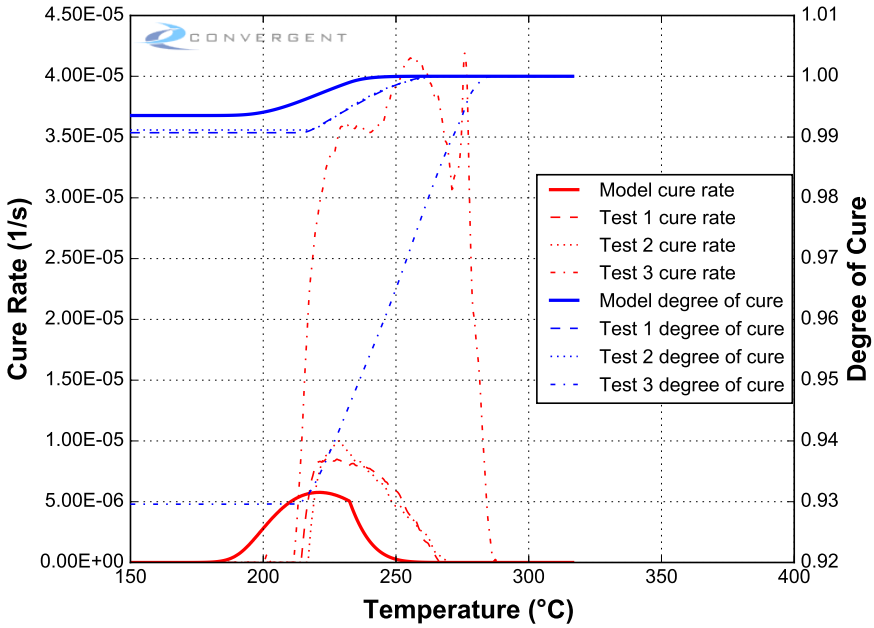

Figure 6.57: Model Prediction: Isothermals 190°C [Ramp].

A summary of all overlaid test categories are shown in Figures 6.58 to 6.61.

Dynamic Tests Overlay

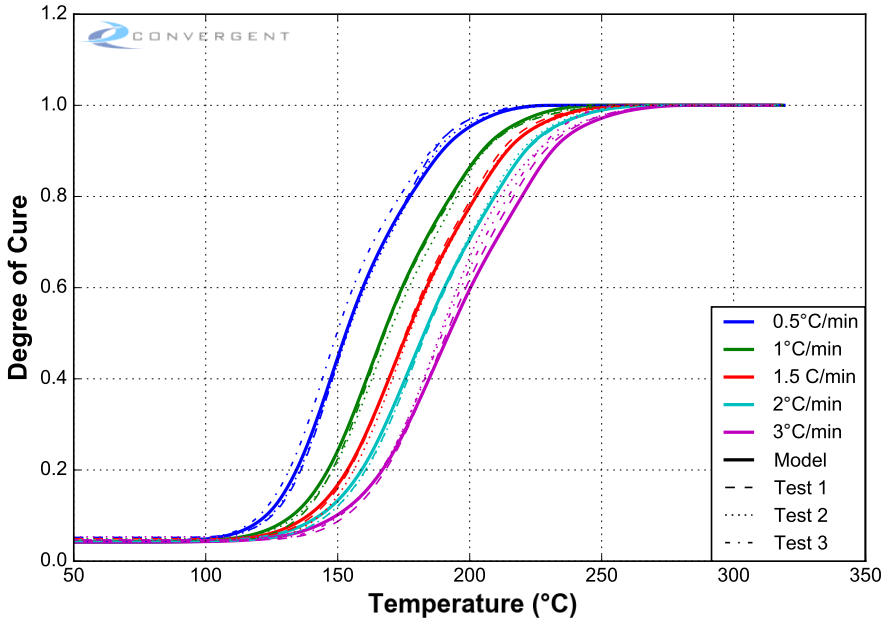

Figure 6.58: Model prediction: Degree of Cure (Dynamics).

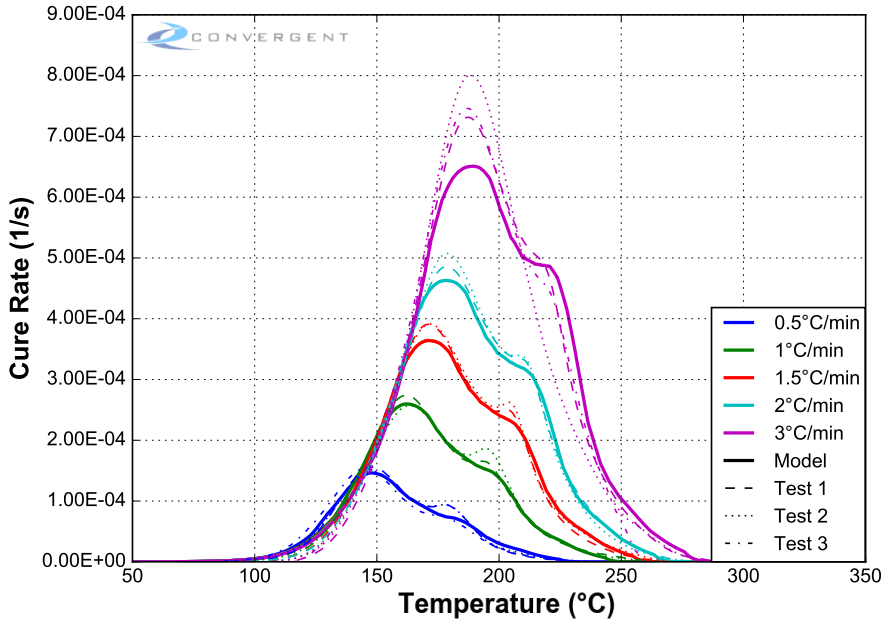

Figure 6.59: Model prediction: Cure Rate (Dynamics).

Isothermal Tests Overlay

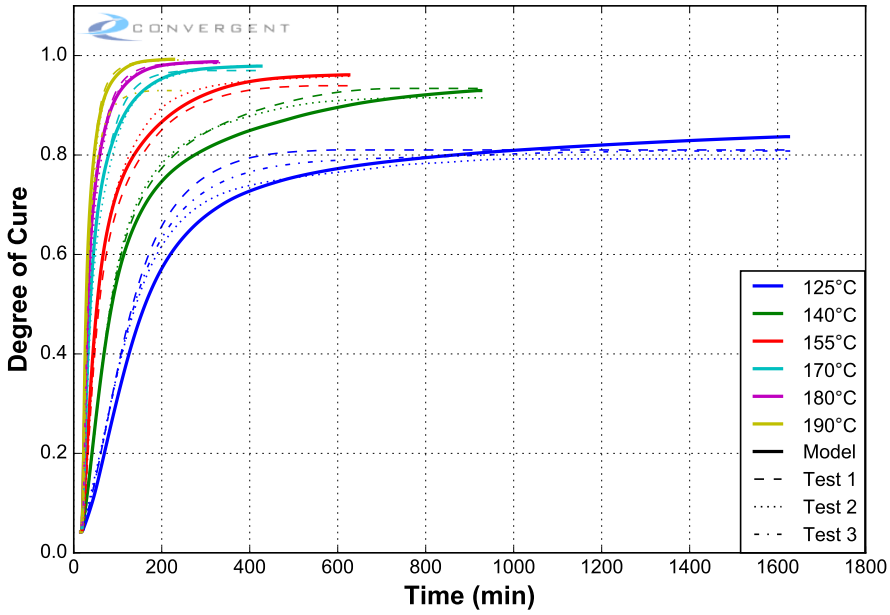

Figure 6.60: Model prediction: Degree of Cure (Isothermals).

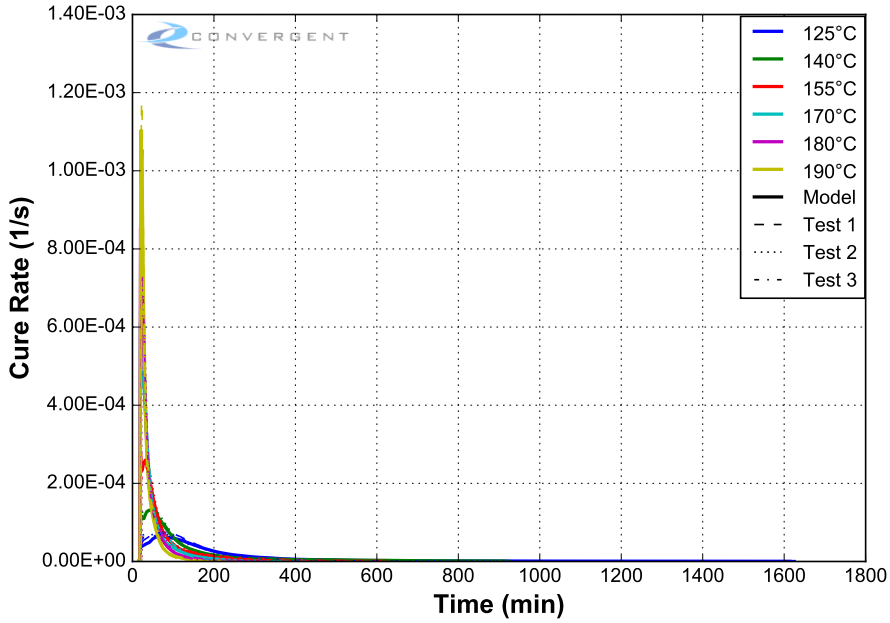

Figure 6.61: Model prediction: Cure Rate (Isothermals).

Interrupted Isothermal Tests

A comparison of glass transition temperatures for the interrupted isothermal tests is shown in Figures 6.62 to 6.65.

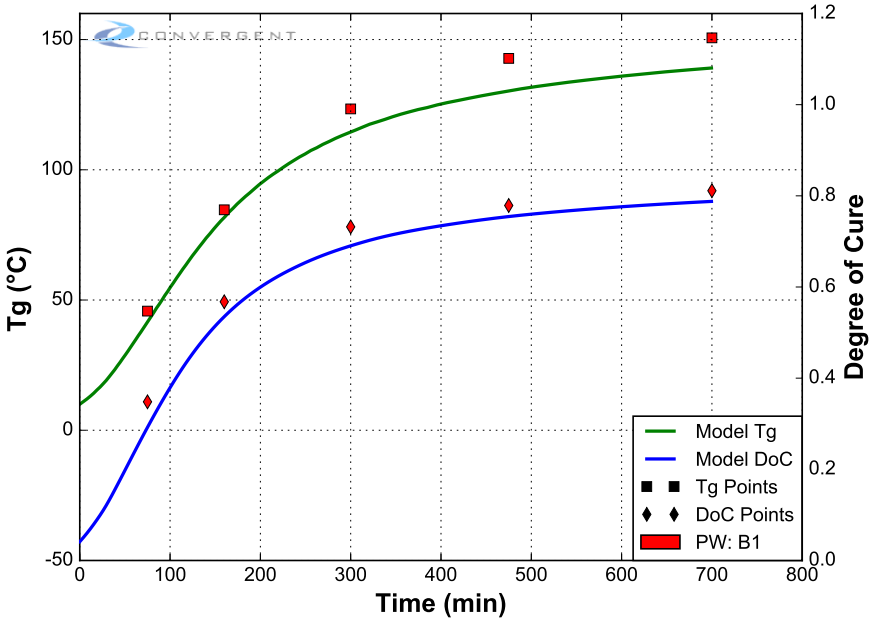

Figure 6.62: Model Prediction: Interrupted isothermals 125°C.

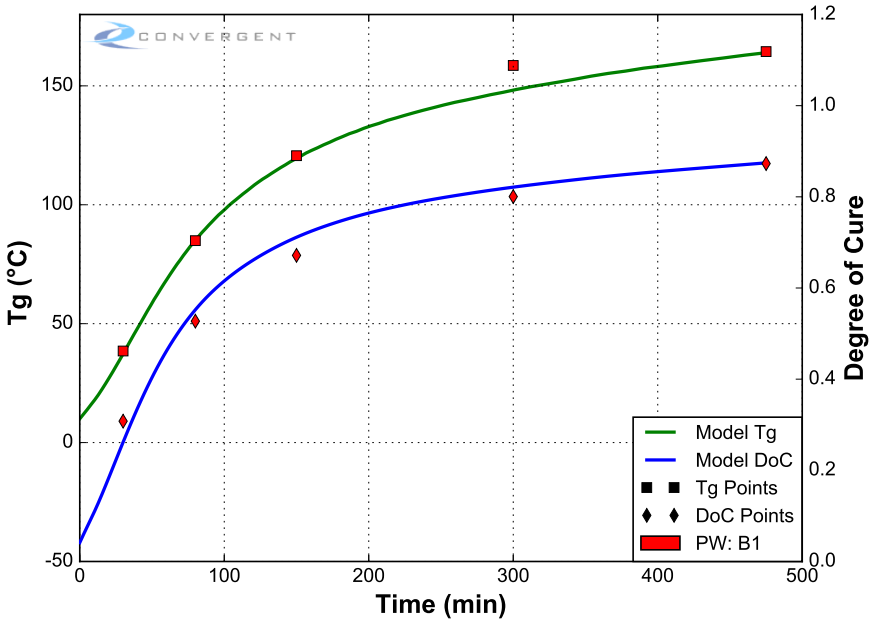

Figure 6.63: Model Prediction: Interrupted isothermals 140°C.

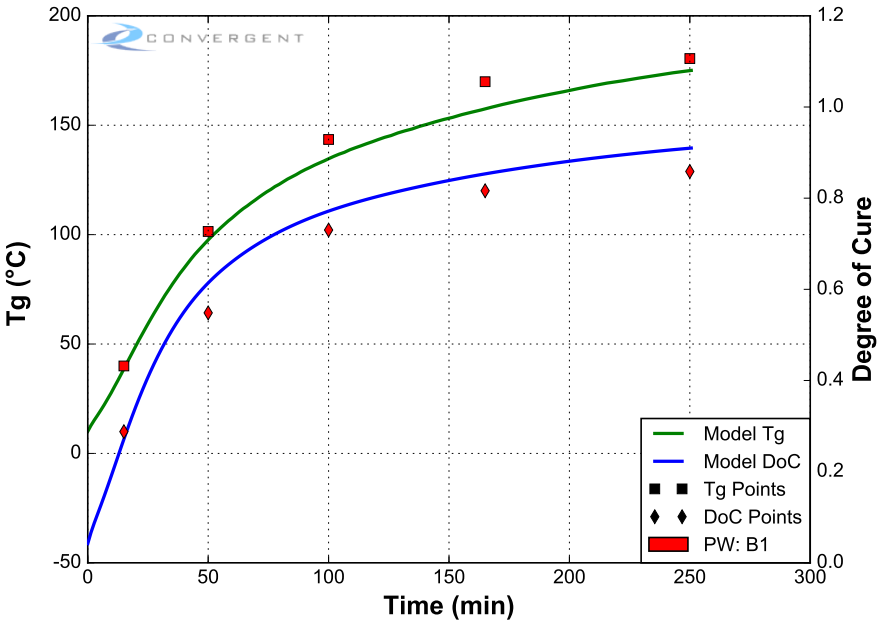

Figure 6.64: Model Prediction: Interrupted isothermals 155°C.

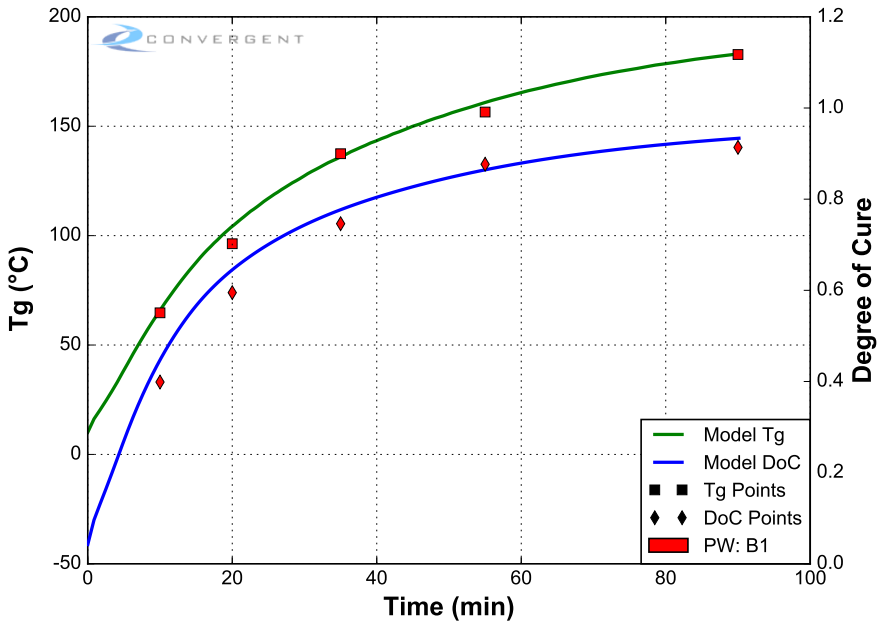

Figure 6.65: Model Prediction: Interrupted isothermals 180°C.

6.9. Cure Kinetics Form and Batch Verification

The model was compared against each of the dynamic tests performed during the form and batch screening tests. The comparison in Figures 6.66 to 6.83 shows the applicability of the model to other forms and/or batches of the same raw material.

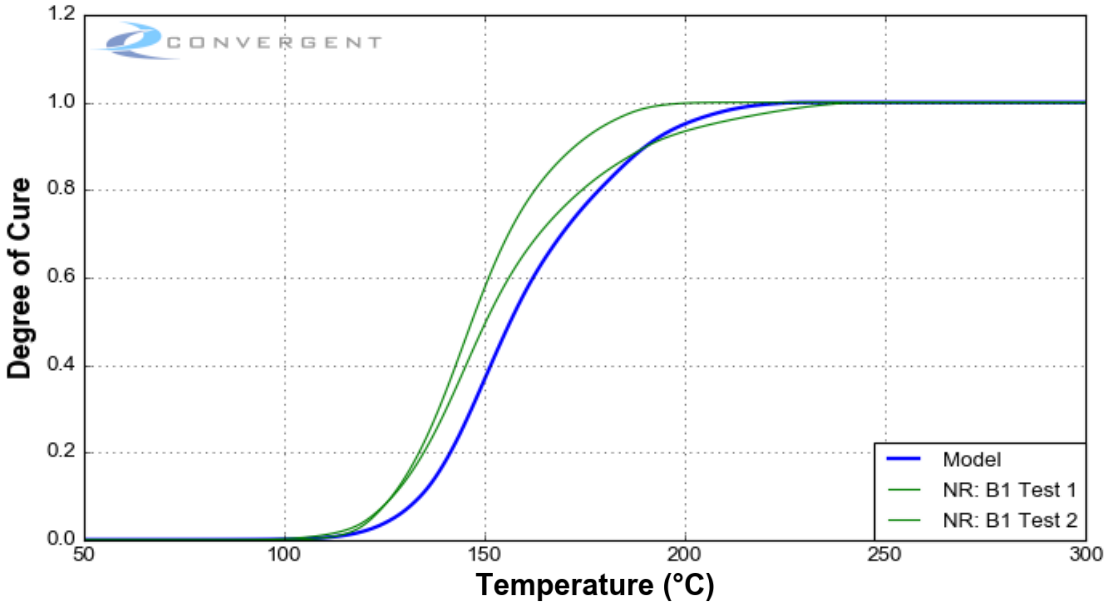

Figure 6.66: NR Form Comparison: Degree of Cure (Dynamics 0.5°C/min).

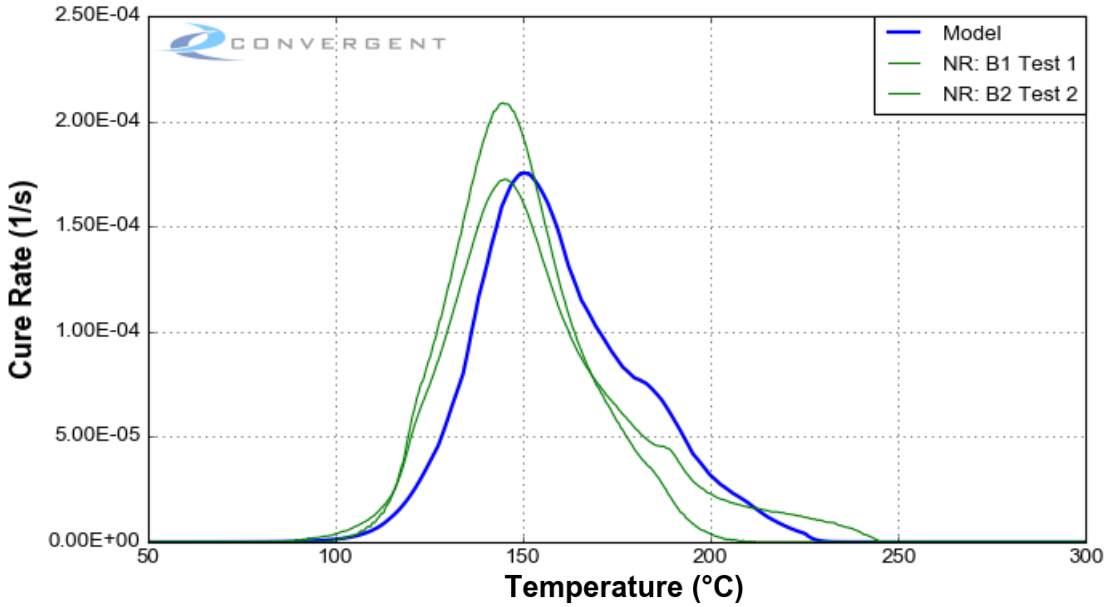

Figure 6.67: NR Form Comparison: Cure Rate (Dynamics 0.5°C/min).

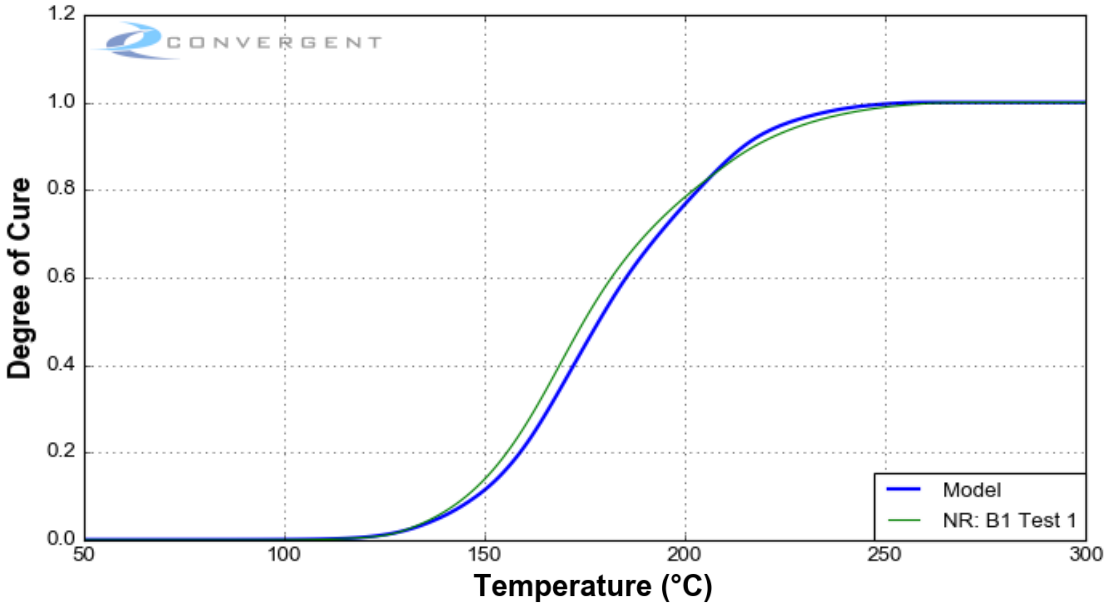

Figure 6.68: NR Form Comparison: Degree of Cure (Dynamics 1.5°C/min).

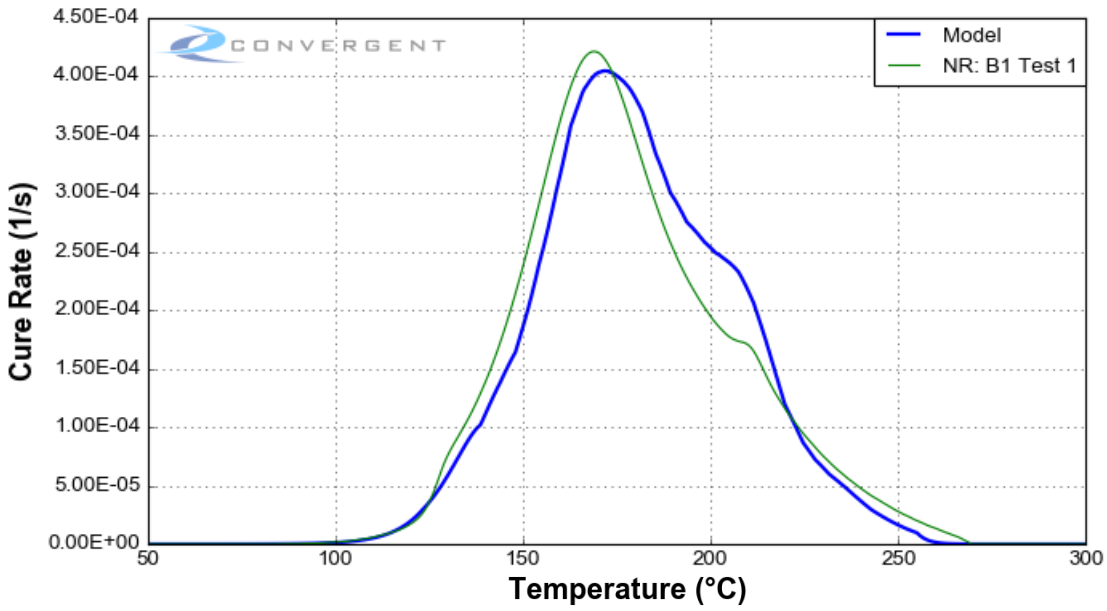

Figure 6.69: NR Form Comparison: Cure Rate (Dynamics 1.5°C/min).

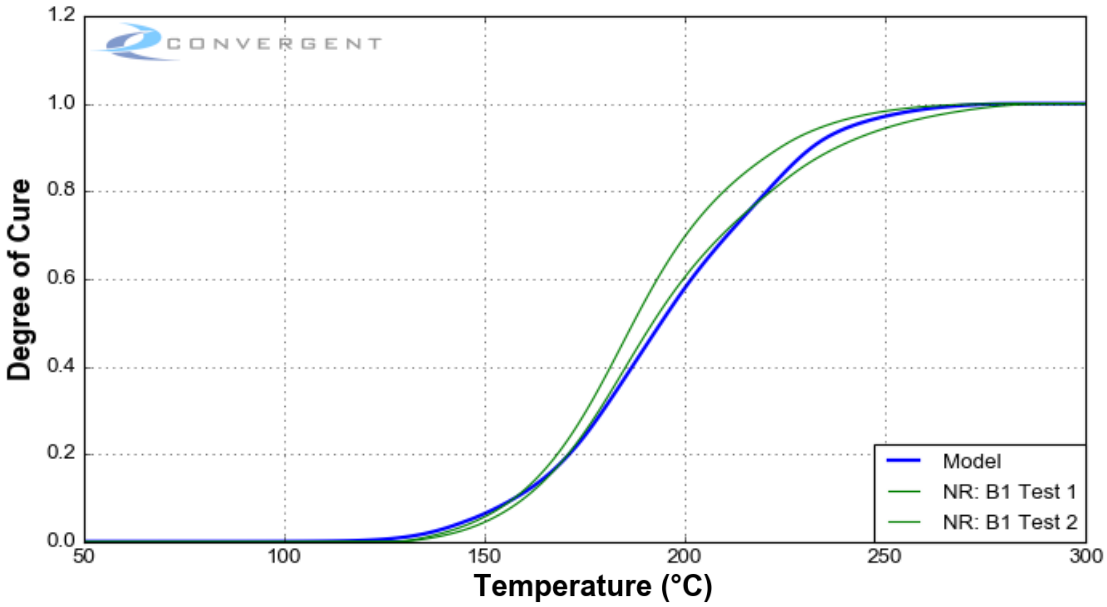

Figure 6.70: NR Form Comparison: Degree of Cure (Dynamics 3°C/min).

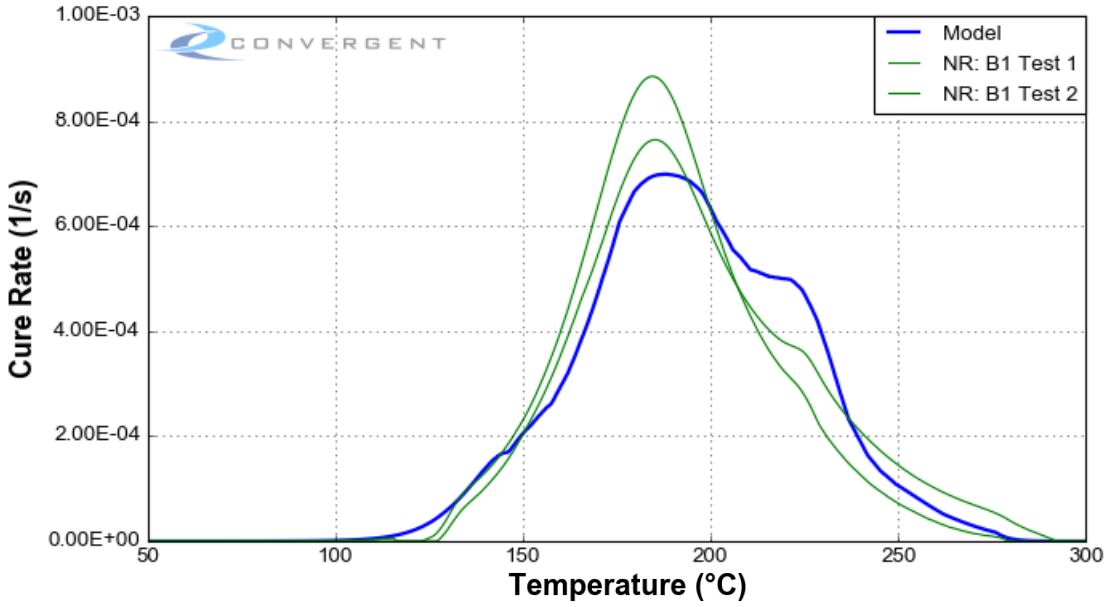

Figure 6.71: NR Form Comparison: Cure Rate (Dynamics 3°C/min).

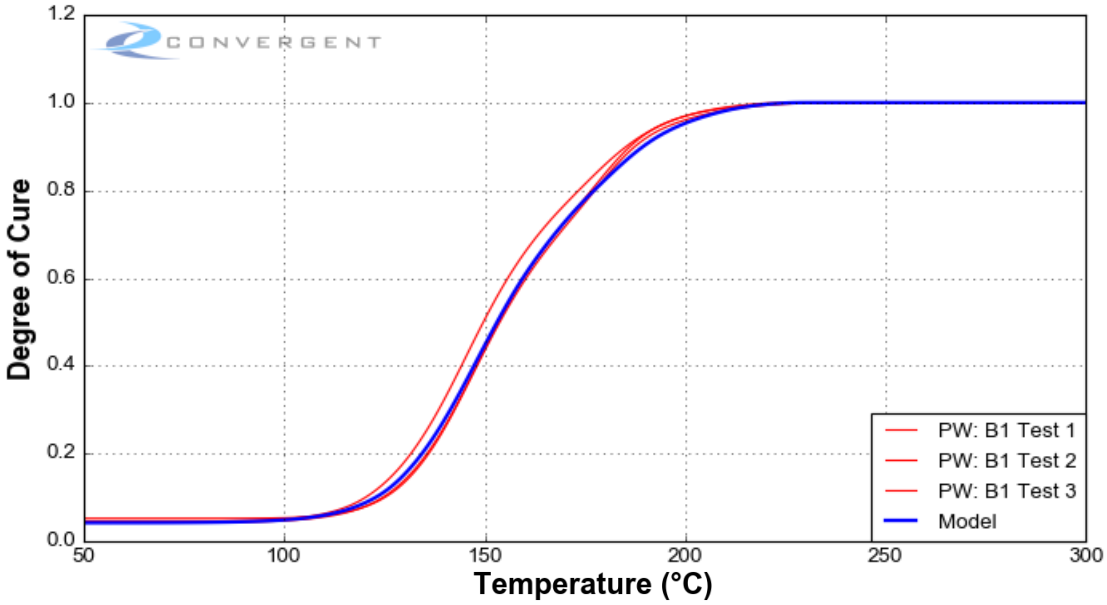

Figure 6.72: PW Form Comparison: Degree of Cure (Dynamics 0.5°C/min).

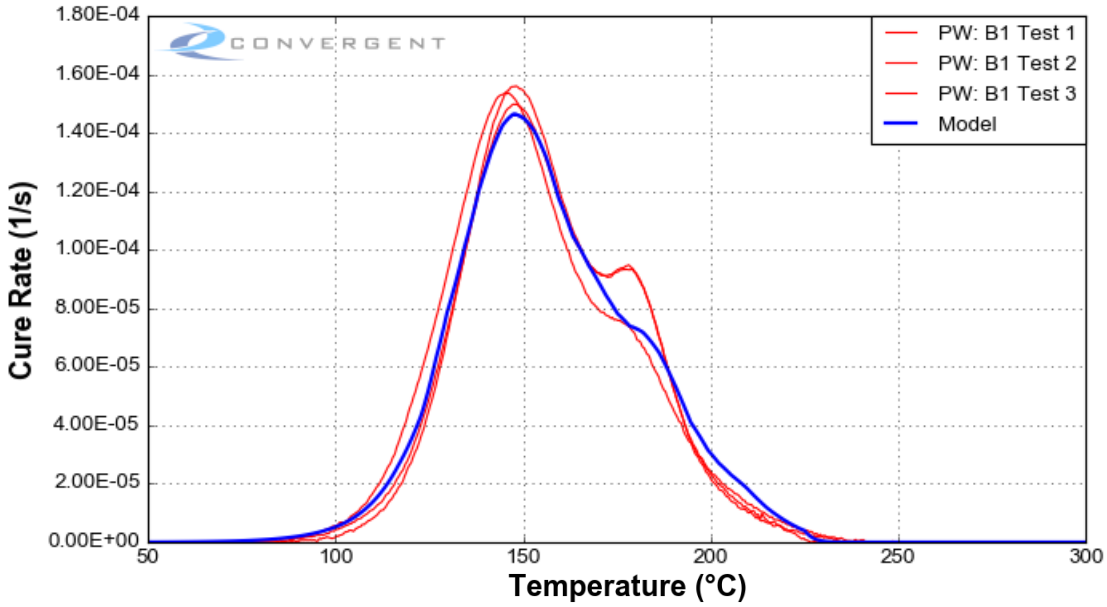

Figure 6.73: PW Form Comparison: Cure Rate (Dynamics 0.5°C/min).

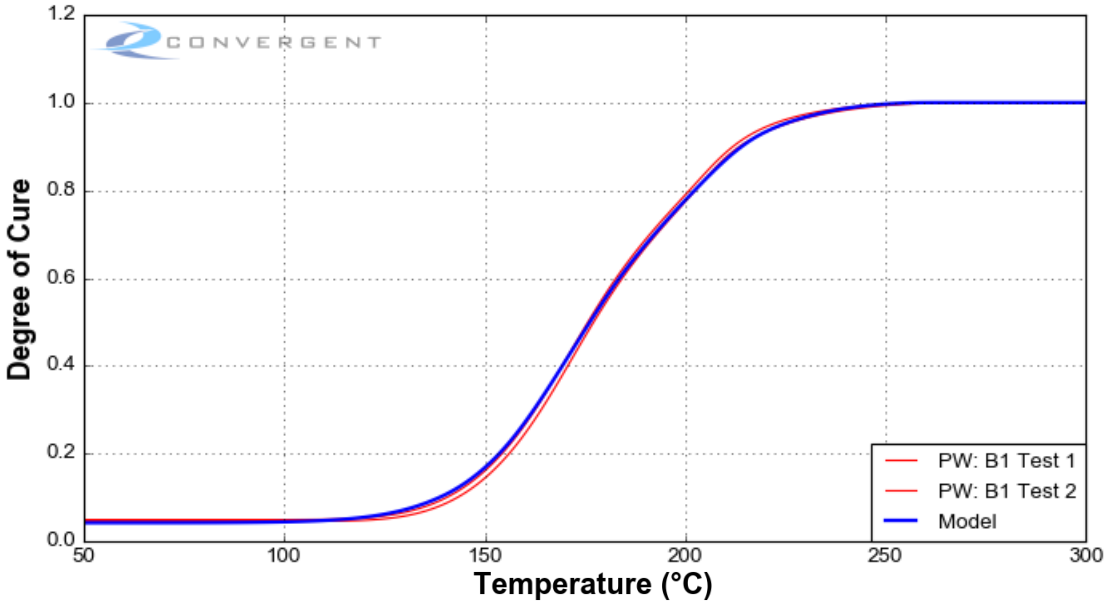

Figure 6.74: PW Form Comparison: Degree of Cure (Dynamics 1.5°C/min).

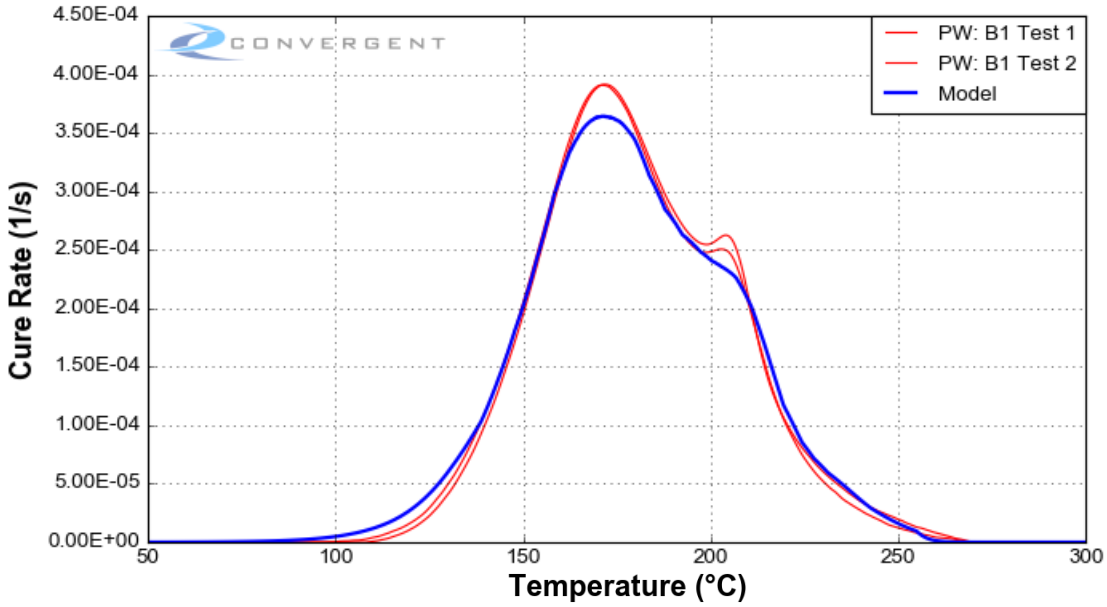

Figure 6.75: PW Form Comparison: Cure Rate (Dynamics 1.5°C/min).

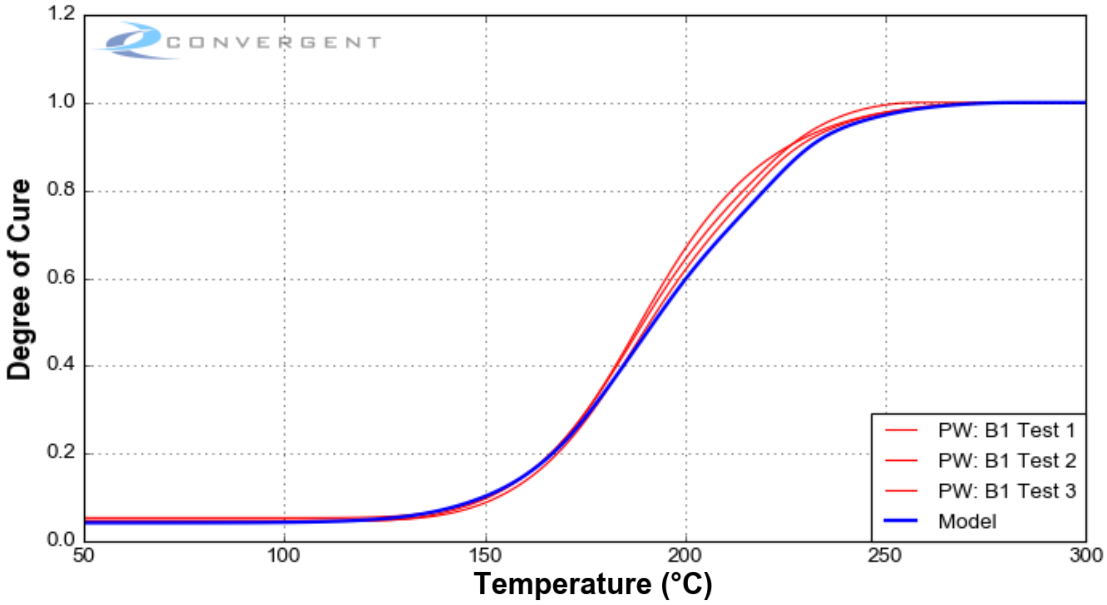

Figure 6.76: PW Form Comparison: Degree of Cure (Dynamics 3°C/min).

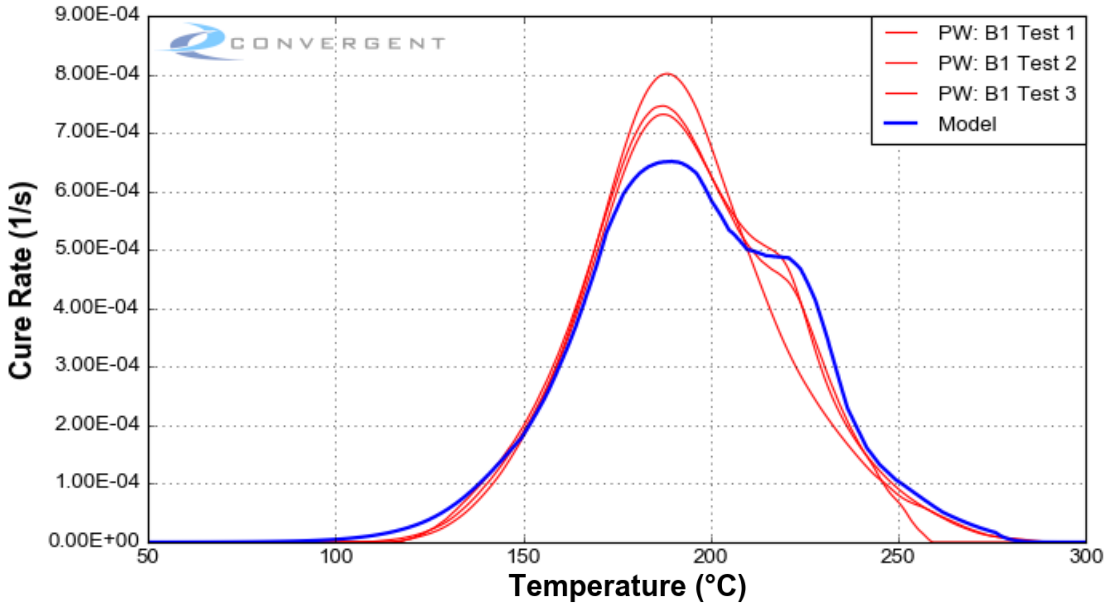

Figure 6.77: PW Form Comparison: Cure Rate (Dynamics 3°C/min).

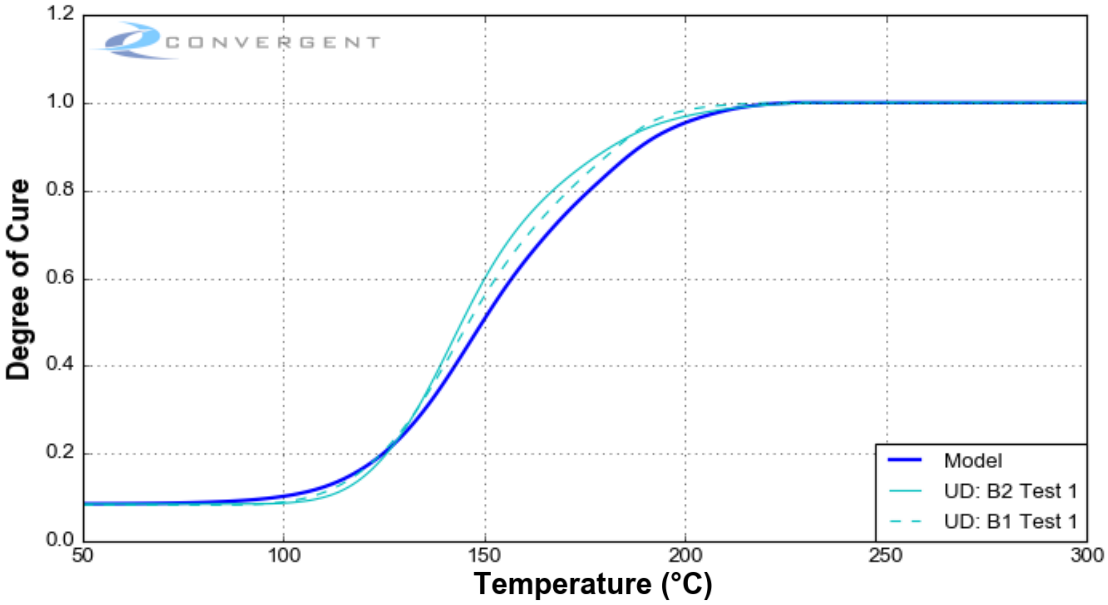

Figure 6.78: UD Form Comparison: Degree of Cure (Dynamics 0.5°C/min).

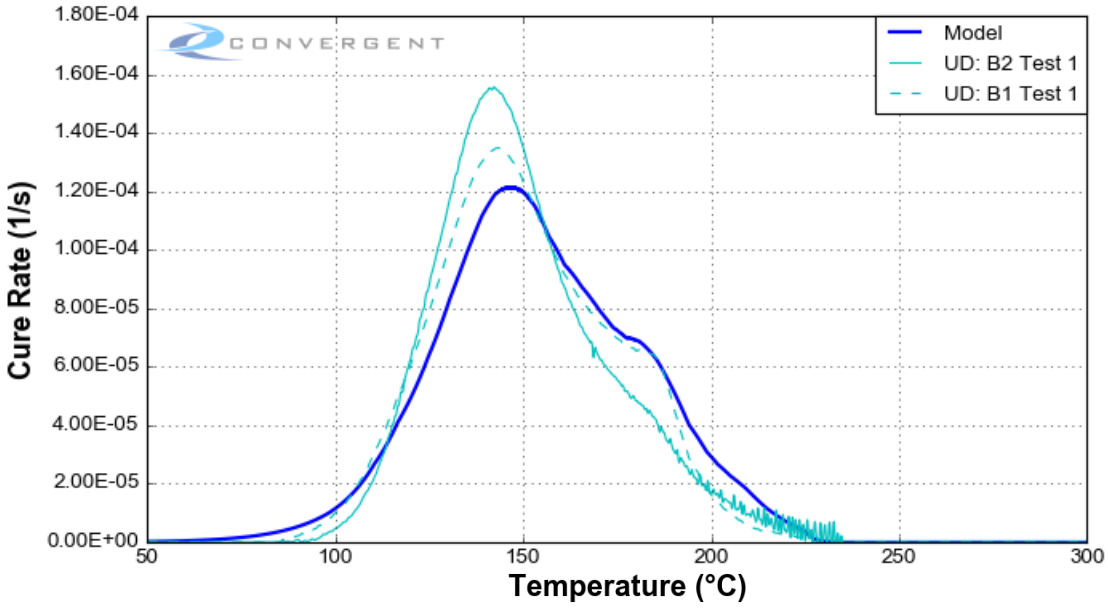

Figure 6.79: UD Form Comparison: Cure Rate (Dynamics 0.5°C/min).

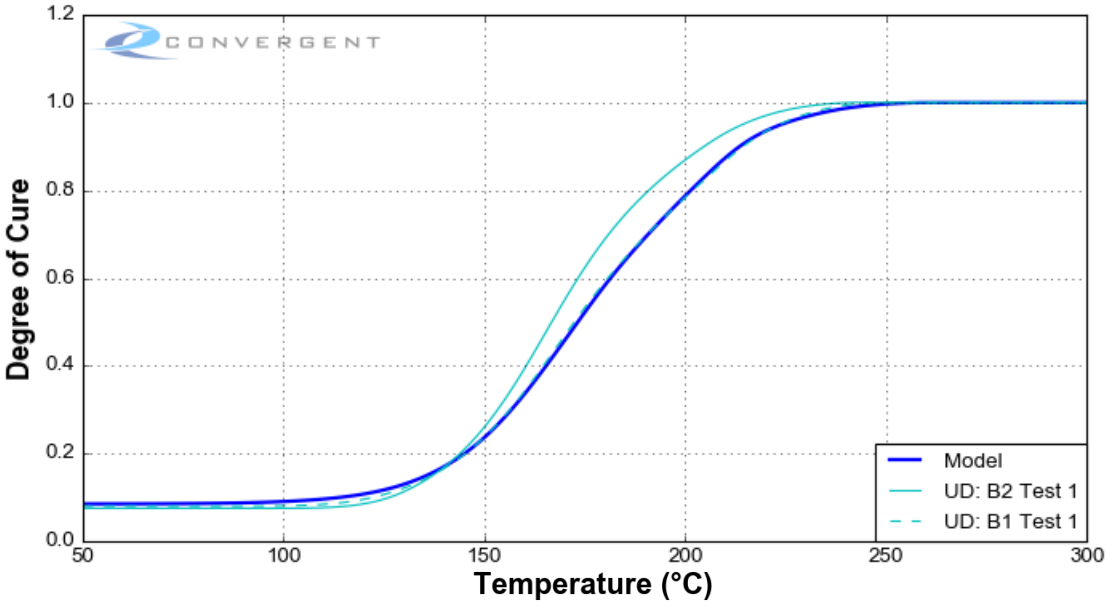

Figure 6.80: UD Form Comparison: Degree of Cure (Dynamics 1.5°C/min).

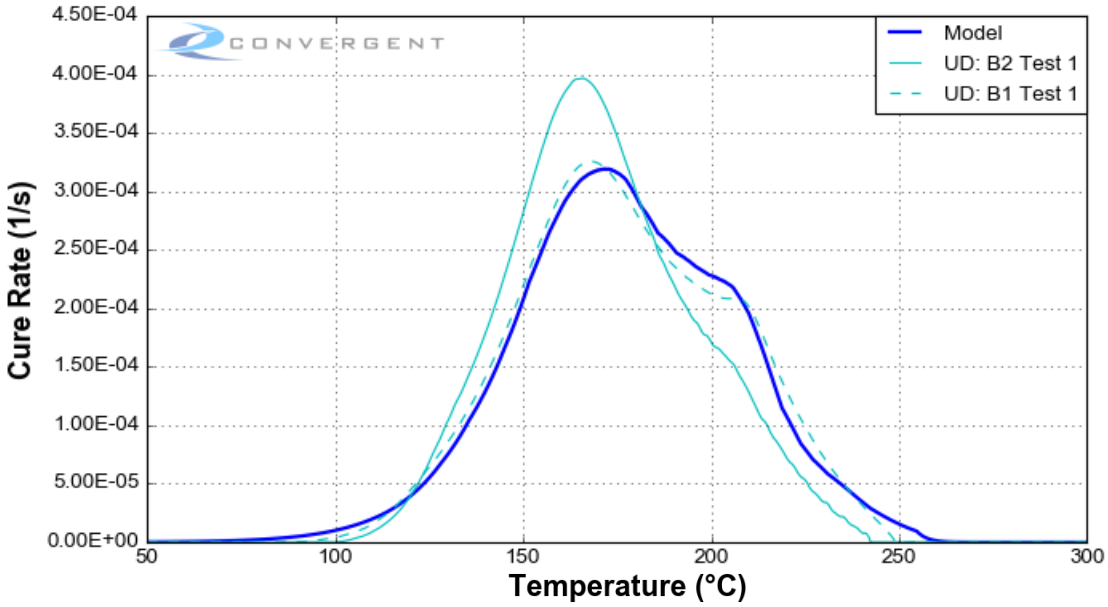

Figure 6.81: UD Form Comparison: Cure Rate (Dynamics 1.5°C/min).

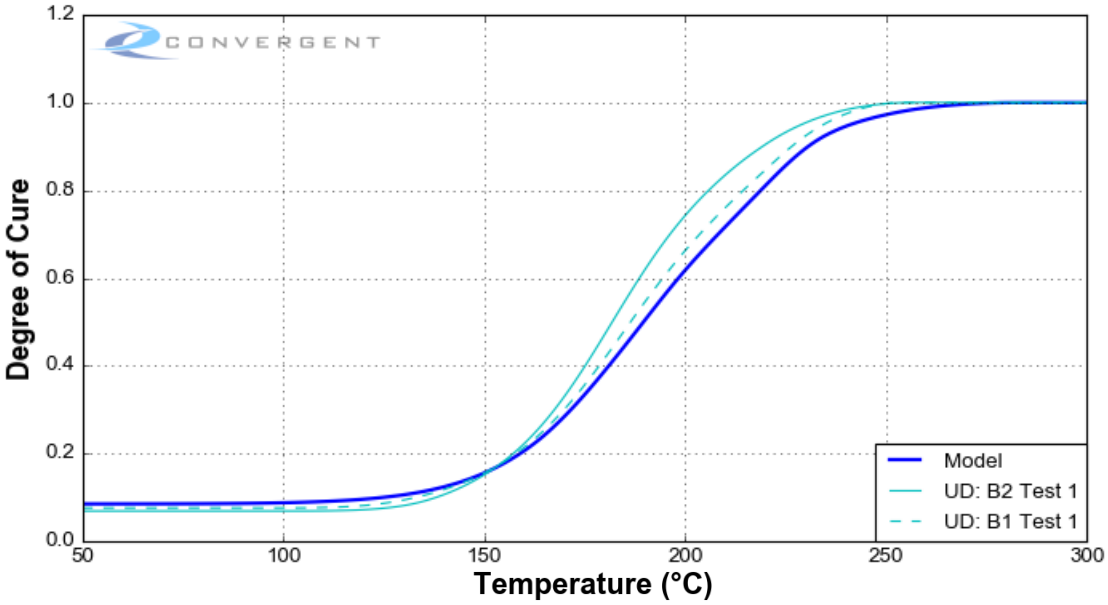

Figure 6.82: UD Form Comparison: Degree of Cure (Dynamics 3°C/min).

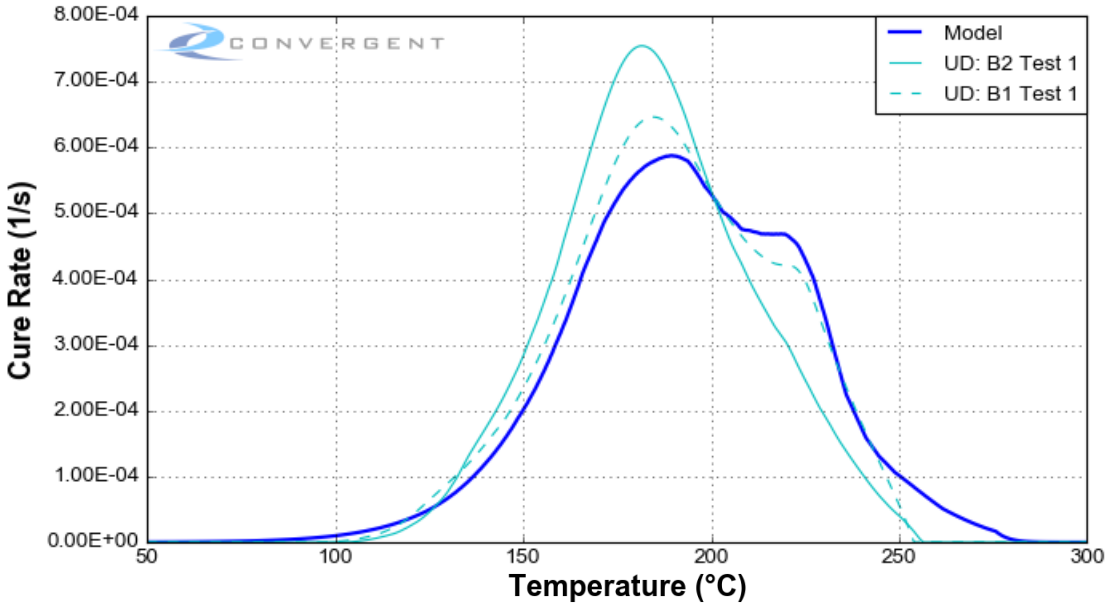

Figure 6.83: UD Form Comparison: Cure Rate (Dynamics 3°C/min).

MRCC Verification Tests

The model was verified by performing cure cycle tests using the manufacturer's recommended cure cycle. The model calculation versus experimental results is shown in Fig. 6.84.

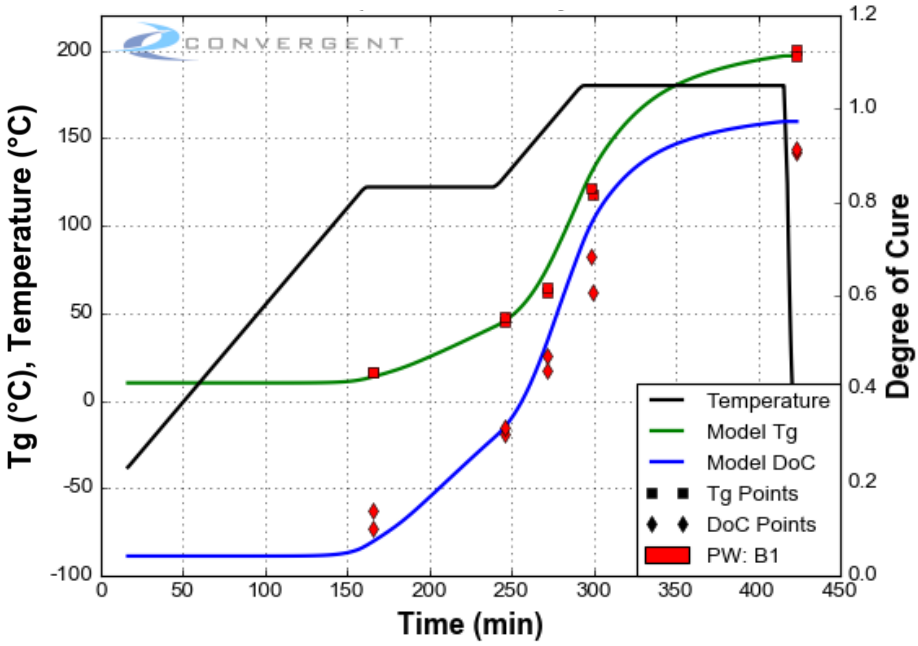

Figure 6.84: Model Prediction: Cure cycles ID: 1.0.

6.10. Cure Kinetics Comments

The cure kinetics model developed was validated for dynamic ramp rates between 0.5ºC/min and 3ºC/min and isothermal hold temperatures between 125ºC and 190ºC.

The spike in cure rate model predictions at the onset of isothermal holds is an artifact of varying instantaneous cure rates between material forms at early degrees of cure. Setting different assumed initial degrees of cure for each material form enables broader model applicability at the cost of inconsistent cure rate measurements in these early cure regions. As a result, there is a bifurcation and general spread in test data in these cure regions. It is not possible to eliminate the cure rate spike without sacrificing the fidelity of dynamic model predictions across all forms. To ensure consistent model fidelity across all forms and tailor the model to temperature and rate regions of greatest interest to the end user, dynamic model predictions for all forms were prioritized over isothermal hold cure rate profiles in early cure regions.

7. Thermo-Chemical Characterization: Heat Capacity

7.1. Introduction

DSC tests were performed to characterize the heat capacity of F7. A TA Instruments Q25 DSC instrument was used for the characterization. Heat capacity was measured during all of the DSC testing outlined in the previous section. A model for the heat capacity as a function of temperature and degree of cure was developed. The heat capacity model was fit to the dynamic and isothermal (hold and ramp) DSC tests.

7.2. Heat Capacity Test Procedures

The heat capacity test procedures were outlined in Section 6.3. The dynamic and isothermal DSC tests were used to characterize the heat capacity.

7.3. Heat Capacity Tests Performed

The heat capacity tests performed were outlined in the cure kinetics section of this report. The majority of DSC test data was generated with uncalibrated direct and reversing heat capacity signals, generating significant variation in test measurements. As a result, these signals were calibrated and test data was generated exclusively to develop the heat capacity model.

7.4. Heat Capacity Raw Data

The raw heat capacity data for the dynamic and isothermal tests are shown Figures 7.1 to 7.7.

Dynamic Tests: Variation with Temperature

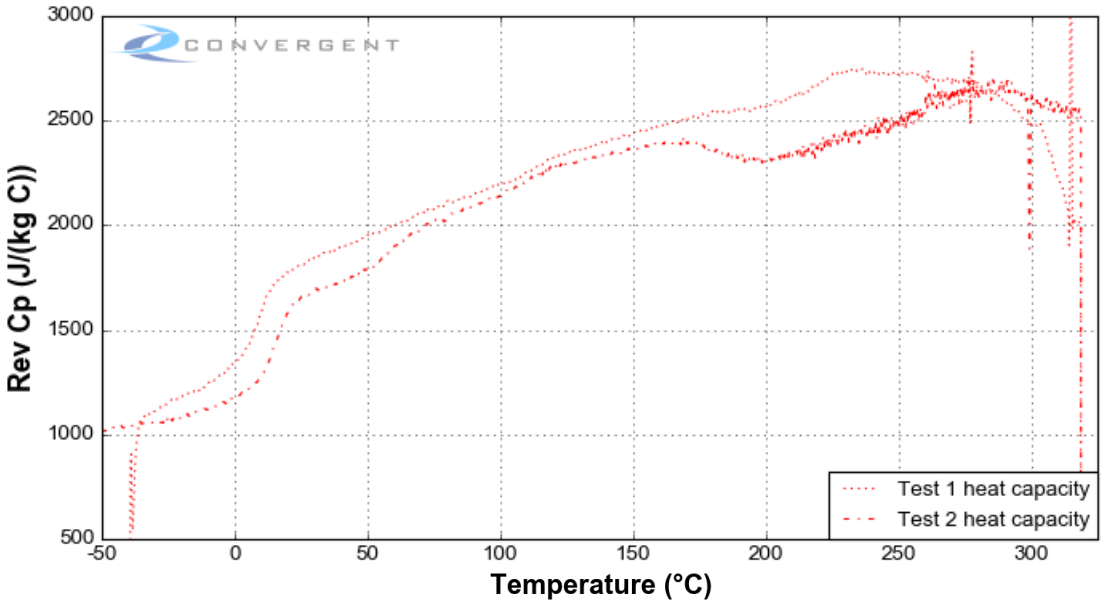

Figure 7.1: Raw test vs Temperature: Dynamics 0.5 C/min.

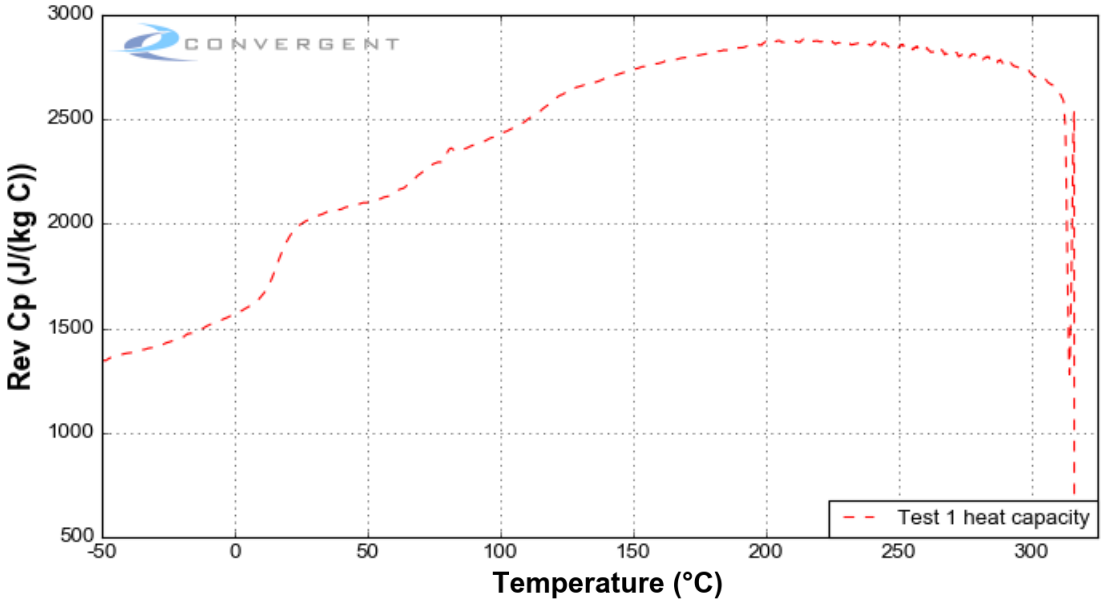

Figure 7.2: Raw test vs Temperature: Dynamics 1.5 C/min.

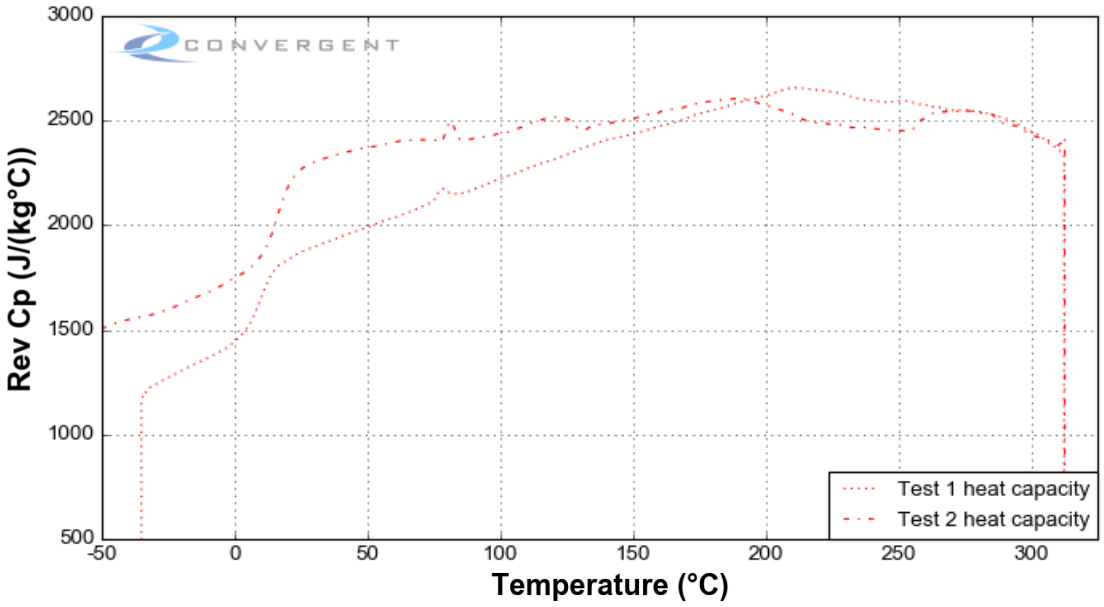

Figure 7.3: Raw test vs Temperature: Dynamics 3°C/min.

Isothermal Tests (Hold): Variation with Time

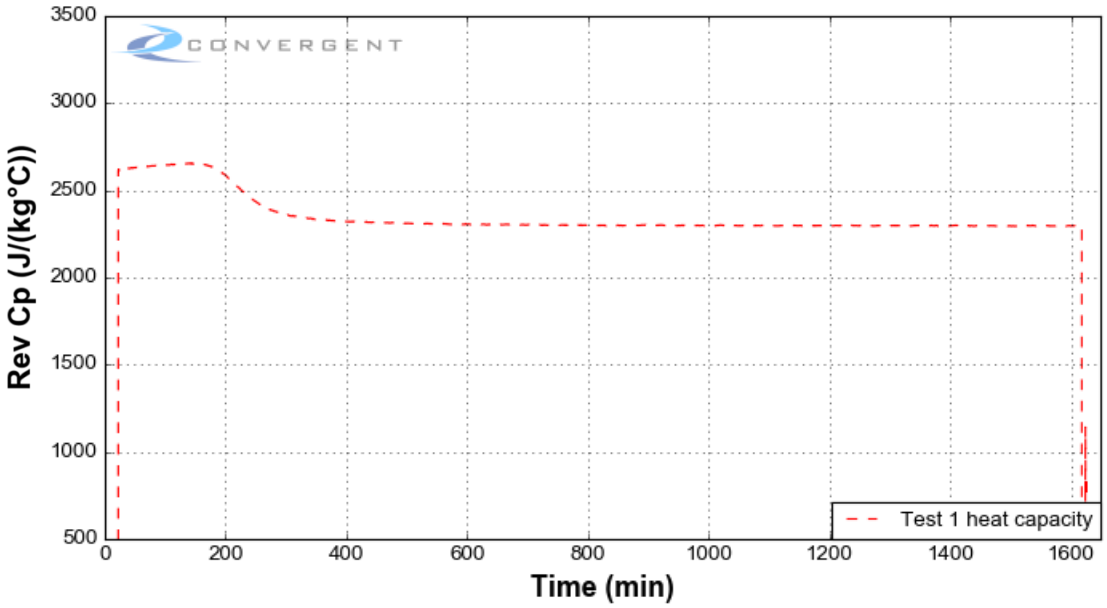

Figure 7.4: Raw test vs Time: Isothermals 125°C [Hold].

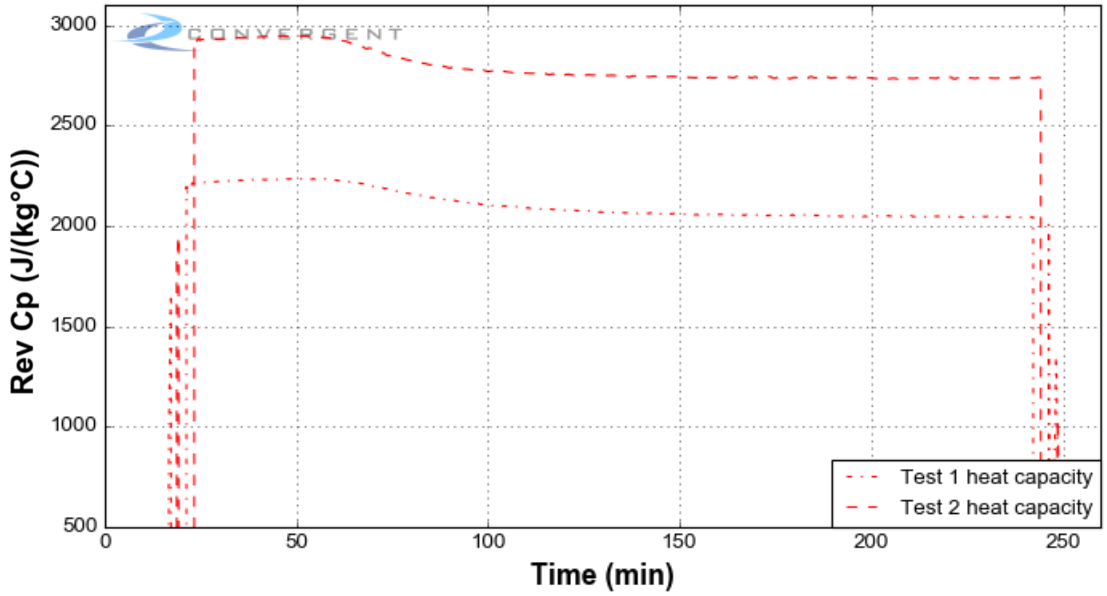

Figure 7.5: Raw test vs Time: Isothermals 190°C [Hold].

Isothermal Tests (Ramp): Variation with Temperature

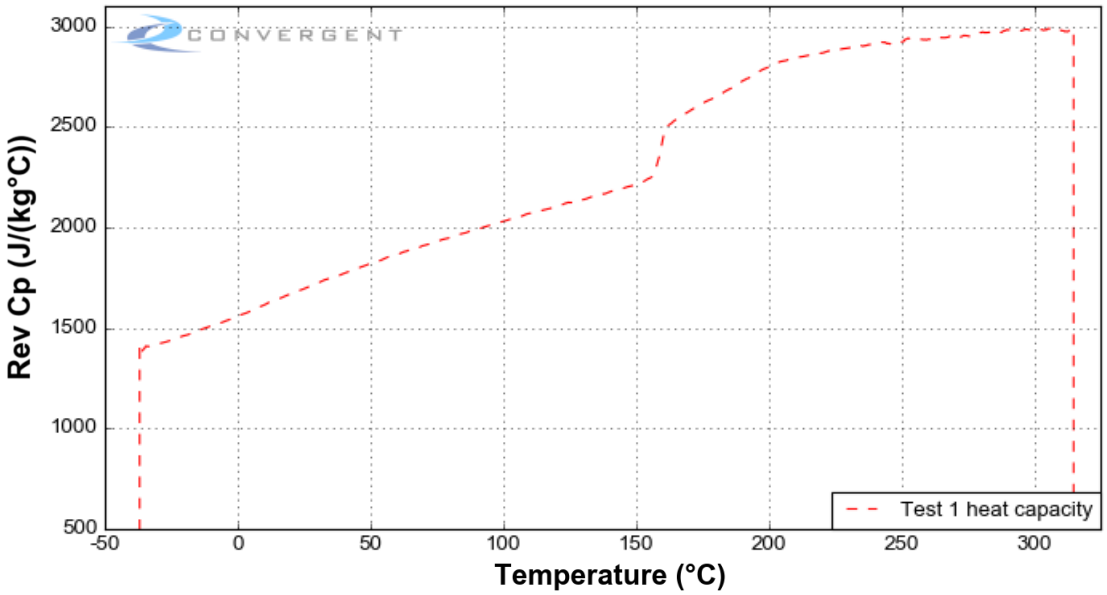

Figure 7.6: Raw test vs Temperature: Isothermals 125°C [Ramp].

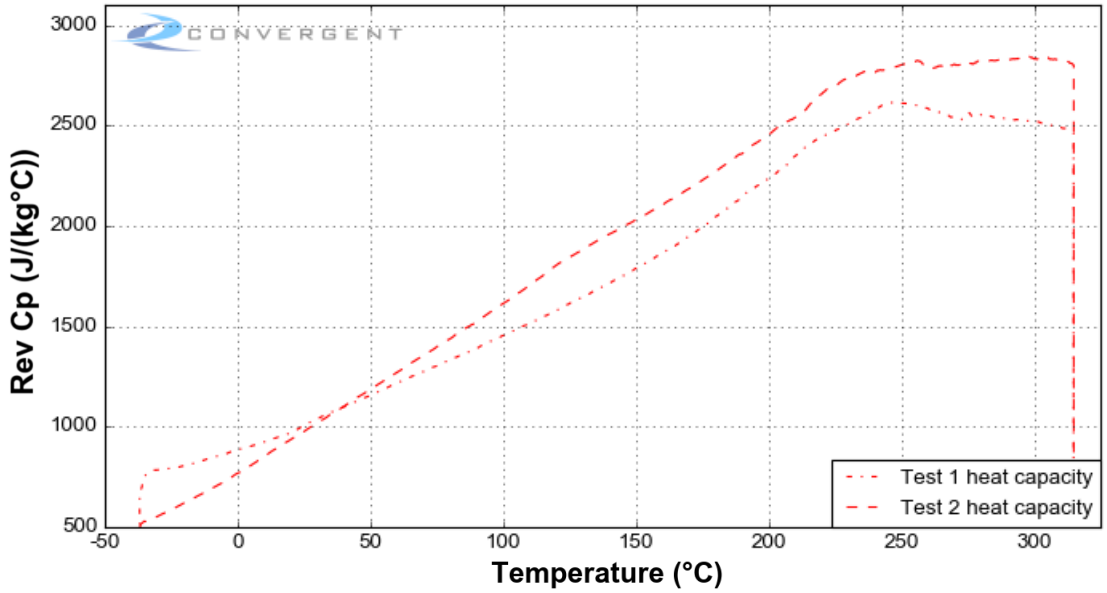

Figure 7.7: Raw test vs Temperature: Isothermals 190°C [Ramp].

7.5. Heat Capacity Data Analysis

The instantaneous heat capacity was obtained from the reversing component of the modulated heat flow in the MDSC tests. In the case where composite material samples are tested, the C_p of the resin (C_{p_r}) was obtained using a rule of mixtures based on the mass fraction of the constituents:

$$C_p = C_{p_r} m_r + C_{p_f}(1 - m_r)$$

The parameters of the resin heat capacity model were fit to the reversing heat capacity of the resin. The heat capacity was assumed to transition between the glassy and rubbery responses with changes in $T - T_g$. The fiber heat capacity model was populated with a datasheet reference value and a temperature dependency parameter that is typical for polyacrylonitrile (PAN) based carbon fibers.

7.6. Heat Capacity Model Fit

Fiber Heat Capacity Model

CCA Fiber Heat Capacity model is defined by:

$$C_p = C_{p_{nom}} + T_f(T - T_0)$$

The M30S fiber heat capacity model constants are given in Table 7.1.

Table 7.1: M30S Fiber Heat Capacity Model Parameters.

Constant	Value	Units
$C_{p_{nom}}$	733.9	$J/(kg.K)$
T_0	20	$°C$
T_f	2.84	$J/(kg.K^2)$

The MR60H fiber heat capacity model constants are given Table 7.2.

Table 7.2: MR60H Fiber Heat Capacity Model Parameters.

Constant	Value	Units
$C_{p_{nom}}$	419.6	$J/(kg.K)$
T_0	20	$°C$
T_f	2.52	$J/(kg.K^2)$

Resin Heat Capacity Model

CCA Resin Heat Capacity model 4 was used:

$$C_p = (1-x)C_p^0 + xC_p^\infty$$

$$C_p^0 = C_{p_r}^0 + \frac{C_{p_g}^0 - C_{p_r}^0}{1 + e^{k^0(T - T_g - \Delta T^0)}}$$

$$C_{p_r}^0 = c_r^0 + s_r^0 T$$

$$C_{p_g}^0 = c_g^0 + s_g^0 T$$

$$C_p^\infty = C_{p_r}^\infty + \frac{C_{p_g}^\infty - C_{p_r}^\infty}{1 + e^{k^\infty(T - T_g - \Delta T^\infty)}}$$

$$C_{p_r}^\infty = c_r^\infty + s_r^\infty T$$

$$C_{p_g}^\infty = c_g^\infty + s_g^\infty T$$

$$T_g = T_g^0 + \frac{\lambda x}{1 - (1-\lambda)x}\left(T_g^\infty - T_g^0\right) + CtoK$$

Note: CtoK is a conversion factor from degrees Celsius to kelvin.

The resin heat capacity model constants are given in Table 7.3:

Table 7.3: Resin Heat Capacity Model Parameters.

Constant	Value	Units
T_g^0	5.5	$°C$
T_g^∞	207	$°C$
λ	0.53	–
s_r^0	5.0	$J/(kg.K^2)$
s_r^∞	1.5	$J/(kg.K^2)$
s_g^0	5.6	$J/(kg.K^2)$
s_g^∞	5.6	$J/(kg.K^2)$
c_r^0	1710	$J/(kg.K)$
c_r^∞	2100	$J/(kg.K)$
c_g^0	1380	$J/(kg.K)$
c_g^∞	960	$J/(kg.K)$
k^0	0.3	–
ΔT^0	3.0	$°C$
k^∞	0.2	–
ΔT^∞	0.0	$°C$

7.7. Heat Capacity Quality of Fit

The model fit and raw heat capacity data for the dynamic and isothermal tests are shown in Figures 7.8 to 7.14.

Dynamic Tests: Variation with Temperature

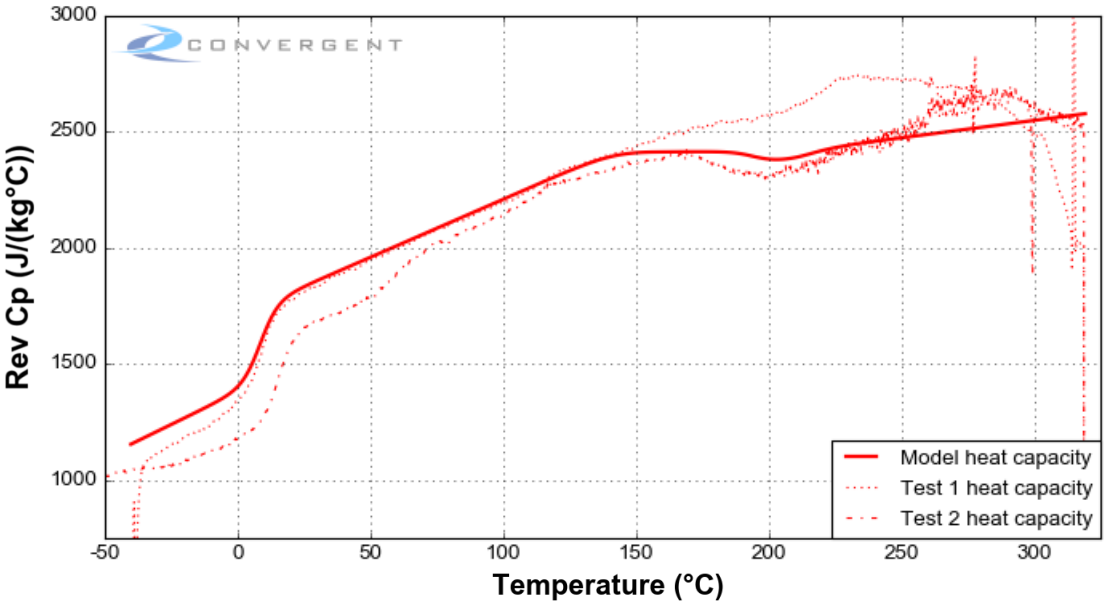

Figure 7.8: Model prediction vs Temperature: Dynamics 0.5 C/min.

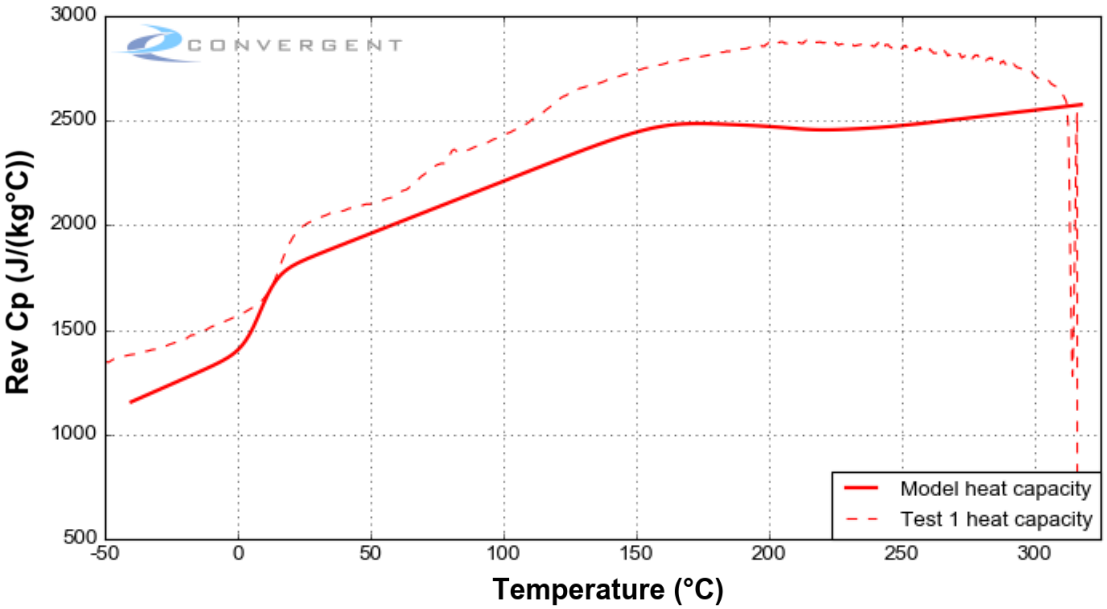

Figure 7.9: Model prediction vs Temperature: Dynamics 1.5°C/min.

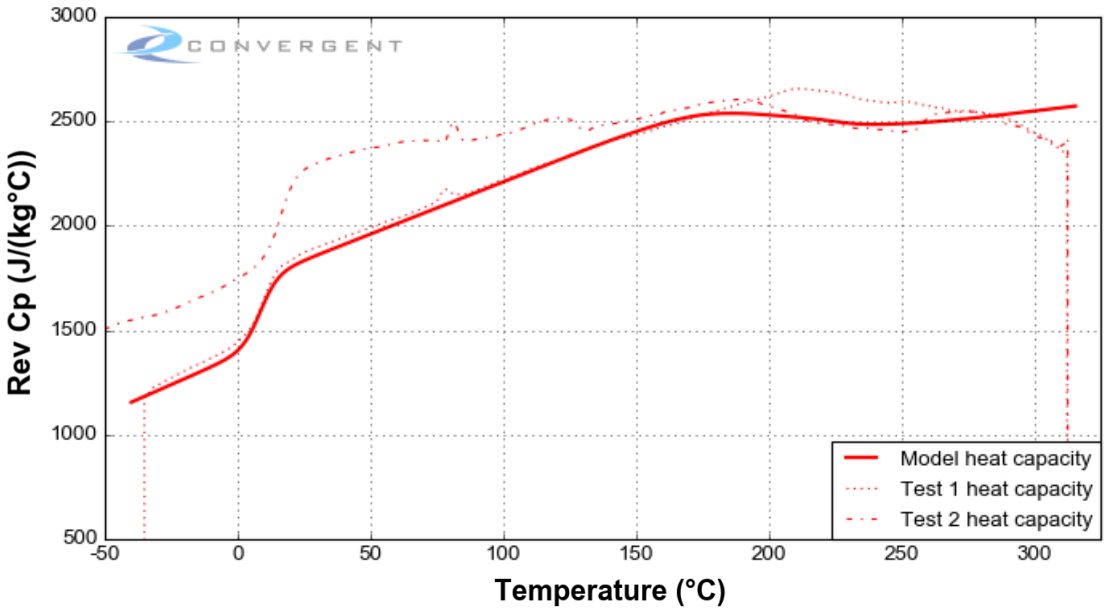

Figure 7.10: Model prediction vs Temperature: Dynamics 3°C/min.

Isothermal Tests (Hold): Variation with Time

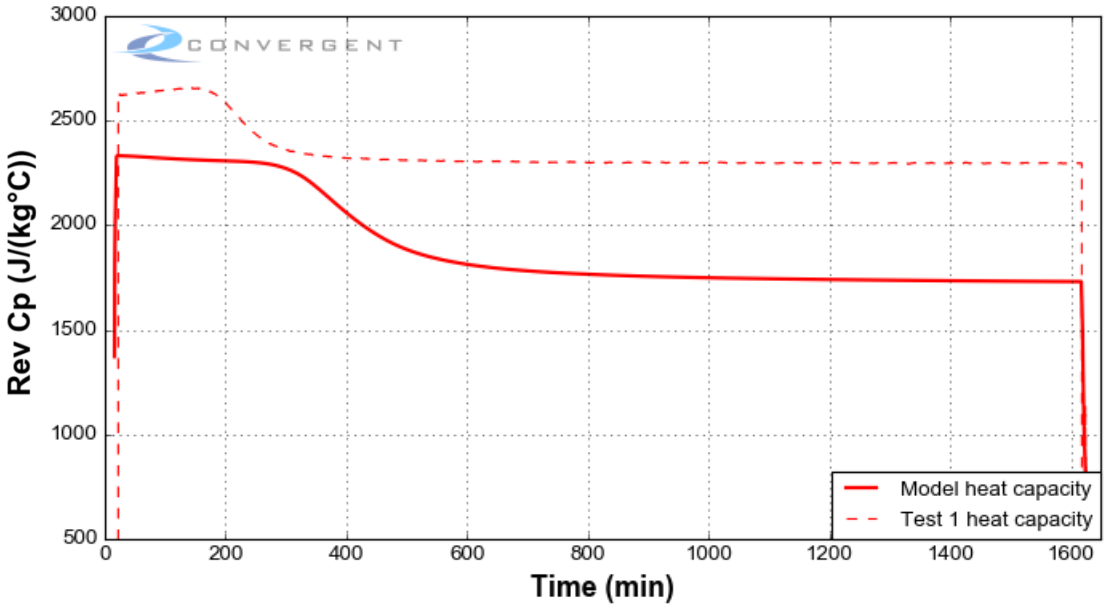

Figure 7.11: Model prediction vs Time: Isothermals 125°C [Hold].

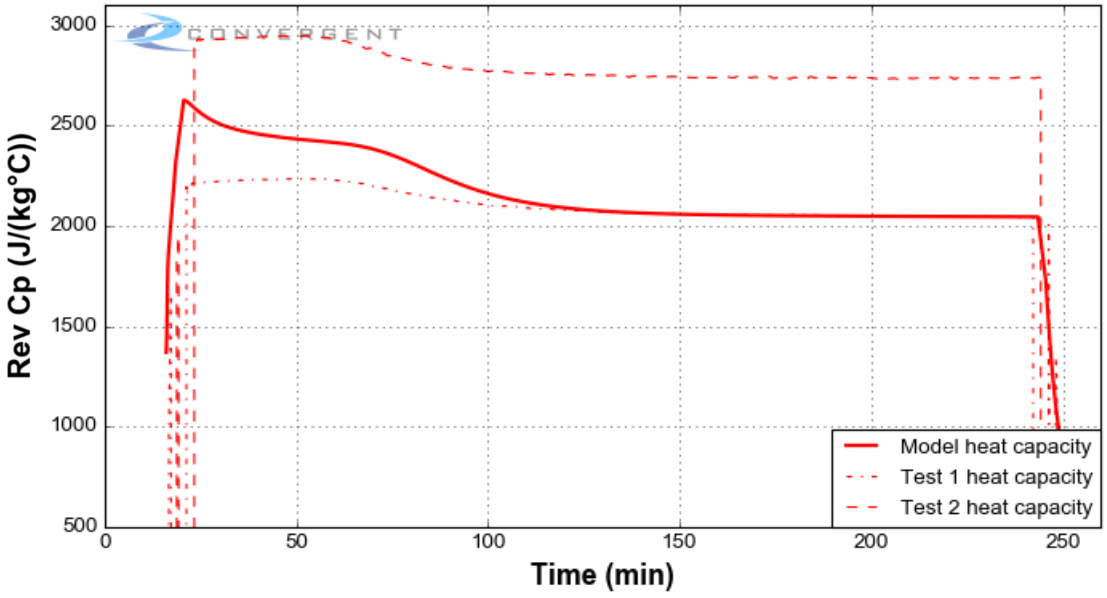

Figure 7.12: Model prediction vs Time: Isothermals 190°C [Hold].

Isothermal Tests (Ramp): Variation with Temperature

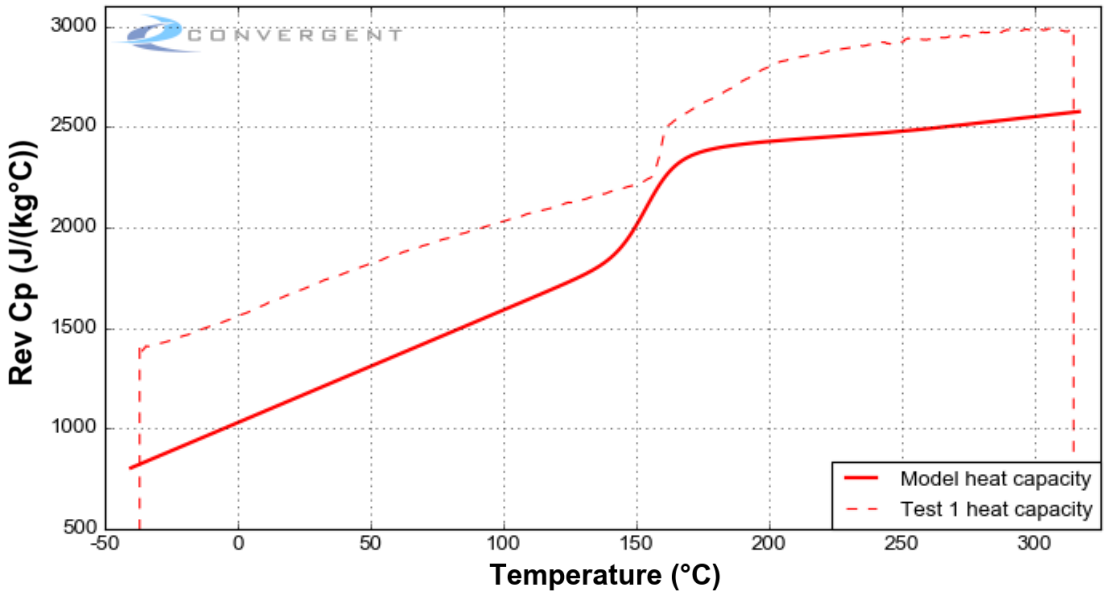

Figure 7.13: Model prediction vs Temperature: Isothermals 125°C [Ramp].

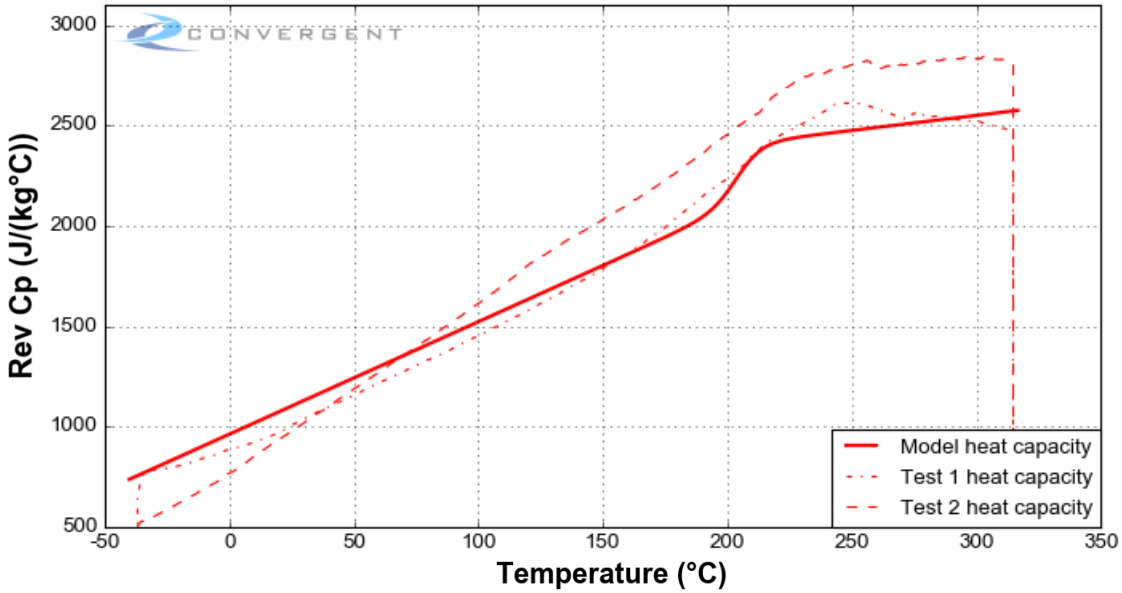

Figure 7.14: Model prediction vs Temperature: Isothermals 190°C [Ramp].

7.8. Heat Capacity Comments

The heat capacity model developed was validated for dynamic ramp rates between 0.5ºC/min and 3ºC/min, isothermal hold temperatures between 125ºC and 200ºC.

While the developed heat capacity model follows the slopes and glass transition step changes observed in test data, the limited quantity of calibrated heat capacity signals inhibits further accuracy in fitting to the absolute values of test data. A future upgrade to this model would benefit greatly from additional heat capacity data for model refinement.

8. Thermo-Chemical Characterization: Thermal Conductivity

The resin thermal conductivity was not characterized by CMTUS. Instead, a typical thermal conductivity model for an epoxy resin was used. Specifically, the conductivity model was based on Andrew A. Johnston model for 8552 resin. For more information on the derivation of these model parameters, please refer to Johnston, A. A. (1997). An integrated model of the development of process-induced deformation in autoclave processing of composite structures (Doctoral dissertation, University of British Columbia), page 115.

The composite thermal conductivity for a unidirectional ply is calculated by:

$$K_{11} = V_f K_{fl} + \left(1 - V_f\right) K_r$$

$$K_{22} = K_{33} = K_r \left[1 - 2\sqrt{\frac{V_f}{\pi}} + \frac{1}{B}\left(\pi - \frac{4}{\sqrt{1 - B^2 \frac{V_f}{\pi}}} \tan^{-1}\left[\frac{\sqrt{1 - B^2 \frac{V_f}{\pi}}}{1 + B\sqrt{\frac{V_f}{\pi}}} \right] \right) \right]$$

$$B = 2\left(\frac{K_r}{K_{ft}} - 1 \right)$$

8.1. Thermal Conductivity Model

Fiber Thermal Conductivity

CCA Fiber Conductivity model 1 was used to calculate the thermal conductivity of the fiber. The thermal conductivity was assumed to be a function of temperature. The conductivity model equation is defined below and parameters are given in Tables 8.1 and 8.2.

$$K_{ft} = K_{t_{nom}} + T_{ft}(T - T_0)$$

$$K_{fl} = K_{l_{nom}} + T_{fl}(T - T_0)$$

Table 8.1: M30S Fiber Thermal Conductivity Model Parameters.

Constant	Value	Units
$K_{t_{nom}}$	10.8	$W/(m.K)$
$K_{l_{nom}}$	38.9	$W/(m.K)$
T_0	0.0	$°C$
T_{ft}	0.0	$W/(m.K^2)$
T_{fl}	0.0	$W/(m.K^2)$

Table 8.2: MR60H Fiber Thermal Conductivity Model Parameters.

Constant	Value	Units
$K_{t_{nom}}$	4.45	$W/(m.K)$
$K_{l_{nom}}$	16.0	$W/(m.K)$
T_0	0.0	$°C$
T_{ft}	0.0	$W/(m.K^2)$
T_{fl}	0.0	$W/(m.K^2)$

Resin Thermal Conductivity

CCA Resin Conductivity model 1 was used to calculate the thermal conductivity of the resin system. The thermal conductivity was assumed to be a function of temperature and degree of cure. The conductivity model equation is defined below and model parameters are given in Table 8.3.

$$K_r = K_0 + T_m(T - T_0) + x_m(x - x_0)$$

Table 8.3: Resin Thermal Conductivity Model Parameters.

Constant	Value	Units
K_0	0.148	$W/(m.K)$
T_0	0.0	$°C$
T_m	3.43E-04	$W/(m.K^2)$
x_0	0.0	–
x_m	6.07E-02	$W/(m.K)$

9. Thermo-Mechanical Characterization: Resin Modulus

9.1. Nomenclature

G_{min} : Minimum shear modulus

K_{min} : Minimum bulk modulus

G_g : Glassy shear modulus

K_g : Glassy bulk modulus

G_r : Rubbery shear modulus

K_r : Rubbery bulk modulus

a_{Tx} : Temperature and degree of cure shift factor

C_T, C_{T_g}, C_2 : Model Constants

f : Frequency

τ_i : Relaxation times for each Maxwell element

g_i : Weight factor for each Maxwell element

T_g : Glass transition temperature

T_g^0 : Glass transition temperature at degree of cure = 0

T_g^∞ : Glass transition temperature at degree of cure = 1

T_{ref} : Reference temperature

T_{gRef} : Glass transition temperature at reference temperature

λ : DiBenedetto equation calibration constant

x_{gel} : Degree of cure at gelation

9.2. Introduction

DMA tests were performed to characterize the modulus development of F7. A model for the resin modulus as a function of temperature and degree of cure was developed. Isotropic material behavior was assumed for the neat resin properties.

9.3. DMA Test Procedures

Bi-Material Beam Tests

To measure the modulus development during cure, a BMB arrangement (developed at Convergent) was used. In the BMB arrangement, the resin was placed on top of a steel shim and loaded in 3-point bending while curing. Testing was performed in a TA Instruments Q800 DMA. Modulus was measured by applying an oscillating displacement at a frequency of 0.1 Hz to the specimen and measuring the corresponding force. The modulus development of the resin was then deconvoluted from the steel shim response.

Isothermal hold tests at various temperatures were performed to capture the modulus development as a function of temperature and degree of cure. The hold temperatures were selected to include and bracket any hold temperatures that were expected to be used in the manufacturing cure cycles. The hold times were selected such that the reaction slows due to diffusion.

Once the isothermal hold segment of a BMB test was completed, the sample was cooled to room temperature and then reheated. The reheat temperature determines whether the material devitrifies or remains in a glassy state during the reheat. The Cure Hardening Instantaneously Linear Elastic (CHILE) modelling approach used in this characterization agrees well with BMB data during cure and during cool down when the material remains glassy, however deviates during the reheat if devitrification occurs. This deviation is due to the combination of physical aging that occurs, resulting in an increase of the instantaneous Tg of the material, and the high sensitivity to temperature of the modulus near Tg. Furthermore, the validity of the CHILE approach is limited to applications in which modulus is increasing or constant, and is not valid for decreasing modulus (material softening).

Homogeneous Resin Beam Tests

To obtain high fidelity data for the glassy modulus as a function of temperature, homogeneous neat resin beams were also tested using a TA Instruments Q800 DMA with the three point bending fixture. This data was used as a reference to scale the BMB data.

All tests performed in the modulus characterization testing of this material used a frequency of 0.1 Hz and temperature ramp rate of 2ºC/min. Homogeneous beam samples were prepared by a casting method developed at Convergent. DSC testing was performed on a small section of each resin beam prior to DMA testing to confirm the degree of cure.

9.4. DMA Tests Performed

The DMA tests performed are summarized below:

- Isothermal bi-material beam tests: six tests at 140ºC to 200ºC
- Dynamic neat resin beam tests: two tests at 2ºC/min from 0ºC up to 320ºC

A summary of the DMA tests performed is shown in Tables 9.1 and 9.2.

Table 9.1: Test Summary (DMA BMB Tests) [Modulus].

Test name	Hold Temperature (°C)	Hold time (°C)
F7-UD-B3-DMA-BMB-140C-350min-1	140	350
F7-UD-B3-DMA-BMB-155C-290min-1	155	290
F7-UD-B3-DMA-BMB-170C-250min-1	170	250
F7-UD-B2-DMA-BMB-180C-180min-1	180	180
F7-UD-B2-DMA-BMB-190C-150min-1	190	150
F7-UD-B2-DMA-BMB-200C-120min-2	200	120

Table 9.2: Test Summary (DMA Neat Resin Tests) [Modulus].

Test name	Ramp rate (°C/min)
PMT F7-NR-B1-DMA-TempSweep-2	2
PMT F7-NR-B1-DMA-TempSweep-3	2

9.5. DMA Raw Bi-Material Beam Modulus Data and Analysis

In order to display the raw resin modulus development data from the DMA BMB tests, some data processing was required. The data from the BMB tests were analyzed according to the technique developed at Convergent. In brief, the equivalent BMB stiffness (EI) was calculated from the measured force, displacement and the phase angle reported by the DMA machine. EI was then deconvoluted into the resin modulus and the model was fit to the data using the temperature and the degree of cure calculated from the cure kinetics model.

The static force and tan delta raw test results as well as the deconvoluted resin modulus for each test condition are shown in the Figures 9.1 to 9.6.

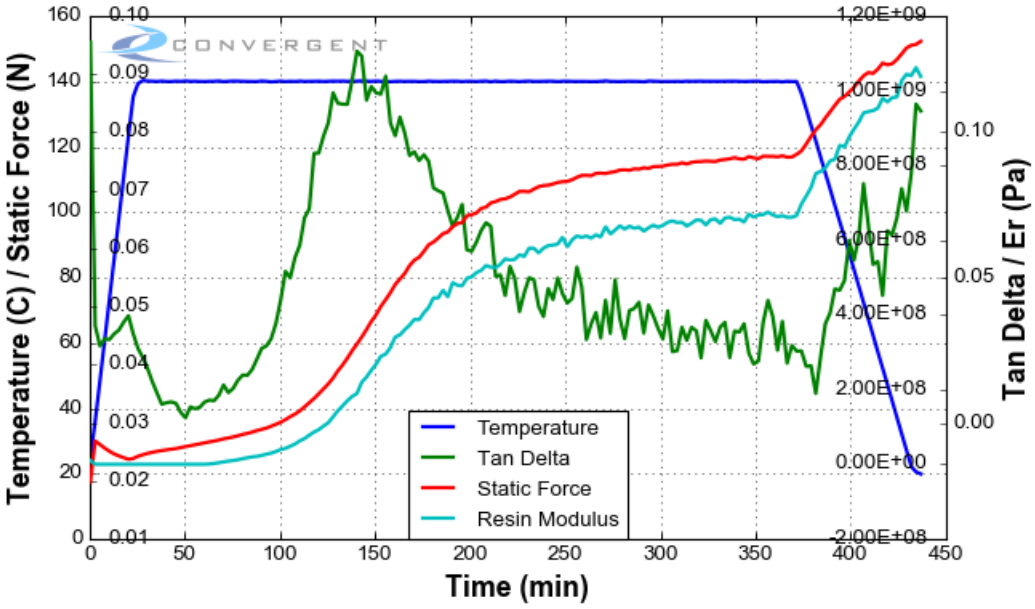

Figure 9.1: Raw Data: F7-UD-B3-DMA-BMB-140C-350min-1.

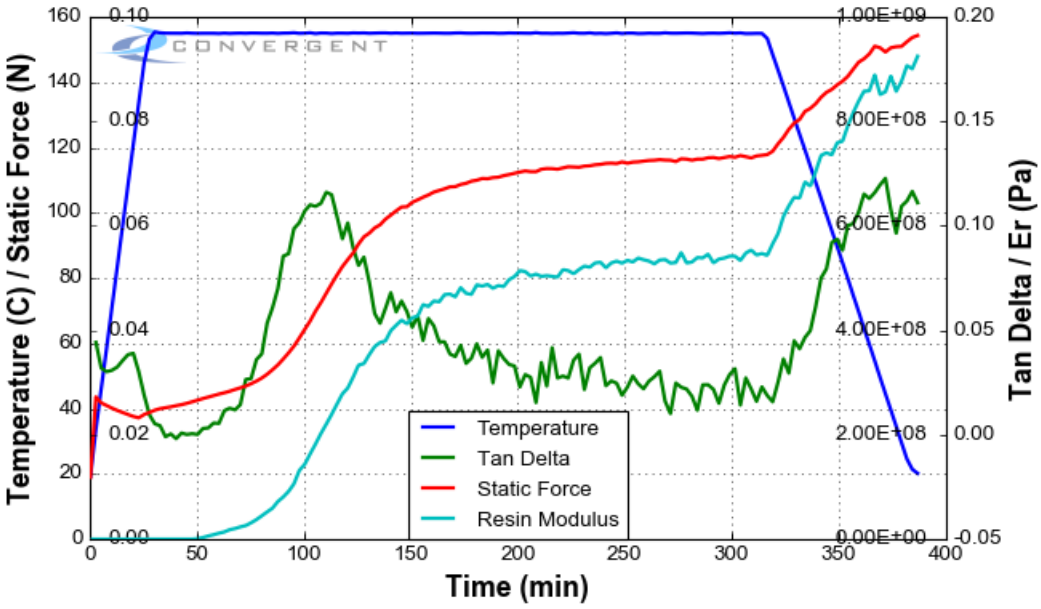

Figure 9.2: Raw Data: F7-UD-B3-DMA-BMB-155C-290min-1.

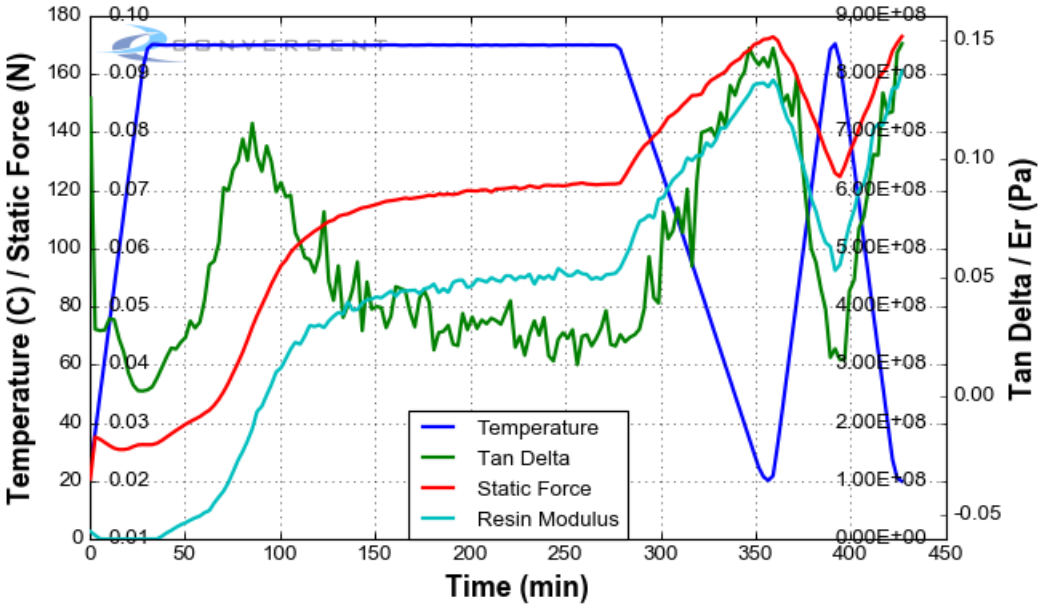

Figure 9.3: Raw Data: F7-UD-B3-DMA-BMB-170C-250min-1.

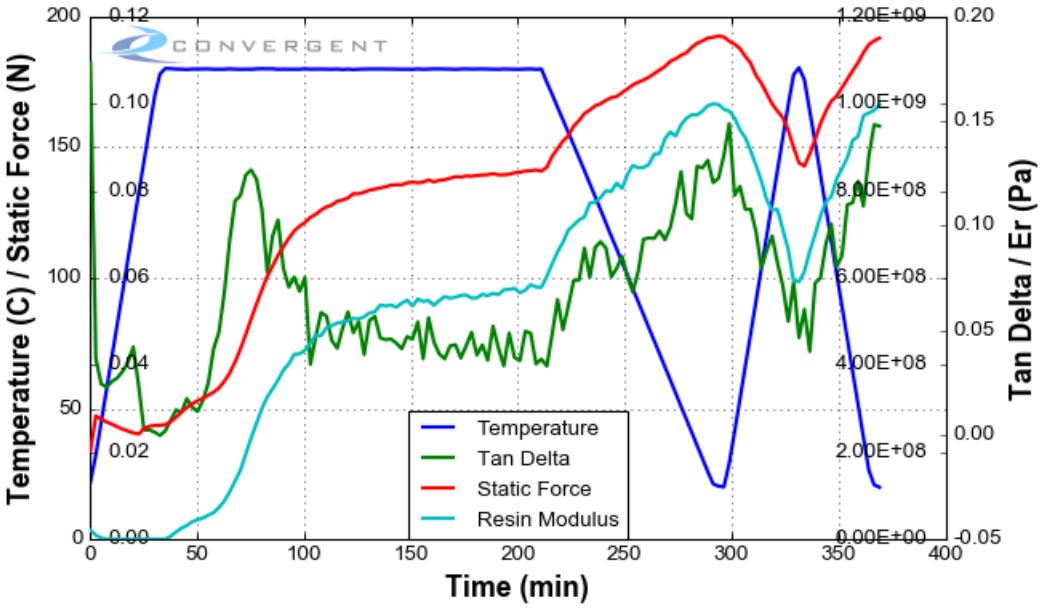

Figure 9.4: Raw Data: F7-UD-B2-DMA-BMB-180C-180min-1.

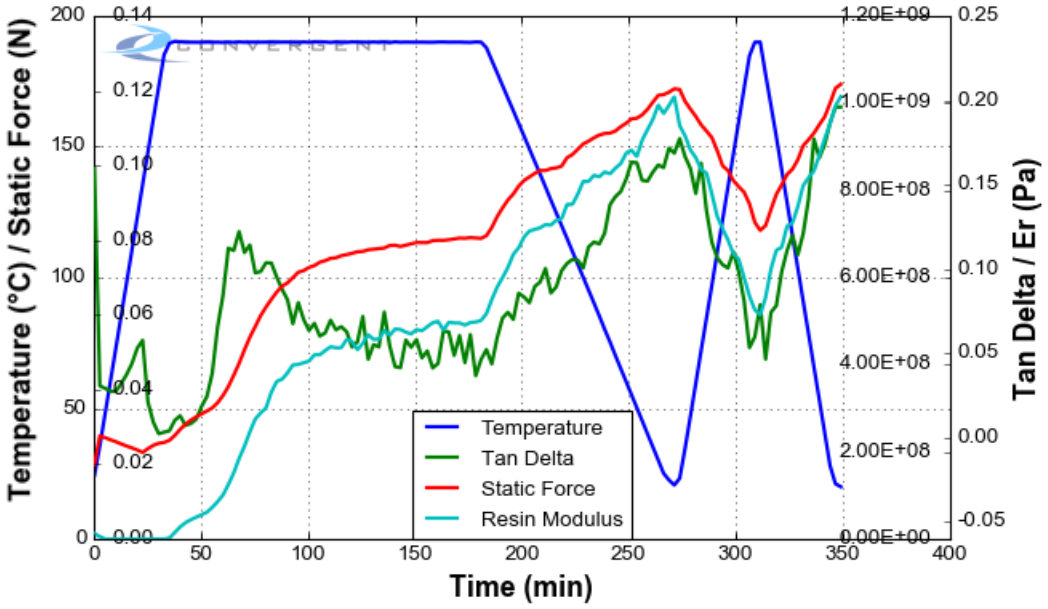

Figure 9.5: Raw Data: F7-UD-B2-DMA-BMB-190C-150min-1.

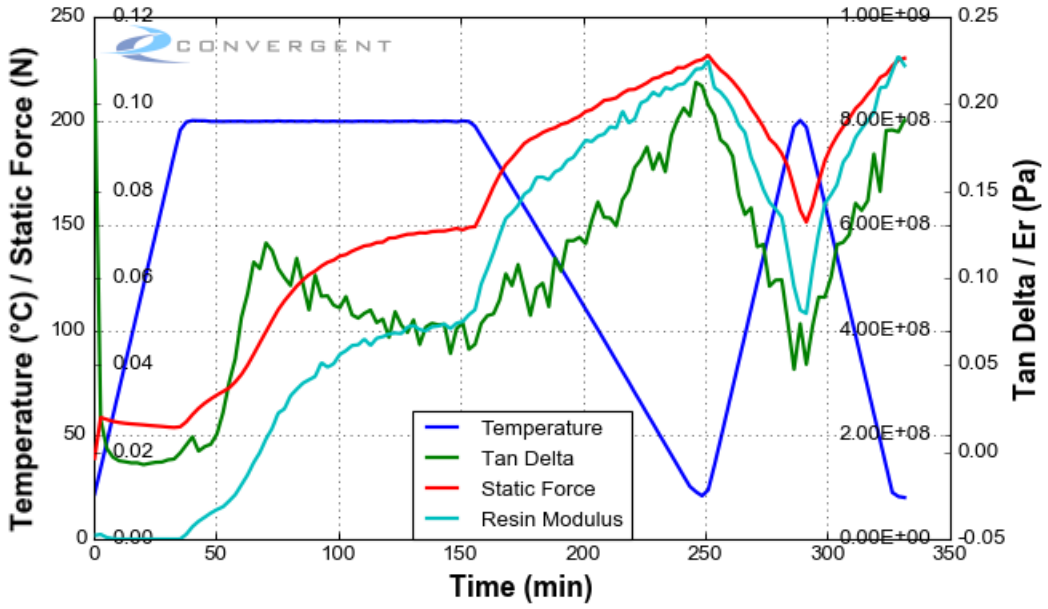

Figure 9.6: Raw Data: F7-UD-B2-DMA-BMB-200C-120min-1.

9.6. DMA Neat Resin Modulus Data Analysis

An overlay of all raw DMA data for the neat resin beam dynamic ramp tests performed is shown in Fig. 9.7.

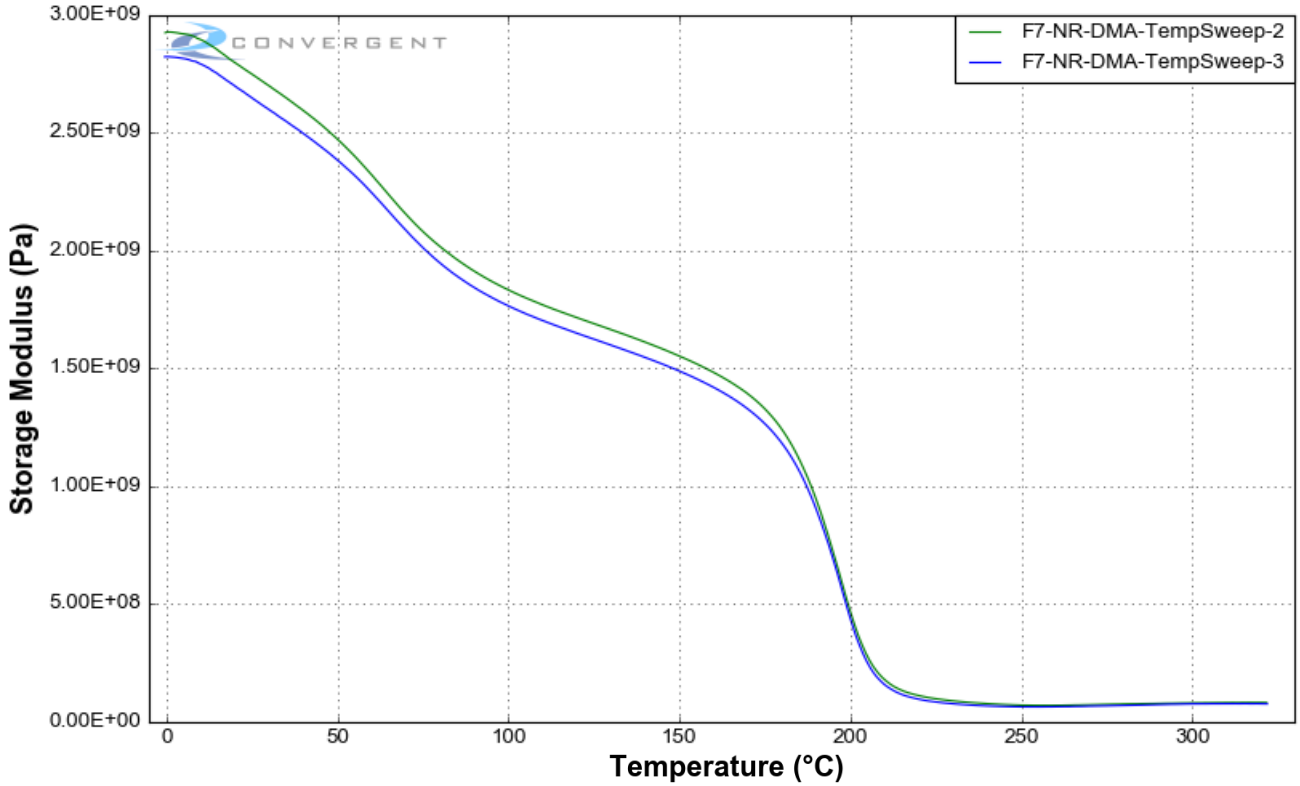

Figure 9.7: Neat resin DMA test data.

9.7. Fiber Elastic Properties

The elastic properties of the AS4 fiber to CCA Fiber Elastic Properties Model 1, which assumes transverse isotropy with temperature dependency for all engineering constants defined by:

$$X = X^{ref} + s_X^T\left(T - T_X^{ref}\right), \qquad X = E_{11}, E_{22}, G_{12}, \nu_{12}, \nu_{23}$$

$$E_{22} = E_{33} \;\; ; \;\; G_{12} = G_{13} \;\; ; \;\; \nu_{12} = \nu_{13}$$

$$G_{23} = \frac{E_{22}}{2(1+\nu_{23})}$$

The model parameters for M30S and MR60H fibers are listed in Tables 9.3 and 9.4.

Table 9.3: M30S Fiber Elastic Properties Model Parameters.

Constant	Value	Units
E_{11}^{ref}	2.94E11	Pa
$s_{E_{11}}^T$	0.0	$Pa/°C$
$T_{E_{11}}^{ref}$	0.0	$°C$
E_{22}^{ref}	2.23E10	Pa
$s_{E_{22}}^T$	0.0	$Pa/°C$
$T_{E_{22}}^{ref}$	0.0	$°C$
G_{12}^{ref}	3.57E10	Pa
$s_{G_{12}}^T$	0.0	$Pa/°C$
$T_{G_{12}}^{ref}$	0.0	$°C$
ν_{12}^{ref}	0.2	-
$s_{\nu_{12}}^T$	0.0	$1/°C$
$T_{\nu_{12}}^{ref}$	0.0	$°C$
ν_{23}^{ref}	0.25	-
$s_{\nu_{23}}^T$	0.0	$1/°C$
$T_{\nu_{23}}^{ref}$	0.0	$°C$

Table 9.4: MR60H Fiber Elastic Properties Model Parameters.

Constant	Value	Units
E_{11}^{ref}	2.94E11	Pa
$s_{E_{11}}^{T}$	0.0	$Pa/°C$
$T_{E_{11}}^{ref}$	0.0	$°C$
E_{22}^{ref}	2.23E10	Pa
$s_{E_{22}}^{T}$	0.0	$Pa/°C$
$T_{E_{22}}^{ref}$	0.0	$°C$
G_{12}^{ref}	3.57E10	Pa
$s_{G_{12}}^{T}$	0.0	$Pa/°C$
$T_{G_{12}}^{ref}$	0.0	$°C$
ν_{12}^{ref}	0.2	-
$s_{\nu_{12}}^{T}$	0.0	$1/°C$
$T_{\nu_{12}}^{ref}$	0.0	$°C$
ν_{23}^{ref}	0.25	-
$s_{\nu_{23}}^{T}$	0.0	$1/°C$
$T_{\nu_{23}}^{ref}$	0.0	$°C$

9.8. Resin Modulus Model Fit

The resin elasticity modulus (E_r) and Poisson's ratio (ν_r) evolutions were fit to CCA Resin Modulus model 13 and CCA Poisson's Ratio model 6, respectively, which are defined by:

$$E_r = \frac{9K'G'}{3K' + G'}$$

$$\nu_r = \frac{3K' - 2G'}{6K' + 2G'}$$

Where G' and K' are defined by:

$$G' = \begin{cases} G_r + (G_g - G_r)\sum_i g_i e^{-\frac{1}{f a_{Tx} \tau_i}} & x > x_{gel} \\ G_{min} & x \leq x_{gel} \end{cases}$$

$$K' = \begin{cases} K_r + (K_g - K_r)\sum_i g_i e^{-\frac{1}{f a_{Tx} \tau_i}} & x > x_{gel} \\ K_{min} & x \leq x_{gel} \end{cases}$$

The temperature and DoC shift factor is defined by:

$$\log(a_{Tx}) = \left(\frac{C_T}{T - T^\infty} - \frac{C_T}{T^{ref} - T^\infty}\right) - \left(\frac{C_{T_g}}{T_g - T^\infty} - \frac{C_{T_g}}{T_g^{ref} - T^\infty}\right)$$

$$T_g = T_g^0 + \frac{\lambda x}{1 - (1 - \lambda)x}\left(T_g^\infty - T_g^0\right)$$

$$T^\infty = T_g - C_2$$

The model constants are given in Tables 9.5 and 9.6.

Table 9.5: Resin Modulus Model Parameters.

Constant	Value	Units
T_g^0	5.5	°C
T_g^∞	207	°C
λ	0.53	–
f	0.1	Hz
C_T	30000.0	°C
C_{T_g}	22000.0	°C
C_2	257	°C
T^{ref}	207	°C
T_g^{ref}	207	°C
G_r	1E7	Pa
G_g	1.05E9	Pa
K_r	3.67E9	Pa
K_g	3.68E9	Pa
x_{gel}	0.5	–
G_{min}	3.33E4	Pa
K_{min}	3.68E9	Pa

Table 9.6: Resin Modulus Prony Series.

g_i	τ_i
0.003861	100000
0.005531	10000
0.041845	1000
0.125378	100
0.119920	10
0.066595	1
0.047967	0.1
0.033354	0.01
0.023151	0.001
0.020631	0.0001
0.018277	1.00E-05
0.016019	1.00E-06
0.014161	1.00E-07
0.012621	1.00E-08
0.010899	1.00E-09
0.010794	1.00E-10
0.014093	1.00E-11
0.016519	1.00E-12
0.019422	1.00E-13
0.022511	1.00E-14
0.025692	1.00E-15
0.029678	1.00E-16
0.032170	1.00E-17
0.028799	1.00E-18
0.027181	1.00E-19
0.025167	1.00E-20
0.023477	1.00E-21
0.021553	1.00E-22
0.020210	1.00E-23
0.017208	1.00E-24
0.015682	1.00E-25
0.011020	1.00E-26
0.018647	1.00E-27
0.022696	1.00E-29
0.012634	1.00E-31
0.012245	1.00E-32
0.013607	1.00E-34

9.9. Resin Modulus Quality of Fit

A comparison of the resin modulus from experimental bi-material beam data and as predicted by the model for each test condition is shown in Figures 9.8 to 9.13.

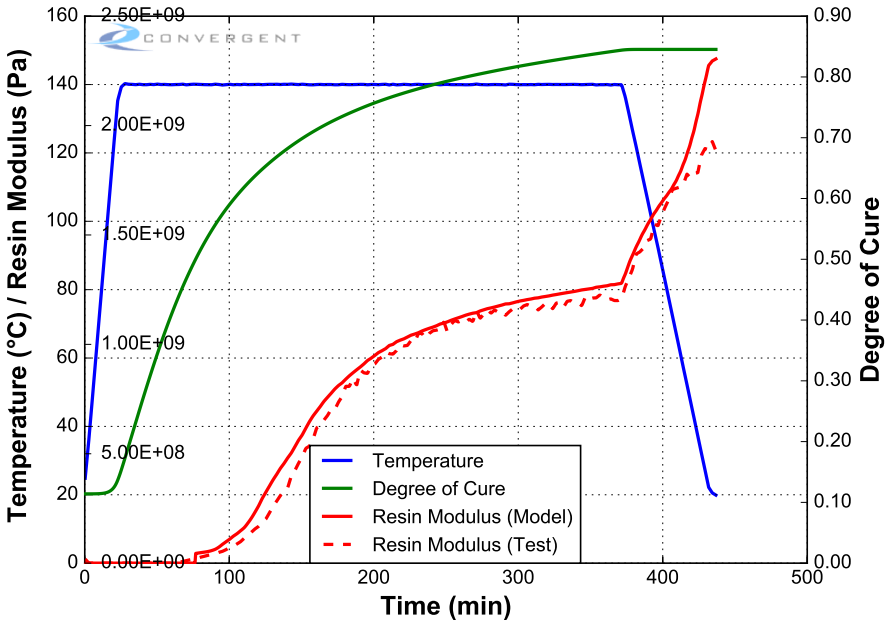

Figure 9.8: Model Prediction: F7-UD-B3-DMA-BMB-140C-350min-1.

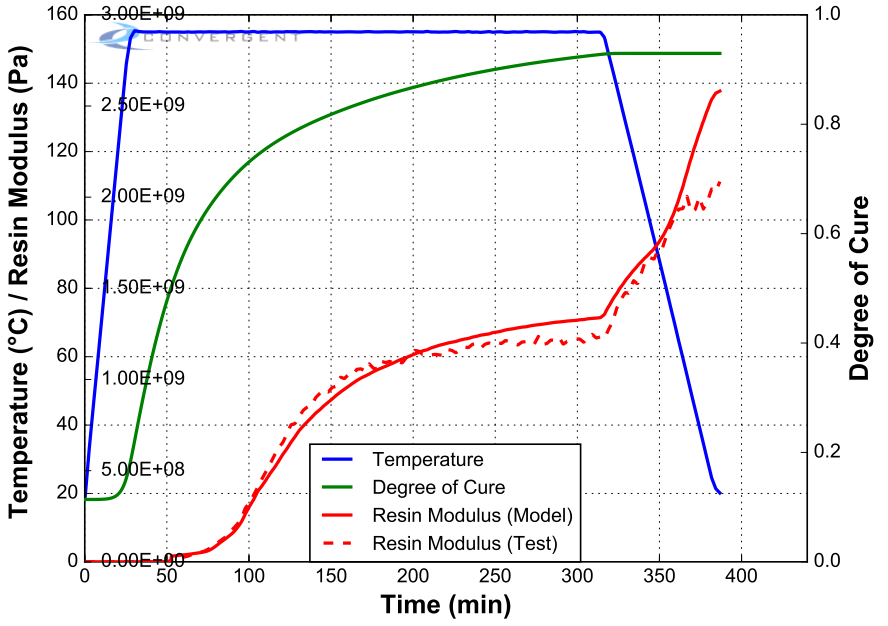

Figure 9.9: Model Prediction: F7-UD-B3-DMA-BMB-155C-290min-1.

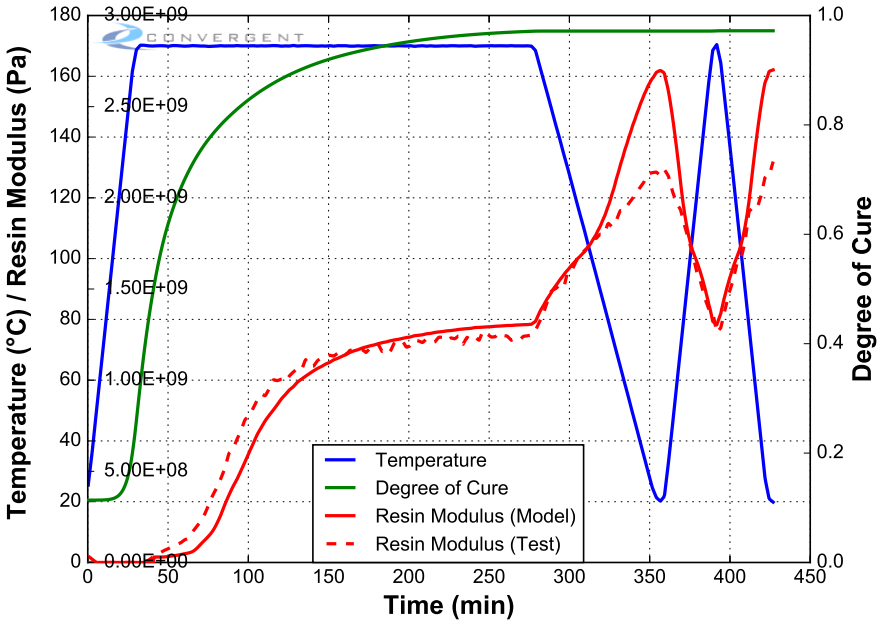

Figure 9.10: Model Prediction: F7-UD-B3-DMA-BMB-170C-250min-1.

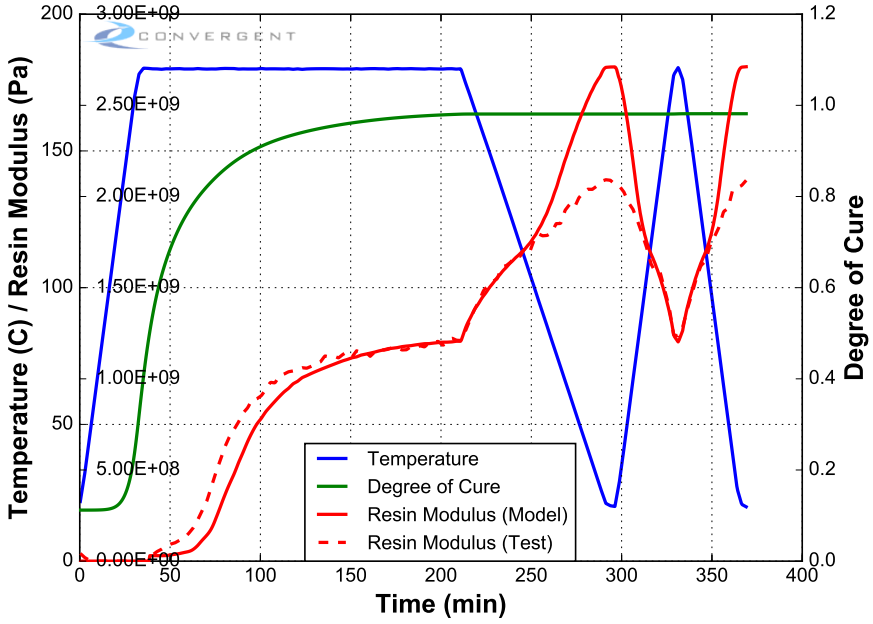

Figure 9.11: Model Prediction: F7-UD-B2-DMA-BMB-180C-180min-1.

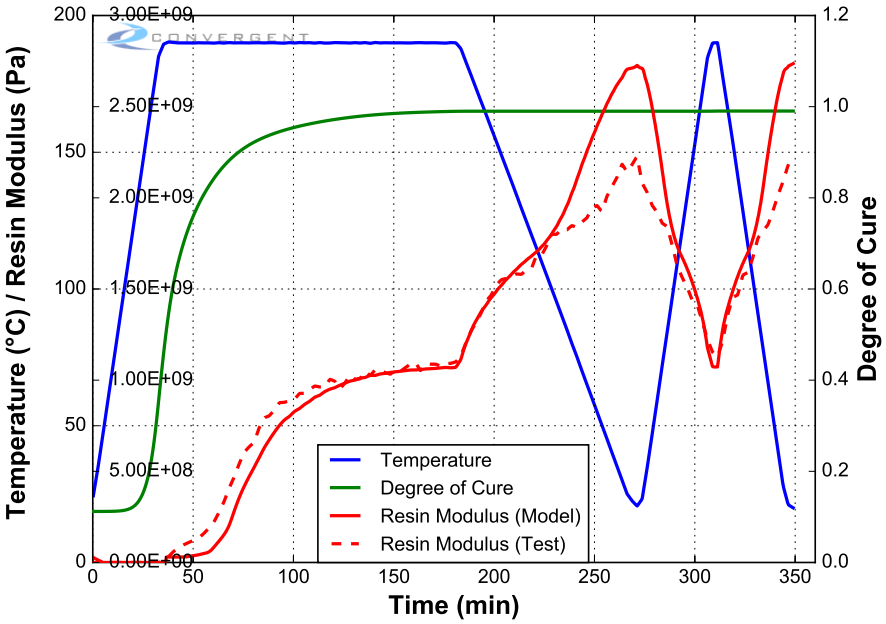

Figure 9.12: Model Prediction: F7-UD-B2-DMA-BMB-190C-150min-1.

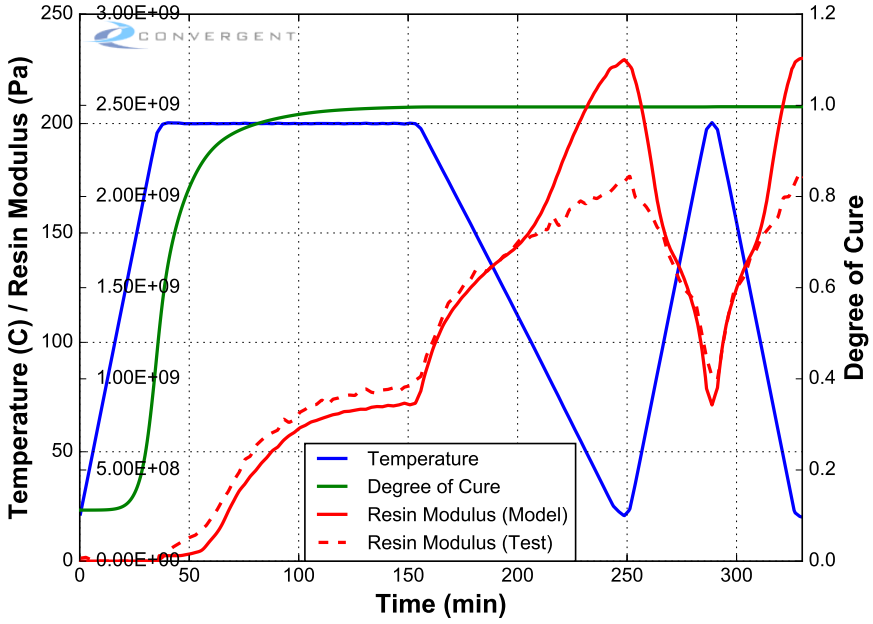

Figure 9.13: Model Prediction: F7-UD-B2-DMA-BMB-200C-120min-2.

A comparison of the resin modulus from experimental neat resin beam data and as predicted by the model is shown in the following figure.

A comparison of the resin modulus from experimental neat resin beam data and as predicted by the model is shown in Fig. 9.14.

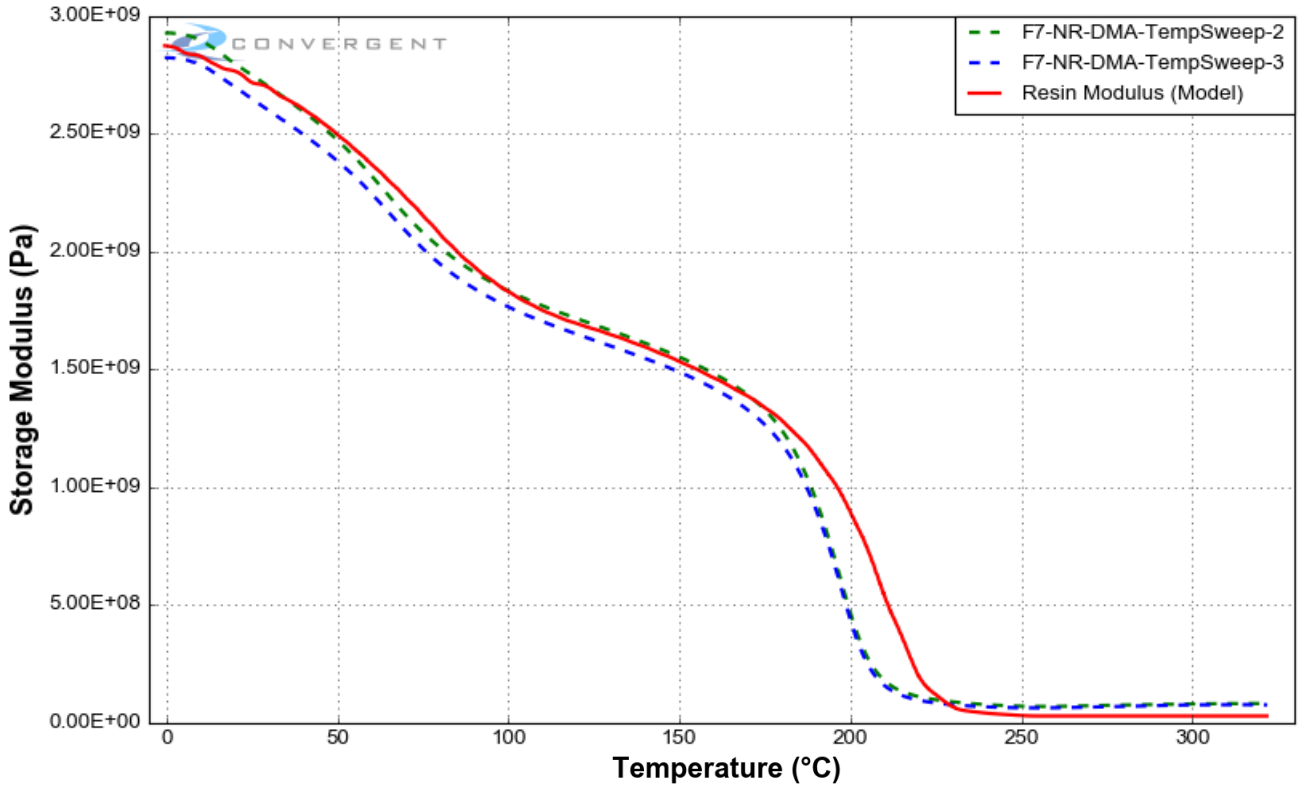

Figure 9.14: Modulus Model Prediction: Neat resin DMA test data.

9.10. Resin Modulus Comments

The resin modulus model developed was validated for cure cycles with hold temperatures between 100ºC and 200ºC. Additionally the resin modulus model was validated in the fully cured state from 20ºC to 200ºC.

10. Thermo-Mechanical Characterization: Resin Thermal Expansion and Cure Shrinkage

10.1. Nomenclature

T_g : Glass transition temperature

T_{g0} : Glass transition temperature at degree of cure = 0

$T_{g\infty}$: Glass transition temperature at degree of cure = 1

λ : DiBenedetto equation calibration constant

α or CTE: Coefficient of thermal expansion

α_{glass} : Glassy state coefficient of thermal expansion

α_{rub} : Rubbery state coefficient of thermal expansion

A, B : $T*'$ Constants

T_{C_i} : $T*'$ Limit

C_{0i}, C_{1i}, C_{2i} : Model Constants

β : Resin instantaneous cure shrinkage factor

10.2. Introduction

The thermal expansion and cure shrinkage models are closely linked. The analysis of these two properties was performed concurrently.

10.3. DMA Test Procedures

BMB Tests

Bi-material three point bend tests were performed using a TA Instruments Q800 DMA machine to measure the deformation of the beam due to curing and temperature change. The same displacement-modulated tests used to determine the resin modulus development properties were used to develop a model for the cure shrinkage and thermal expansion properties of the material. The displacement of the bi-material sample (position at zero applied dynamic force) was measured as the resin/prepreg material cured under the test conditions. The methodology for the tests performed was discussed in the previous section.

10.4. DMA Tests Performed

The DMA tests performed were outlined previously in the Resin Modulus section of this report.

10.5. DMA Raw BMB Displacement Data

The complete displacement history of the tests are shown in Figures 10.1 to 10.6. The isothermal hold portion was used to determine the resin cure shrinkage and the cool-down portion was used to determine the resin CTE.

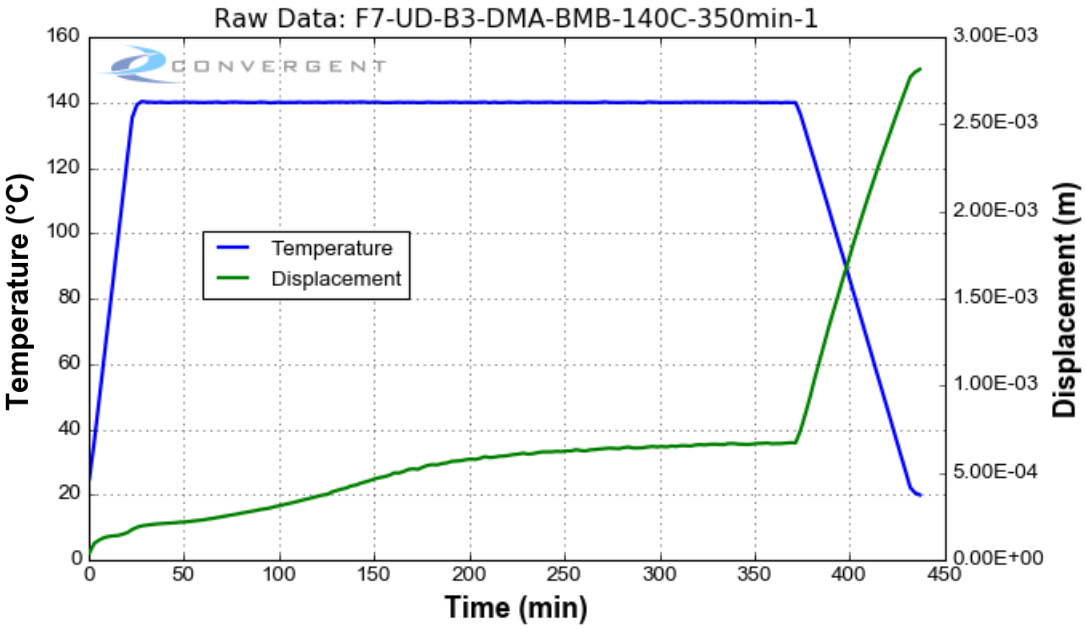

Figure 10.1: Raw Data: F7-UD-B3-DMA-BMB-140C-350min-1.

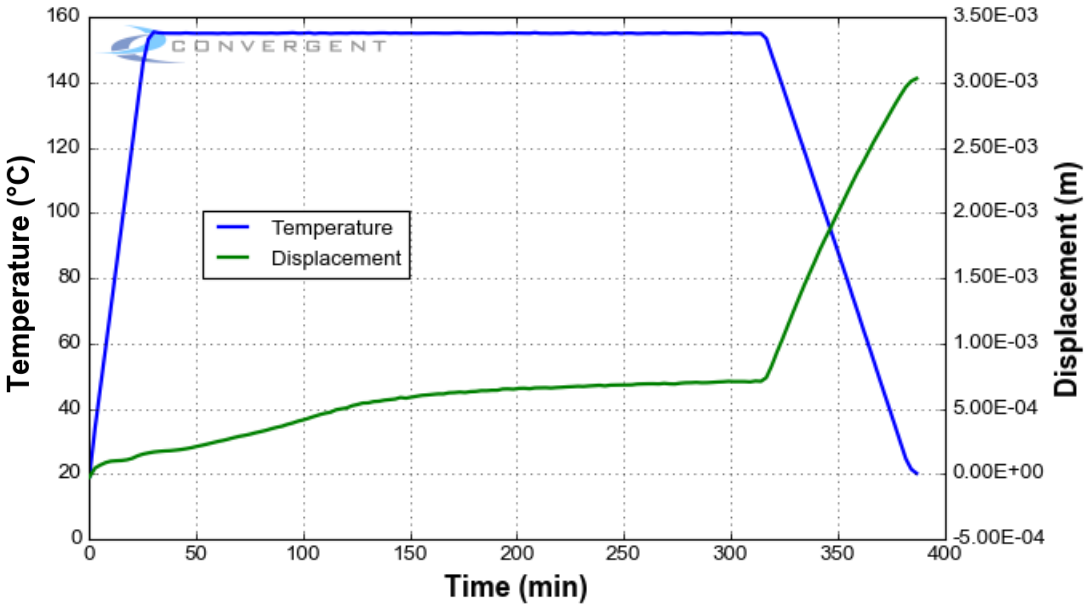

Figure 10.2: Raw Data: F7-UD-B3-DMA-BMB-155C-290min-1.

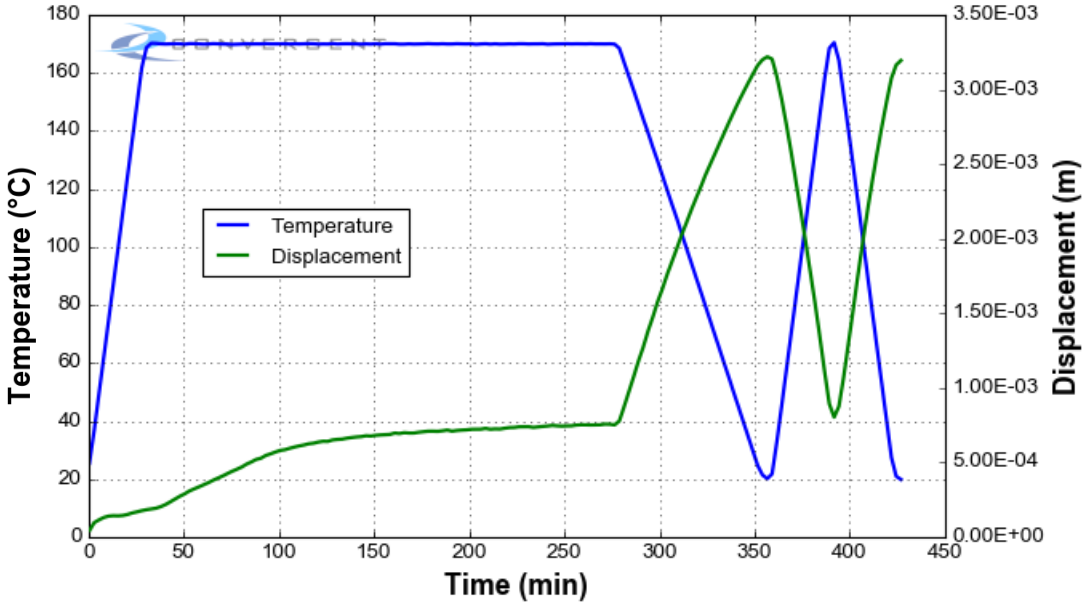

Figure 10.3: Raw Data: F7-UD-B3-DMA-BMB-170C-250min-1.

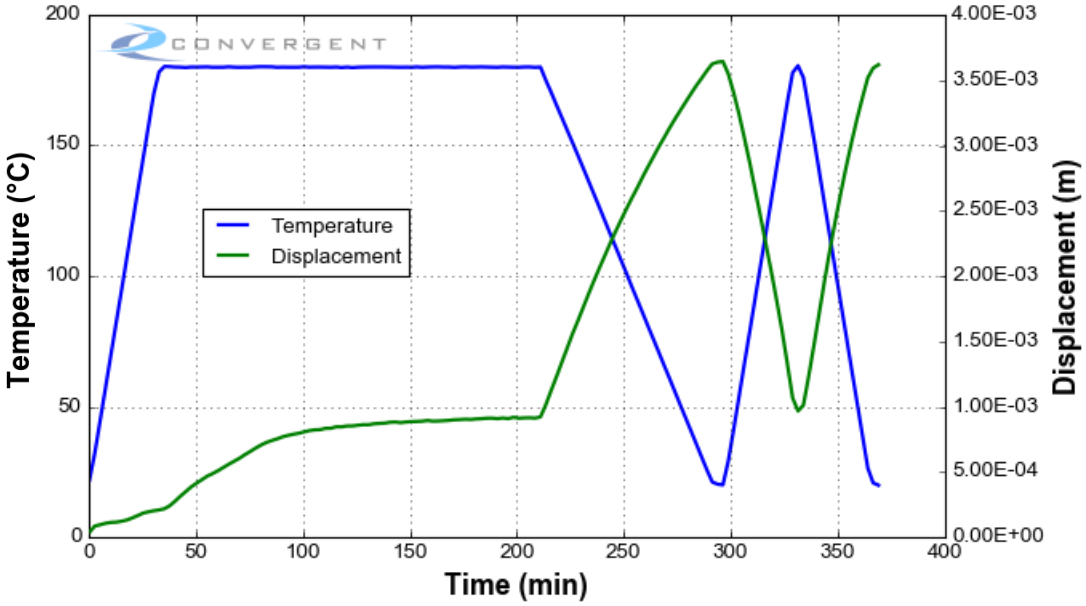

Figure 10.4: Raw Data: F7-UD-B2-DMA-BMB-180C-180min-1.

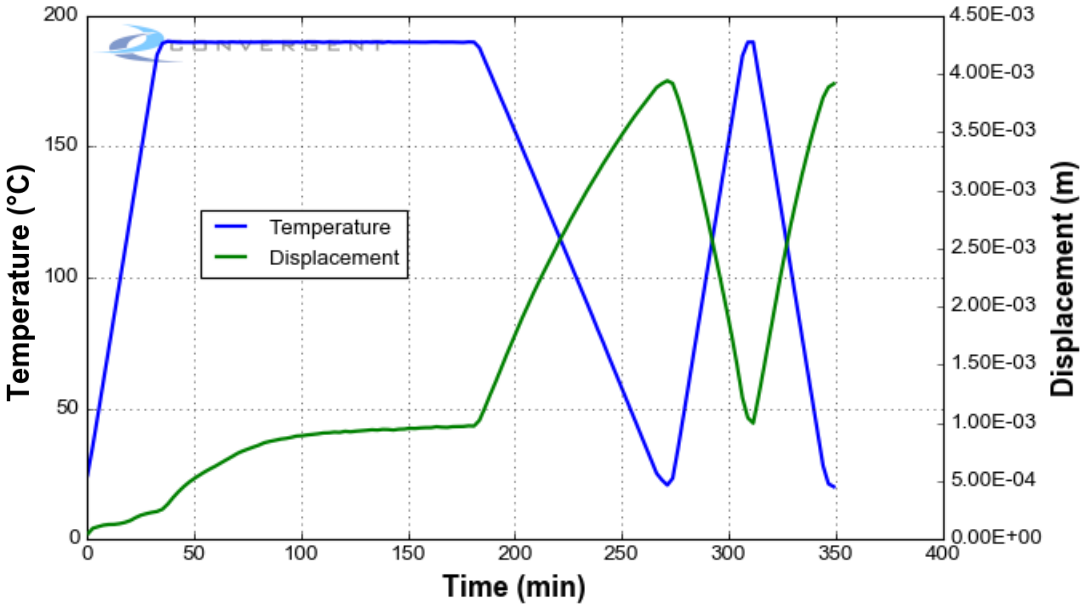

Figure 10.5: Raw Data: F7-UD-B2-DMA-BMB-190C-150min-1.

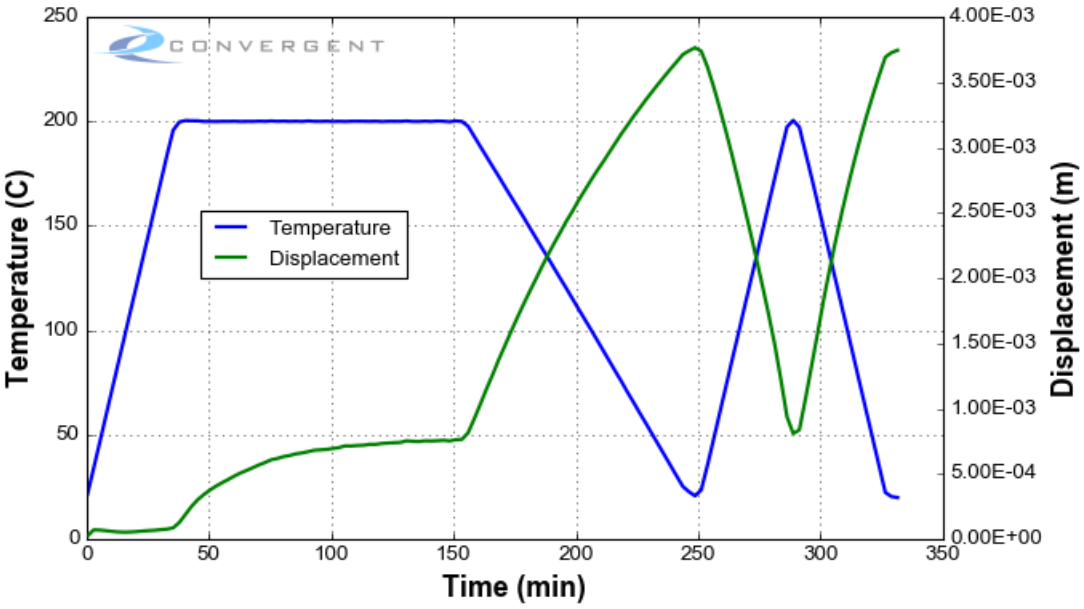

Figure 10.6: Raw Data: F7-UD-B2-DMA-BMB-200C-120min-1.

10.6. Thermo-Mechanical Analyzer Test Procedures

Homogeneous Resin Beam Thermo-Mechanical Analyzer (TMA) Tests

Dynamic ramp tests were performed on neat resin samples using a TA Instruments Q400 TMA to measure the linear expansion due to temperature change. Samples were heated and cooled at 2ºC/min. The length of the sample was measured throughout the thermal cycle.

10.7. TMA Tests Performed

The TMA tests performed are summarized below:

- Dynamic neat resin beam tests: 1 test at 2ºC/min from 0ºC up to 235ºC, 1 test at 2ºC/min from 0ºC up to 290ºC
- Dynamic MR60H unidirectional laminate beam tests: 3 tests at 2ºC/min from 0ºC up to 235ºC

A summary of the TMA tests performed is shown in Table 10.1.

Table 10.1: Test Summary (TMA Tests) [Modulus].

Test name	Ramp rate (°C/min)
F7-UD-B1-TMA-DIR1-1	2
F7-UD-B1-TMA-DIR2-1	2
F7-UD-B1-TMA-DIR3-1	2
F7-NR-B1-TMA-DIR1-2	2
F7-NR-B1-TMA-DIR1-2	2

10.8. TMA Raw Data

The change in sample length from the TMA testing is shown in Figures 10.7 to 10.11.

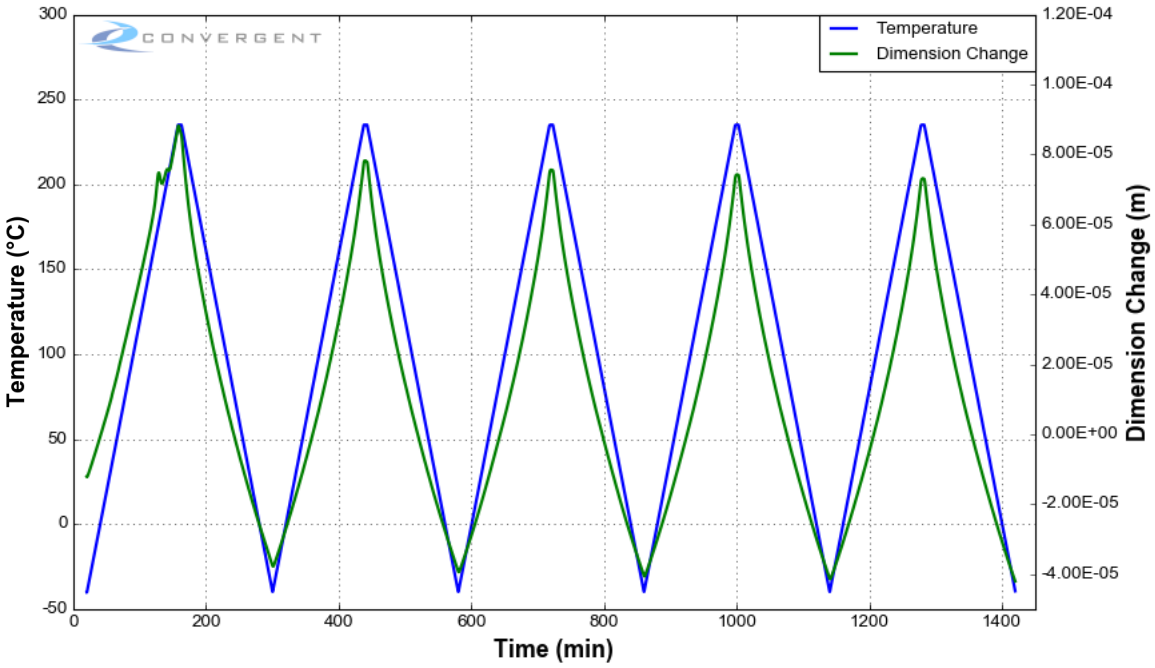

Figure 10.7: Neat Resin TMA Test Data Showing the Sample Dimension Change: Sample 1.

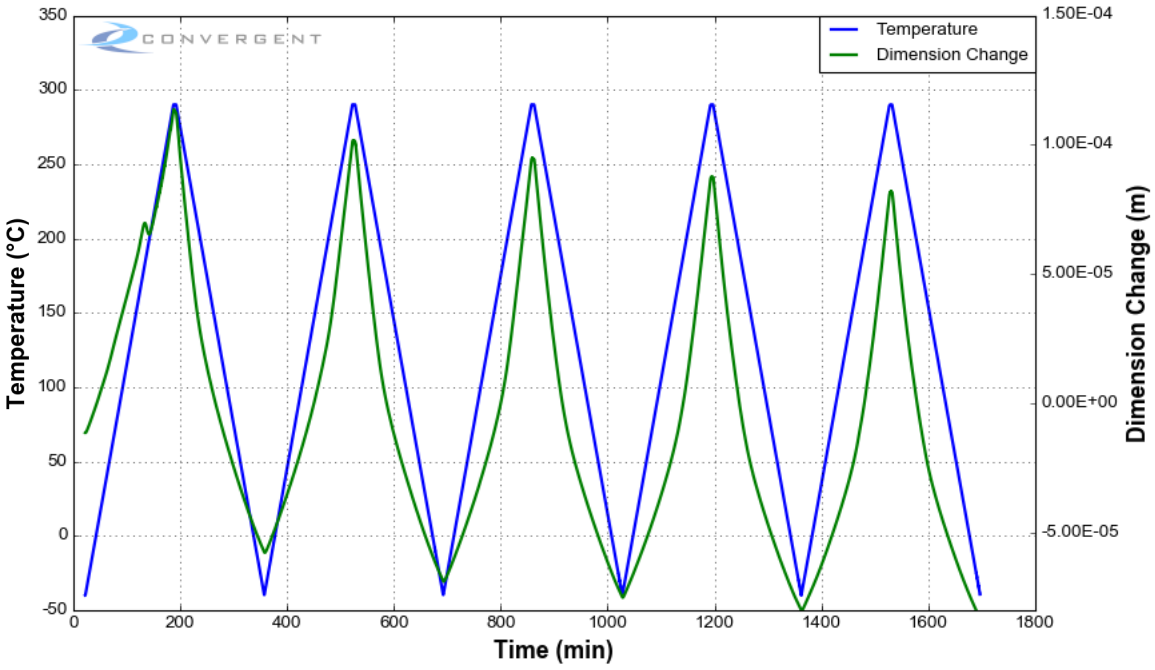

Figure 10.8: Neat Resin TMA Test Data Showing the Sample Dimension Change: Sample 2.

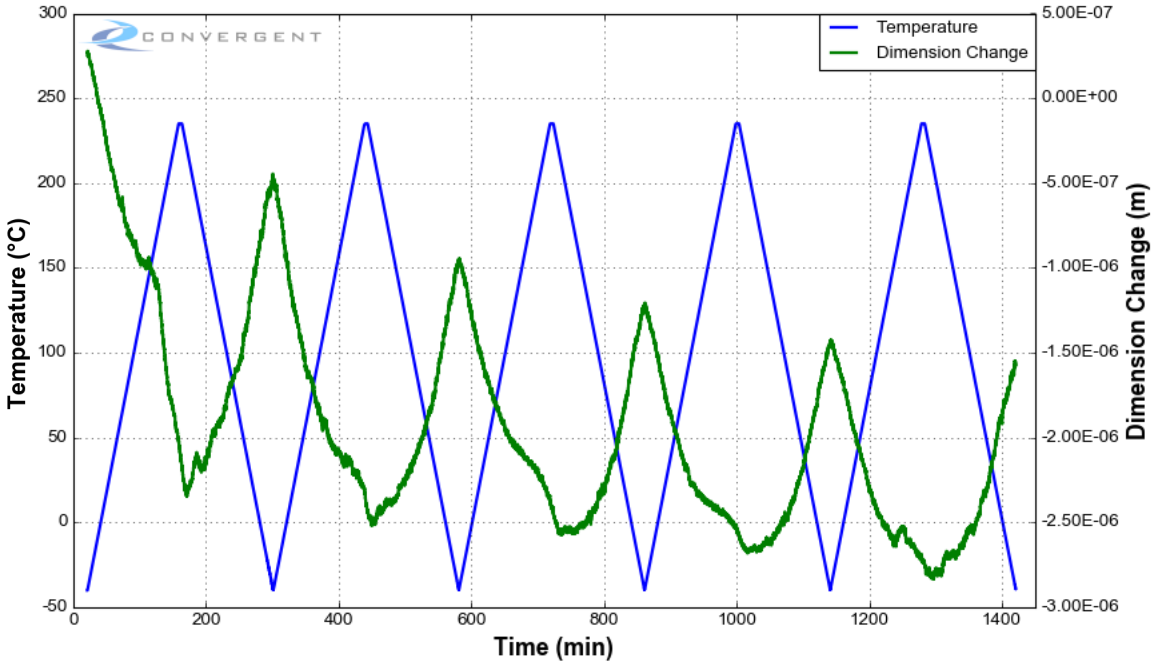

Figure 10.9: MR60H Unidirectional Laminate TMA Test Data Showing the Sample Dimension Change: Direction 1.

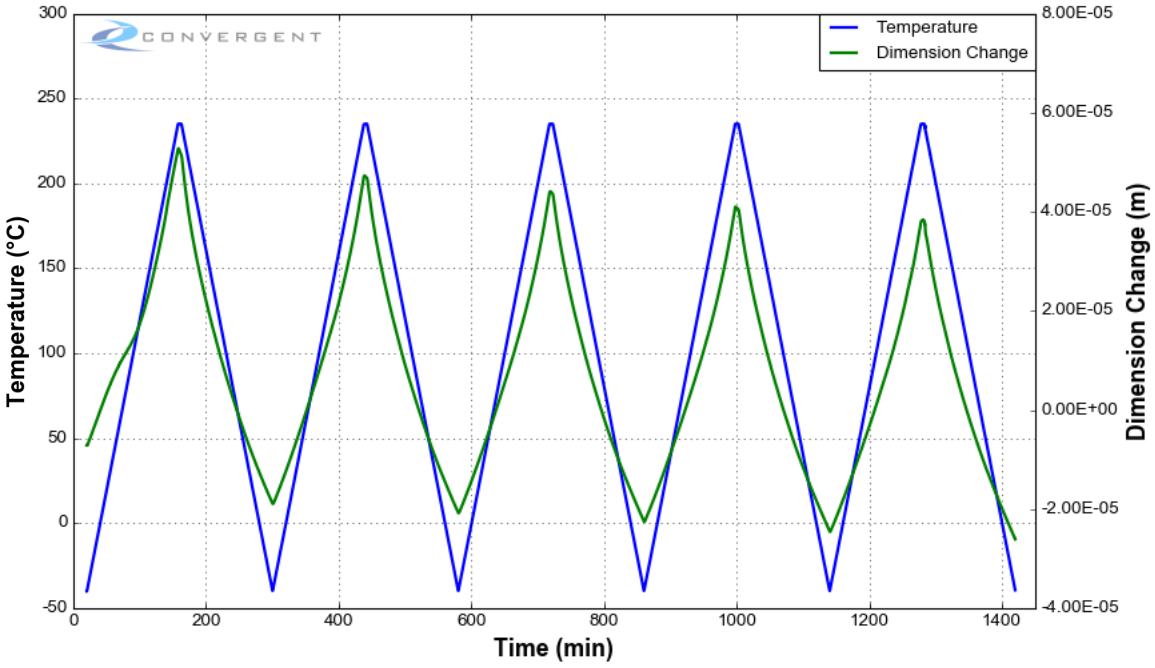

Figure 10.10: MR60H Unidirectional Laminate TMA Test Data Showing the Sample Dimension Change: Direction 2.

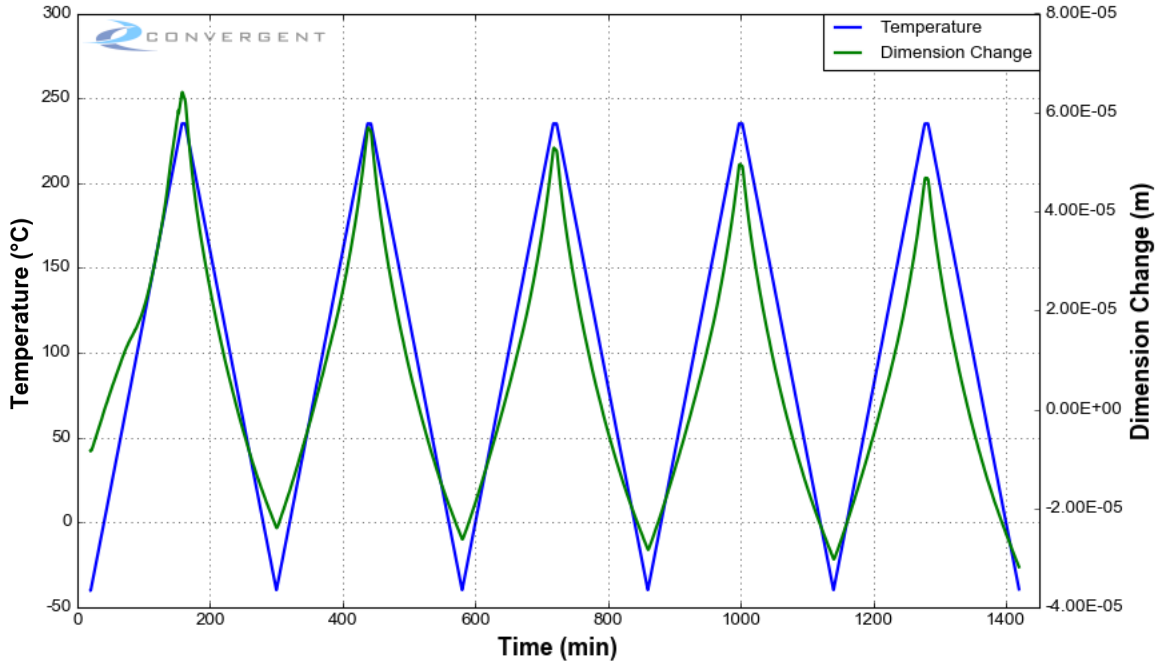

Figure 10.11: MR60H Unidirectional Laminate TMA Test Data Showing the Sample Dimension Change: Direction 3.

10.9. TMA Data Analysis

The calculated instantaneous CTE test data generated from the TMA testing is shown in Figures 10.12 to 10.16.

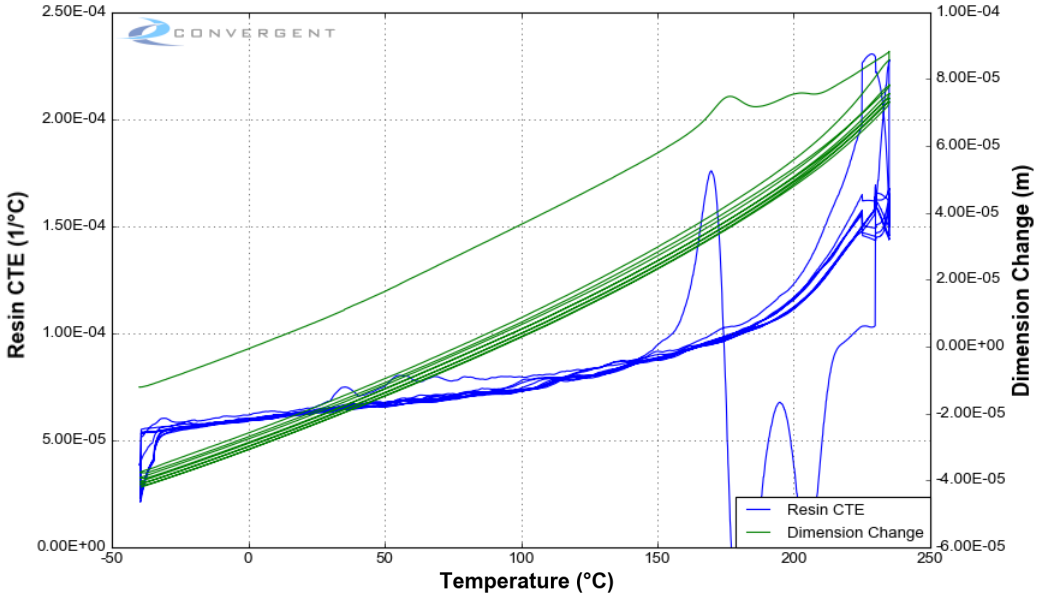

Figure 10.12: Neat Resin TMA Test Data Showing the Sample Length and Instantaneous CTE: Sample 1.

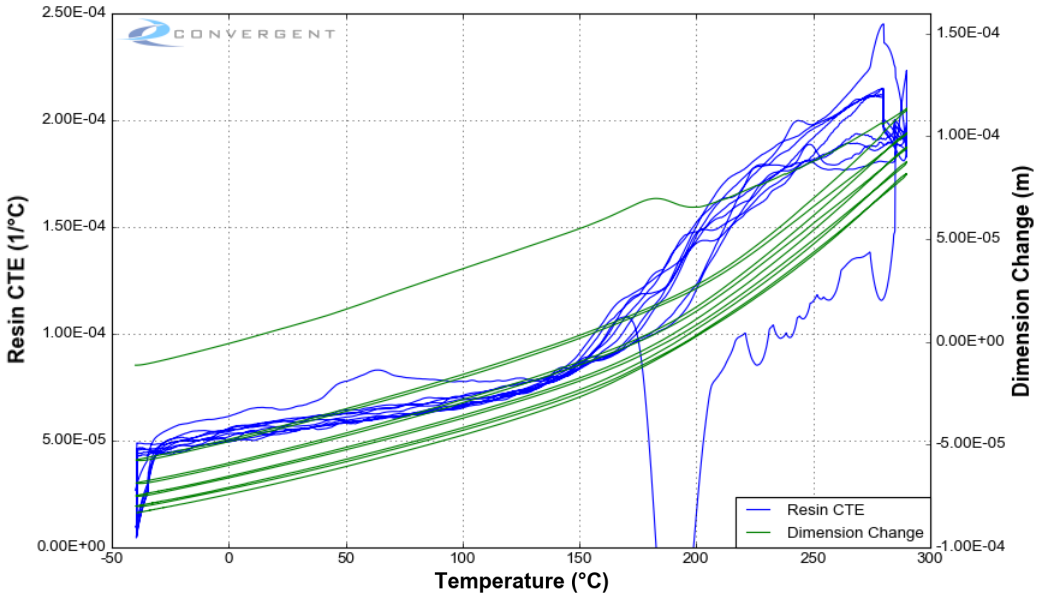

Figure 10.13: Neat Resin TMA Test Data Showing the Sample Length and Instantaneous CTE: Sample 2.

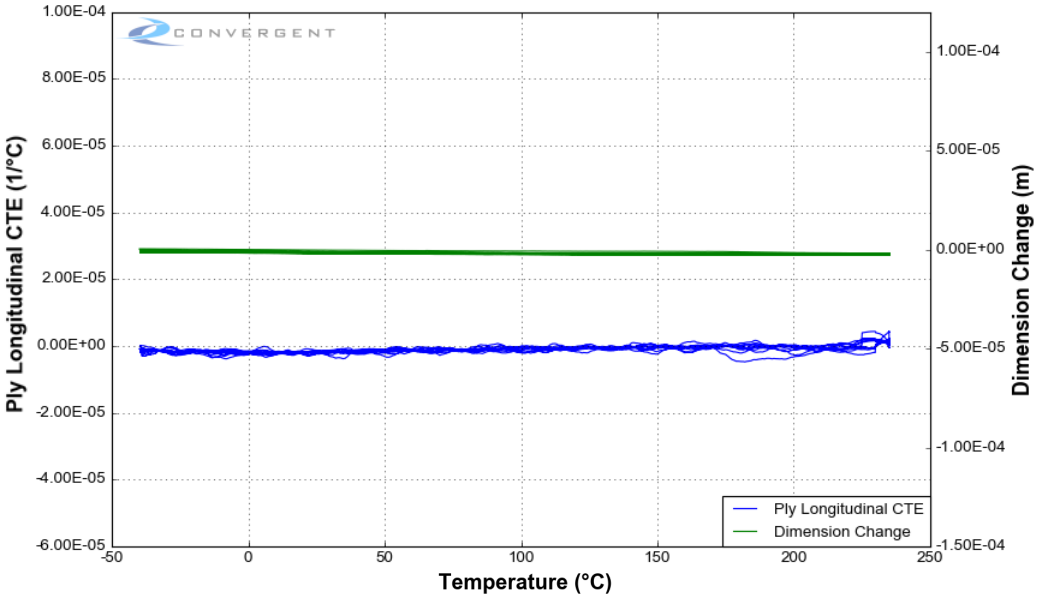

Figure 10.14: MR60H Unidirectional Laminate TMA Test Data Showing the Sample Length and Instantaneous CTE: Direction 1.

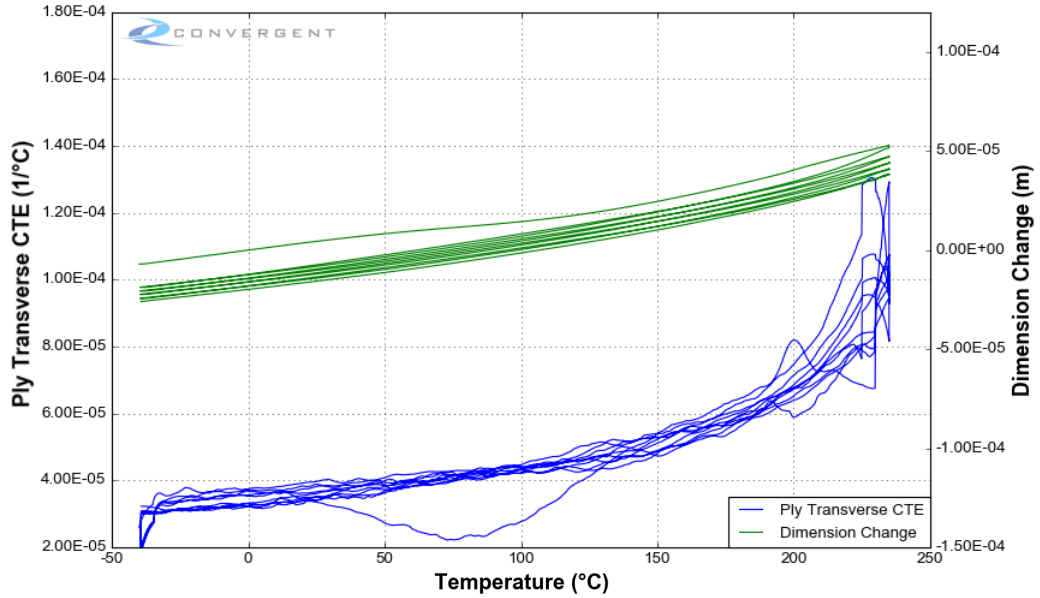

Figure 10.15: MR60H Unidirectional Laminate TMA Test Data Showing the Sample Length and Instantaneous CTE: Direction 2.

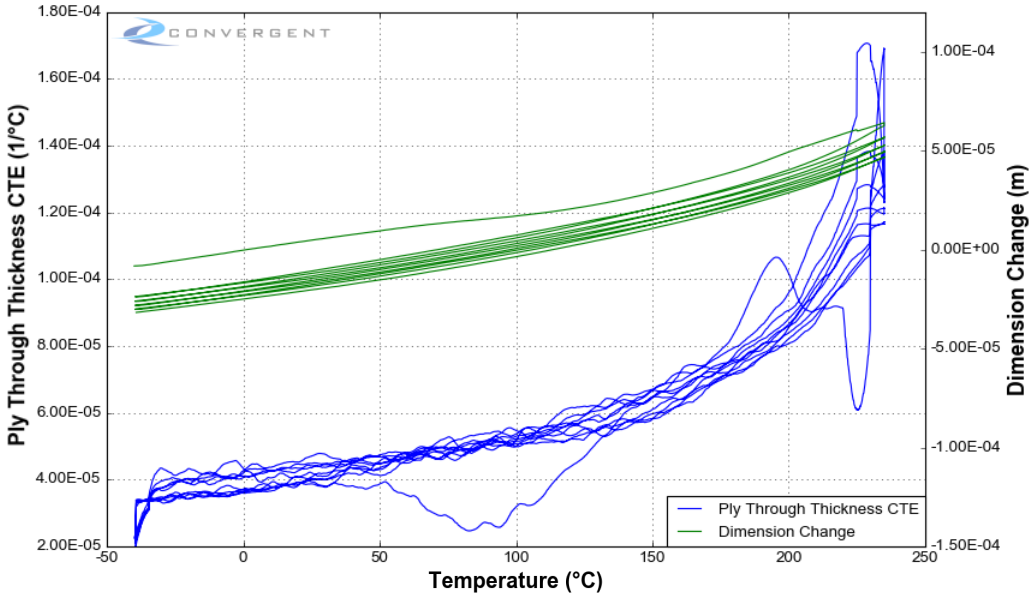

Figure 10.16: MR60H Unidirectional Laminate TMA Test Data Showing the Sample Length and Instantaneous CTE: Direction 3.

10.10. Thermal Expansion and Cure Shrinkage Model Fit

The data was analyzed by converting the displacement data into thermal strains, and examining the data in T-Tg space. The thermal expansion and cure shrinkage models were then fit to the data.

Thermal Expansion Model Fit

CCA resin thermal expansion model 5 is used to model resin thermal strains. Model parameters are defined in Table 10.2.

$$\frac{d\epsilon}{dT} = \alpha$$

$$\alpha = \begin{cases} \alpha_{glass} & T^{*'} \le T_{C1} \\ C_{01} + C_{11}T^{*'} + C_{21}\left(T^{*'}\right)^2 & T_{C1} < T^{*'} \le T_{C2} \\ C_{02} + C_{12}T^{*'} + C_{22}\left(T^{*'}\right)^2 & T_{C2} < T^{*'} \le T_{C3} \\ C_{03} + C_{13}T^{*'} + C_{23}\left(T^{*'}\right)^2 & T_{C3} < T^{*'} \le T_{C4} \\ \alpha_{rub} & T_{C4} < T^{*'} \end{cases}$$

$$T^{*'} = A.T - B.T_g$$

$$T_g = T_g^0 + \frac{\lambda x}{1-(1-\lambda)x}\left(T_g^\infty - T_g^0\right)$$

Table 10.2: Resin Thermal Expansion Model Parameters.

Constant	Value	Units
T_g^0	5.5	°C
T_g^∞	207	°C
λ	0.53	–
A	1.0	–
B	0.73	–
T_{C1}	-188.687	°C
T_{C2}	-11.5384	°C
T_{C3}	48.0728	°C
T_{C4}	80.6428	°C
α_{rub}	0.000149	1/°C
α_{glass}	5.43E-05	1/°C
C_{01}	8.27E-05	1/°C
C_{11}	1.51E-07	$1/°C^2$
C_{21}	0.0	$1/°C^3$
C_{02}	8.66E-05	1/°C
C_{12}	4.86E-07	$1/°C^2$
C_{22}	0.0	$1/°C^3$
C_{03}	5.24E-05	1/°C
C_{13}	1.20E-06	$1/°C^2$
C_{23}	0.0	$1/°C^3$

Cure Shrinkage Model Fit

CCA resin cure shrinkage model 10 is used to model resin cure shrinkage strains. Model Parameters are defined in Table 10.3.

$$\frac{d\epsilon}{dx} = \beta = -\alpha_{CS}\frac{B}{A}\frac{dT_g}{dx}$$

$$\alpha_{CS} = \begin{cases} \alpha_{CS_{glass}} & T^{*'} \le T_{C1} \\ C_{01} + C_{11}T^{*'} + C_{21}\left(T^{*'}\right)^2 & T_{C1} < T^{*'} \le T_{C2} \\ C_{02} + C_{12}T^{*'} + C_{22}\left(T^{*'}\right)^2 & T_{C2} < T^{*'} \le T_{C3} \\ C_{03} + C_{13}T^{*'} + C_{23}\left(T^{*'}\right)^2 & T_{C3} < T^{*'} \le T_{C4} \\ \alpha_{CS_{rub}} & T_{C4} < T^{*'} \end{cases}$$

$$T^{*'} = A.T - B.T_g$$

$$T_g = T_g^0 + \frac{\lambda x}{1-(1-\lambda)x}\left(T_g^\infty - T_g^0\right)$$

Table 10.3: Resin Cure Shrinkage Model Parameters.

Constant	Value	Units
T_g^0	5.5	°C
T_g^∞	207	°C
λ	0.53	–
A	1.0	–
B	0.73	–
T_{C1}	-193.210	°C
T_{C2}	-29.6301	°C
T_{C3}	48.0728	°C
T_{C4}	87.5244	°C
α_{rub}	1.32E-04	$1/°C$
α_{glass}	0.0	$1/°C$
C_{01}	3.15E-05	$1/°C$
C_{11}	1.63E-07	$1/°C^2$
C_{21}	0.0	$1/°C^3$
C_{02}	4.06E-05	$1/°C$
C_{12}	4.68E-07	$1/°C^2$
C_{22}	0	$1/°C^3$
C_{03}	-2.08E-05	$1/°C$
C_{13}	1.75E-06	$1/°C^2$
C_{23}	0.0	$1/°C^3$

10.11. Thermal Expansion and Cure Shrinkage Quality of Fit

To verify the quality of the model fit, the predictions of the model were compared to the experimental data. These comparisons are shown in Figures 10.17 to 10.22.

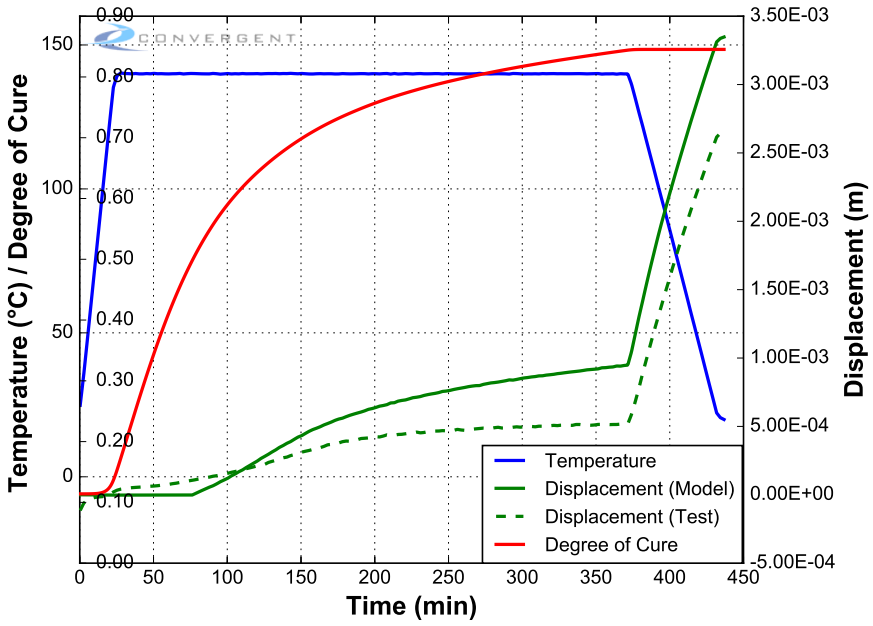

Figure 10.17: Model Prediction: Isothermals 140°C.

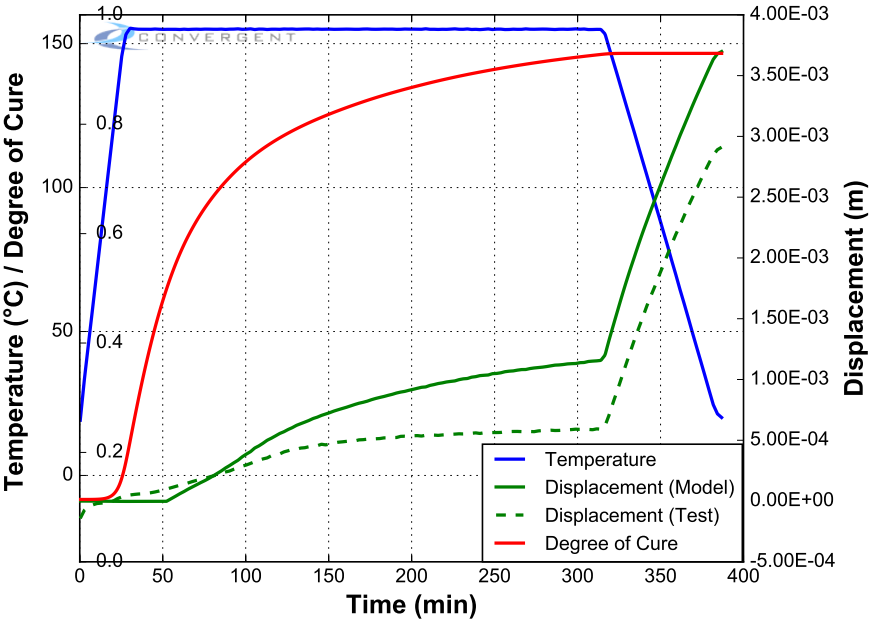

Figure 10.18: Model Prediction: Isothermals 155°C.

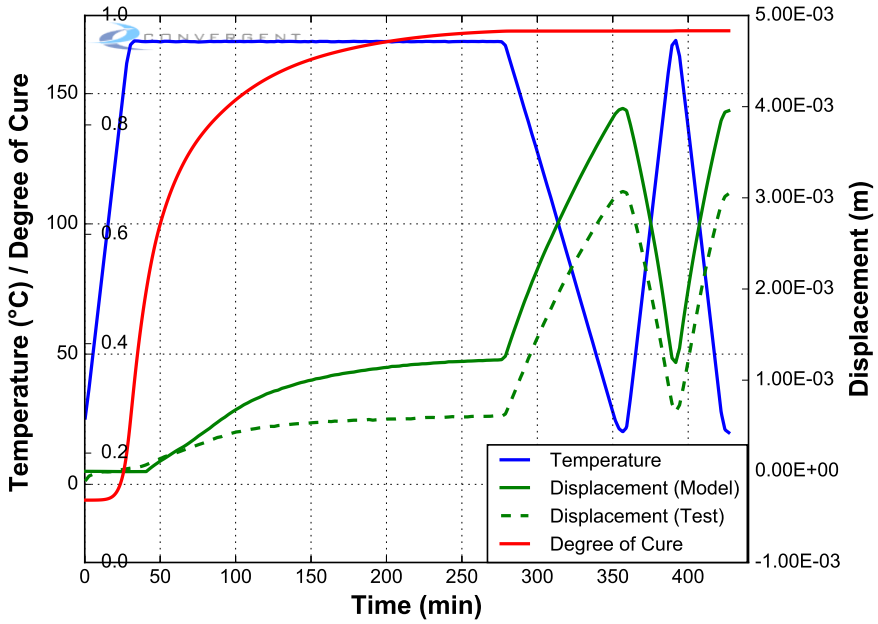

Figure 10.19: Model Prediction: Isothermals 170°C.

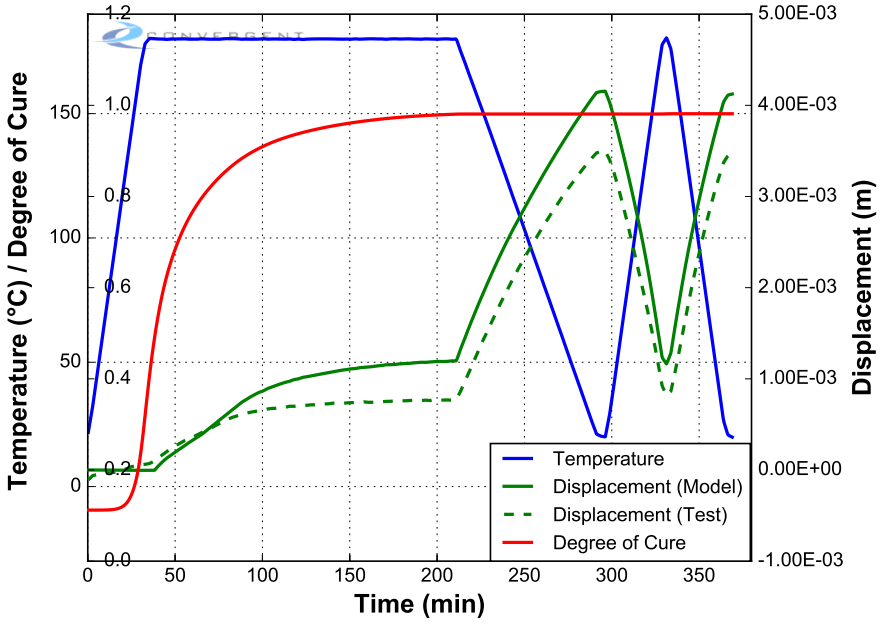

Figure 10.20: Model Prediction: Isothermals 180°C.

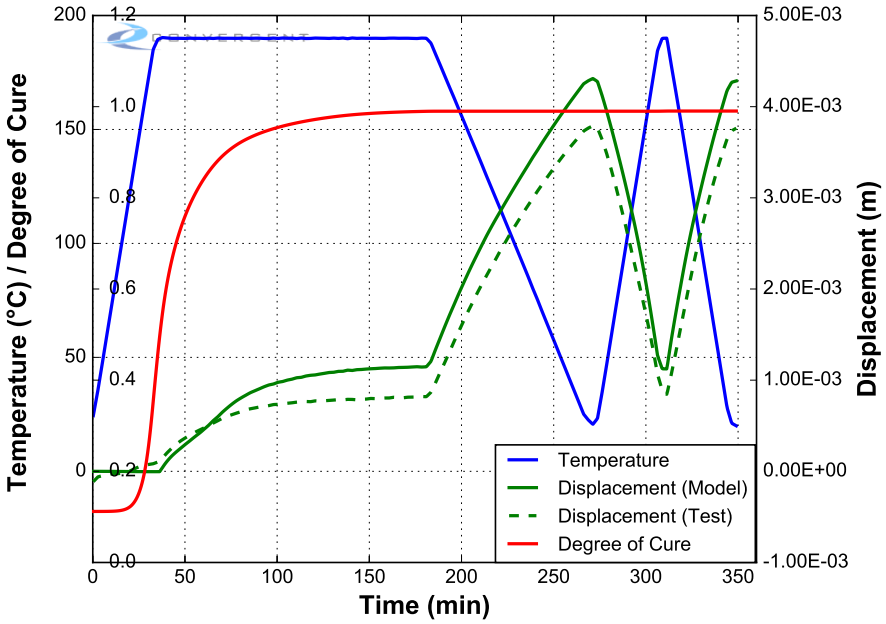

Figure 10.21: Model Prediction: Isothermals 190°C.

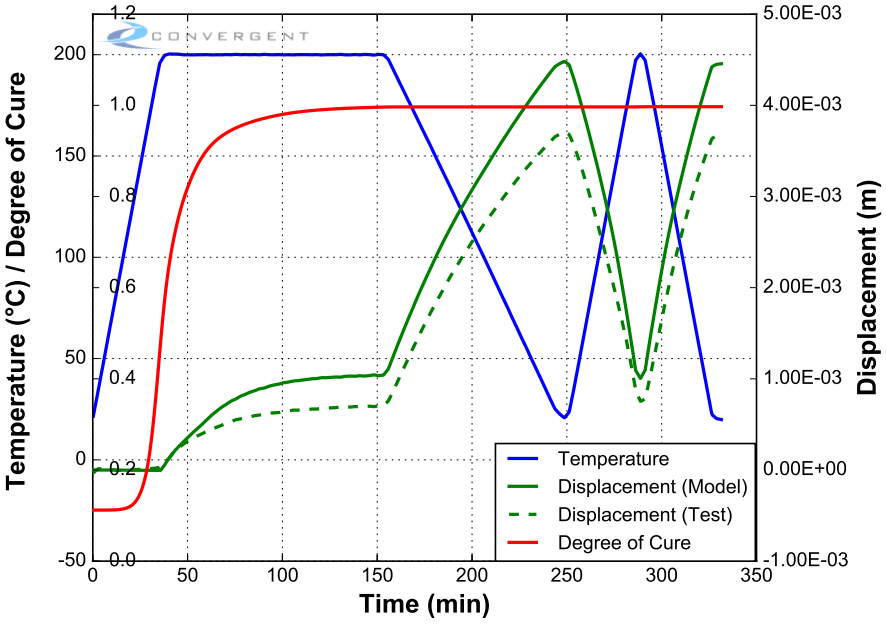

Figure 10.22: Model Prediction: Isothermals 200°C.

A comparison of the experimental TMA data and the behavior as predicted by the model is shown in Figures 10.23 to 10.26.

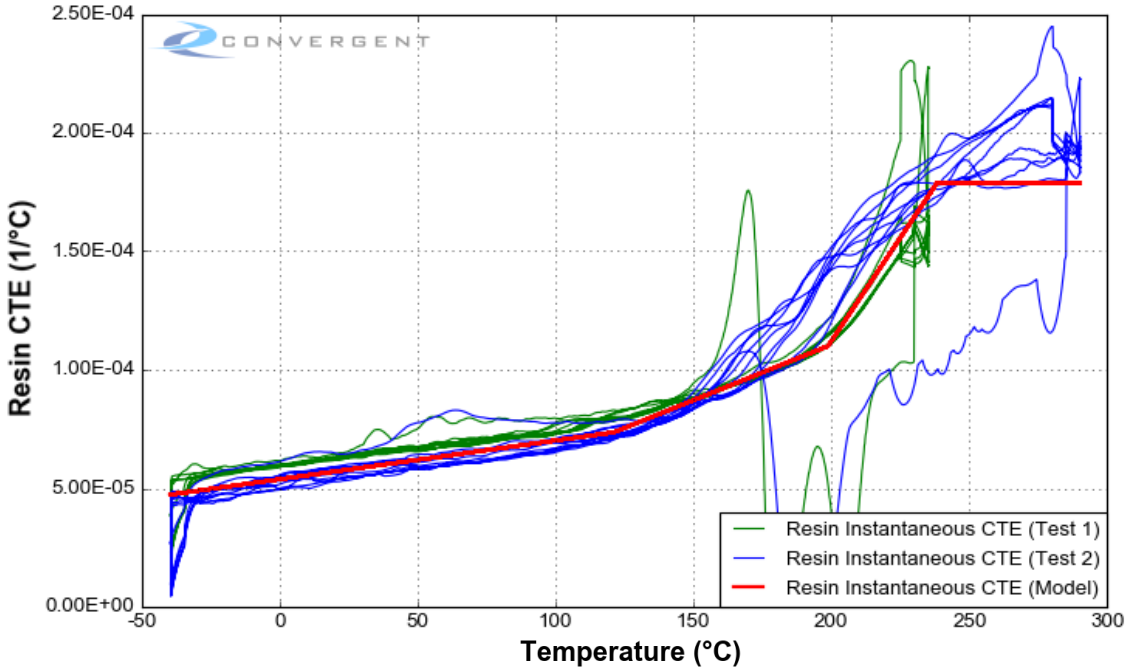

Figure 10.23: CTE Model Prediction: Neat resin TMA test data.

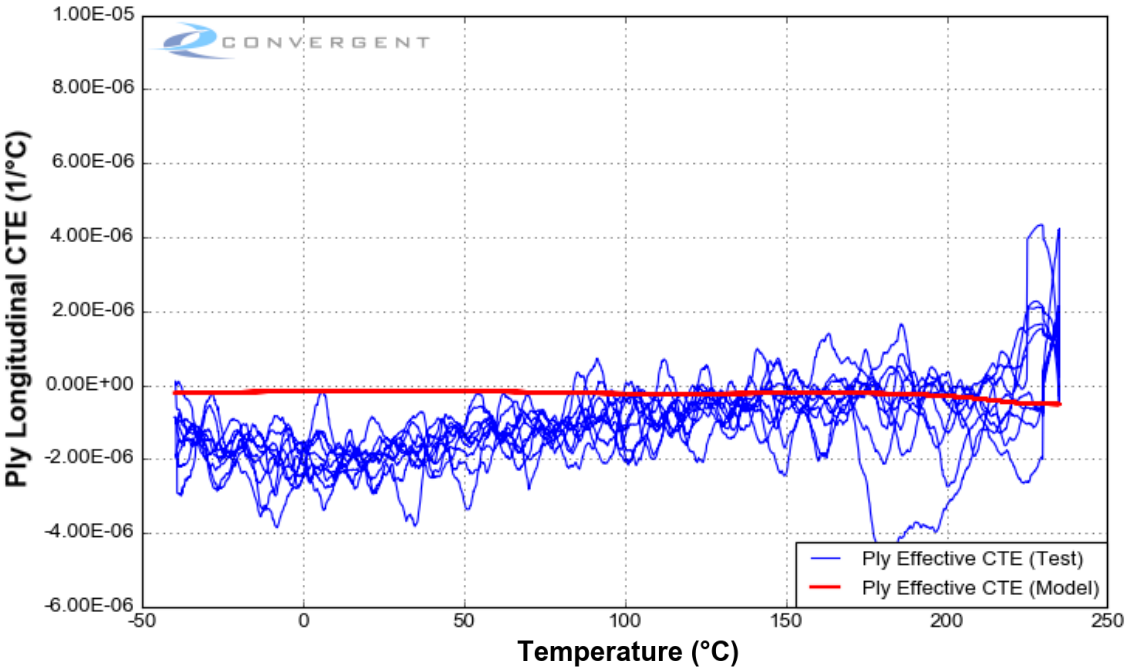

Figure 10.24: CTE Model Prediction: MR60H Unidirectional Laminate TMA test data: Direction 1.

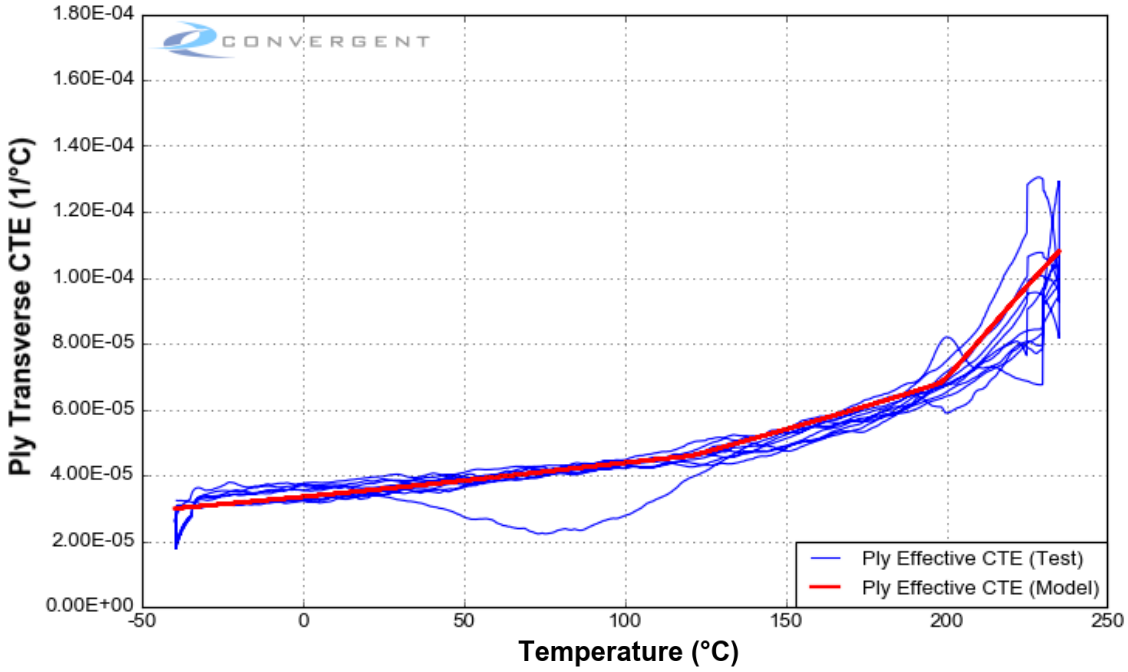

Figure 10.25: CTE Model Prediction: MR60H Unidirectional Laminate TMA test data: Direction 2.

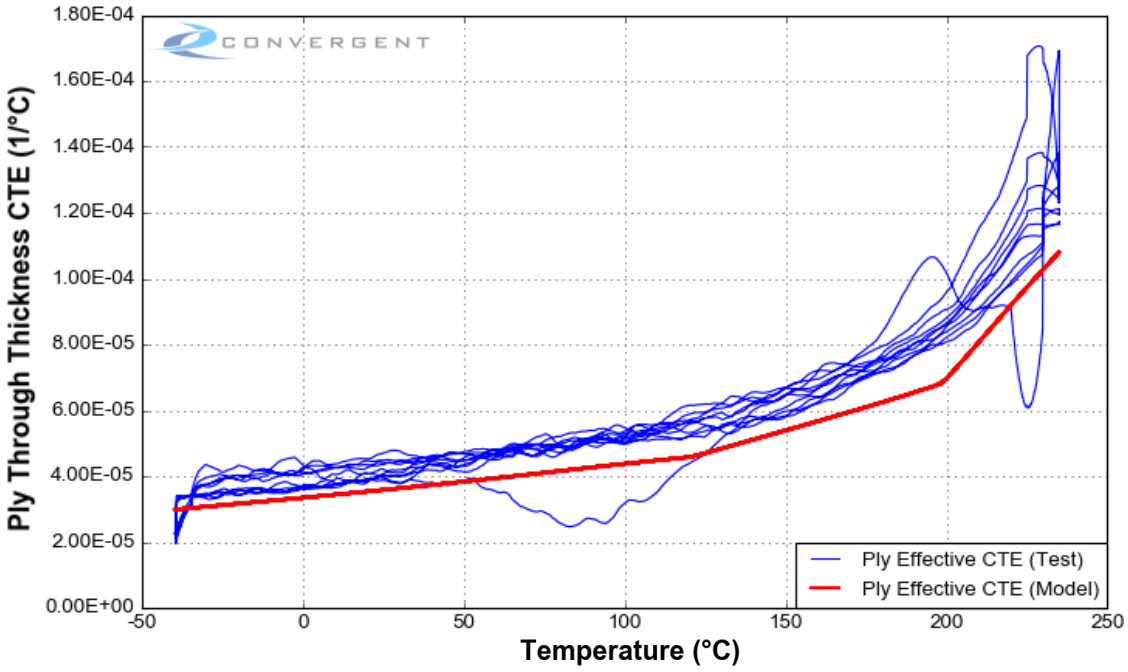

Figure 10.26: CTE Model Prediction: MR60H Unidirectional Laminate TMA test data: Direction 3.

10.12. Thermal Expansion and Cure Shrinkage Comments

The CTE and cure shrinkage models developed are validated for cure cycles within the range of temperatures between 140ºC and 200ºC. The CTE model was fit to the neat resin tests and compared to the UD laminate level tests. This model fit shows good prediction of the laminate level tests with minor deviation from those performed in Direction 3. Additionally, the CTE model is validated for fully cured material from 20ºC to 290ºC based on an additional test performed to capture the rubbery region. The CTE model developed in Revision 2 effectively captures material response at higher temperature regions with negligible effects to other model predictions. This iteration is an improvement over the previous version which was limited in accurate model predictions to a maximum temperature of 235ºC.

It is noted that the low temperature BMB displacement is over-predicted by the models. The reason for this was not fully resolved in this work. The cured resin DMA and TMA data is considered higher confidence than the Bi-Material Beam tests and priority was given to fit to this data. The CTE model fit to the resin TMA data was compared against the UD laminate TMA data with only minor deviations, further building confidence in the CTE model.

It should also be noted that there was some uncertainty in the cure kinetics model in the early stages of the isothermal holds as discussed in the thermo-chemical comments section. There was also uncertainty around the initial degree of cure of each form tested. While every effort was made to resolve these, these two factors could result in minor differences in the experiment and model degree of cure history used to predict the BMB deflections.